Author:
Owen, Alun

Title:
Is photodegradation the critical pathway in the transformation of DOM in aquatic systems during autumn and winter

Is photodegradation the critical pathway in the transformation of DOM in aquatic systems during autumn and winter?

Alun Thomas Owen

A dissertation submitted to the University of Bristol in accordance with the requirements for award of the degree of Masters by Research (MScR) in the Faculty of Science - Geographical Sciences November 2018

Word Count: 16,677

Abstract

Dissolved Organic Matter (DOM) is ubiquitous to almost every aquatic system on earth, it affects nutrient loadings, metals concentrations and can impact upon human health. The last few decades have provided a vast insight into the transformation of DOM via microbial organisms but less so has been done on how the sun can affect DOM transformations (photodegradation).

The impact that photodegradation can have on aquatic DOM in the summer months has been extensively studied but DOM transformations in autumn and winter are currently poorly understood. With the increasing uncertainty from climate change there is a pressing need to better understand how photodegradation is impacting sites of different DOM character.

In order to bridge this research gap 6 sites were identified of varying land use and DOM character in Conwy and Hampshire Avon catchments. Samples taken at each site were divided between unfiltered samples and samples that had been filtered through a 0.1 µm cellulose nitrate filtered to remove any biota. This was to compare the effects of photodegradation alone vs the effect of photodegradation and the breakdown via biota on the transformation of DOM. The samples were incubated in autumn and winter at the same temperature and solar intensity of the month they were sampled in order to compare the transformations observed. Each day macronutrients, UV and fluorescence measurements were taken to monitor the change over 1 week.

The data analysis showed that DOM varied in concentration and composition between seasons and that photodegradation was still occurring even in winter. The data emphasised that neither photodegradation nor biodegradation were mutually exclusive and that more work needs to be done to identify the compound specific DOM transformations in autumn and winter.

Acknowledgments

I would firstly like to say a big thank you to my supervisor Penny Johnes for without her continued support and critique I would have been unable to complete this thesis to the best of my ability. I would also like to say thank you to Dr Christopher Yates who kept me sane in the lab whilst trying to analyse 300 samples a week on top of my MScR experiment and his continued support and late night “quick question?” I would also like to thank the DOMAINE team in Conwy that aided my sample collection. I finally would like to give a massive thankyou to my amazing fiancée Ben, who really would not have made this thesis possible without the continued support and cups of tea whilst I was angrily trying to work out why Matlab wasn’t working !! I really couldn’t have done it without you all.

Author's declaration:

I declare that the work in this dissertation was carried out in accordance with the requirements of the University's *Regulations and Code of Practice for Research Degree Programmes* and that it has not been submitted for any other academic award. Except where indicated by specific reference in the text, the work is the candidate's own work. Work done in collaboration with, or with the assistance of, others, is indicated as such. Any views expressed in the dissertation are those of the author.

SIGNED: ..... DATE:.....

Contents

List of Tables

List of Equations

List of Figures

Glossary

- DOM: Dissolved Organic Matter
- POM: Particulate Organic Matter
- DOC: Dissolved Organic Carbon
- DIC: Dissolve Inorganic Carbon
- POC: Particulate Organic Matter
- HMW: High Molecular Weight
- LMW: Low Molecular Weight
- TDP: Total Dissolved Phosphate
- PP: Particulate Phosphate
- DOP: Dissolved Organic Phosphate
- TDN: Total Dissolved Nitrogen
- PON: Particulate Organic Nitrogen
- TON: Total Oxidisable Nitrogen
- DON: Dissolved Organic Nitrogen
- DNRA: dissimilatory nitrate reduction to ammonia
- CDOM: Chromophoric Dissolved Organic matter
- FDOM: Fluorescent Dissolved Organic matter
- EEM: Excitation Emission Matrix
- RU: Raman Units
- S_r: Slope Ratio
- LOD: Limit of Detection
- UF: Unfiltered
- F: Filtered

1. Introduction

DOM can be found in almost all aquatic waters and plays a vital role in nutrient cycling within river systems. It can either be heterotrophic (produced within the river catchment) or autotrophic (produced in situ via microbial and or algal processing or photodegradation). A large portion of DOM is made up of CDOM, this plays an integral part in DOM transformation as light especially in the UV region can break down usually inaccessible HWM compounds into LMW compounds that are easily metabolised by biota. Photodegradation can also have an impact upon inorganic nutrient cycling in river systems for example nitrate can undergo photomineralisation to produce nitrite and an oxygen radical.

CDOM can act as a "sun screen" absorbing harmful UV light that could damage algal and microbial cells inhibiting nutrient cycling. But in large concentrations it can completely absorb light inhibiting photosynthesis. A sub fraction of CDOM is fluorescent DOM (FDOM) that will fluoresce under certain wavelengths of light. FDOM provides valuable insights into the origin and transformations of DOM; Peak T for instance can be used as a proxy to estimate the metabolism of biota and or the amount of sewage present in a sample. Peaks A & C are indicators of the amount of humic like (generally HMW compounds) present (see Figure 1) . The ratios of these peaks can also indicate the freshness of DOM.

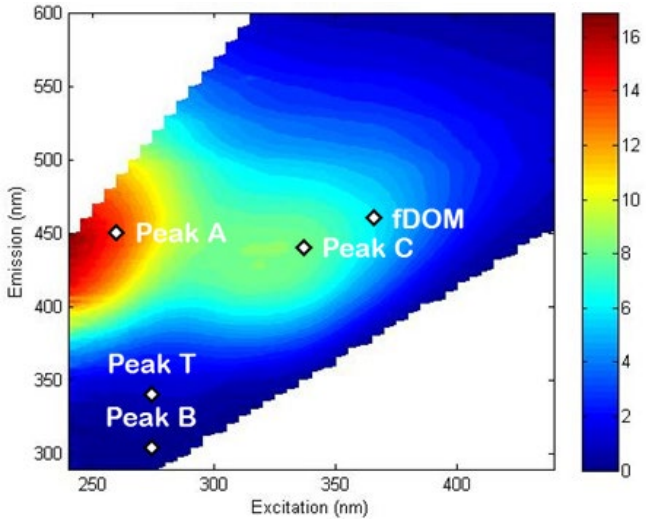

Figure 1: The position of fluorescent peaks in soil leachate (U.S. Geological Survey, 2016)

Recent literature has only really highlighted the implications of photodegradation in areas with high CDOM such as peat systems due to their high concentrations of plant material, but there is a distinct lack of research in areas with low CDOM such as groundwater fed systems and even less so during autumn and winter. This study is aiming to bridge that gap by comparing the effects of photodegradation on sites in areas of high and low CDOM concentrations between autumn and winter.

2. Literature review

2.1. Dissolved Organic Matter (DOM)

DOM is a ubiquitous component of natural waters, operationally defined as comprising any organic compound passing through a 0.45 µm filter (Evans et al., 2005). DOM is the bulk term for the combined fractions of dissolved organic carbon (DOC), dissolved organic nitrogen (DON) and dissolved organic phosphorus (DOP). DOM is one of the largest biologically active carbon reservoirs and (Cole et al., 2007) has estimated that global inland waters receiving approximately 1.9 Pg C annually from the terrestrial landscape, of which about 0.2 Pg C is buried in aquatic sediments, 0.8 Pg C is returned to the atmosphere and the remaining 0.9 Pg C is delivered to the oceans via streams, rivers, lakes and transitional waters.

In the last 2 decades researchers have used the terms humic acids, fulvic acids and humin to describe the DOM pool according to their solubility. However, with such broad definitions recent trends have shifted to using molecular weight as a classification system. For example HMW fractions have been found to have higher concentrations of aromatic, carboxyl-rich humic substances and defined as >1000 Da (Daltons), (Fagerberg et al., 2009; Simjouw et al., 2005). Whereas LMW fractions had typically high concentrations of smaller, more labile compounds such as aliphatic, sugars and amino acids (Woods et al., 2010) and were <1000Da (Fagerberg et al., 2009; Simjouw et al., 2005)

Much of the recycling of DOM is dependent on its composition, this is due to the highly heterogenous nature of DOM consisting of a complex mixture of organic functional groups and is received from multiple sources (Hedges, 1992; Miller and Zepp, 1995). Consequently, DOM has multiple pathways, it may be transformed through burial to sediments (Hedges, 1992), in the food web via the microbial loop (Findlay and Sinsabaugh, 2003) or be mineralized to carbon dioxide via photochemical and microbial oxidation (Mopper et al., 2015). It also influences the solubility and bioavailability of organic pollutants and heavy metals (Findlay and Sinsabaugh, 2003). DOM character is influenced by a variety of factors due to its surrounding landscape such as soil source and or vegetation and the biotic and

abiotic processing in stream and soil (Watts et al., 2001), this could be changed in the future by a climate change (Ritson et al., 2014).

Major sources of DOM in freshwaters can be categorised into 2 groups, depending on whether the sources are located within the water body (autochthonous) or the wider catchment (allochthonous). Autochthonous DOM is derived by in situ production and/or removal from the water column or sediments via microbial processes and has been suggested to produce a high proportion of LMW compounds (Chróst and Faust, 1983; Yates et al., 2016) . Terrigenous DOM (allochthonous) from natural organic matter (NOM) sources in areas with minimal anthropogenic inputs are thought to be comprised of a high proportion of HMW compounds derived from the microbial breakdown of dead organic matter compared to anthropogenically impacted catchments (Seitzinger and Sanders, 1997; Zou et al., 2004), which are then delivered to waters via hydrological flow pathways (Harjung et al., 2016; Yates et al., 2016).

In anthropogenically impacted catchments supporting intensive animal agriculture and discharging treated sewage effluent to water bodies, the allochthonous DOM is likely to have a greater proportion of LMW compounds derived from microbial processing of organic wastes. Finally, a further allochthonous source of DOM in waters is from the exchange of dust and gaseous phase substances with the atmosphere (Benner and Kaiser, 2011; Yang et al., 2016).

Some components of DOM are coloured and are referred to as chromophoric dissolved organic matter (CDOM). These originate from the decomposition of plant matter by microorganisms within the aquatic environment, as well as through the transport of partially-transformed organic material from river reaches upstream and the surrounding terrestrial environment (Jaffé et al., 2008; Yamashita and Tanoue, 2008). CDOM can generally be separated into two major classes: HMW compounds and protein-like substances with a lower molecular weight (Coble, 1996; Yamashita and Tanoue, 2008). The HMW substances are complex mixtures of aromatic and aliphatic compounds derived from the partial decay of dead organic matter, while protein-like substances such as amino acids can be are produced either in situ (autochthonous) such as those produced as a result of cell

multiplication and metabolic processing (Coble et al., 2014) or within the catchment (allochthonous) (Su et al., 2015) such as those contained in human and animal wastes.

In high concentrations CDOM may inhibit the light available for primary production for plants rooted within the water body, and the epilithic algal community growing on the sediment substrate. However CDOM can also reduce the amount of damaging UV-B radiation whilst allowing UVA and photosynthetically active radiation to be much more efficiently transmitted into the water (Mei et al., 2010; Walsh et al., 2003; Zepp et al., 2003).

The rate at which different DOM compounds are broken down is highly variable within water bodies, for example large aromatic structures, are broken down slowly by microorganisms, whereas leachates generally containing LMW compounds from living vegetation and fresh litter have a larger proportion of LMW carbohydrates, which are more readily transformed (Marschner and Kalbitz, 2003).

A large proportion of DOM in aquatic ecosystems is derived from terrestrial sources (Houser *et al.,* 2005; Rasilo *et al.,* 2015). Consequently, processes controlling DOM composition and concentration in fluvial systems are largely determined by conditions in the catchment area (Houser *et al.,* 2005). Thus, DOM concentration and chemistry in any water body, as sampled at any point in time and space, will reflect the combined influences of terrestrial biogeochemical cycling of organic matter and the discharge regime of the catchment, which is influenced by factors such as the hydrogeology of the catchment, and climate including precipitation and temperature.

Low order streams are the first important link in the transport of DOM from their soil sources to the aquatic environment, because they integrate chemical compounds from groundwater, surrounding landscape and in-stream processes (Mosher et al., 2015). When anthropogenic disturbances alter and or block flow pathways connecting terrestrial sources to the river and hence altering the natural state (Grimm et al., 2008). They can impact the quality of DOM transported to inland waters, because different carbon pools are activated and transported under baseflow versus overland and near surface quick flow conditions (Seifert et al., 2016).

Vegetation and land use will also impact on DOM composition, for example lowland catchments in the UK have a higher proportion of intensively farmed landscapes, larger population densities and a high proportion of flow migrating along through flow and base flow pathways linking source to stream as opposed to upland systems (Yates et al., 2016). These differing characteristics of the NOM and anthropogenically derived DOM sources in each catchment will then impact on the composite DOM character instream. The position within the stream network will also be important, as DOM processing will increase as material moves from the headwaters to lower reaches of the water body.

In upland catchments such as peat systems that are water-saturated, organic rich soils have been recognised as a major source of DOM in surface waters (Billett et al., 2006; Hope et al., 1997) although forests, heath and moorlands with non-saturated organic soils are also significant sources (Aitkenhead and McDowell, 2000; Berg et al., 2012). Moving away from upland headwaters there are increasing inputs of DOM from agricultural and urban sources (Hope et al., 1997) including livestock wastes and the discharge of organic-rich sewage effluent. However, in less populated upland headwaters with natural or semi-natural vegetation rather than agriculture as the dominant land cover, the dominant source of DOC is likely to be from terrestrial NOM stores.

Large increases in dissolved organic carbon (DOC) concentrations have been observed in UK surface waters (Evans et al., 2005; Freeman et al., 2001; Worrall et al., 2004) as well as parts of Northern Europe and North America (Monteith et al., 2007), attributed by a number of authors to a combination of climate change(Ritson et al., 2014; Zepp et al., 2003), recovery of systems from acidification (Monteith et al., 2007; Sawicka et al., 2017), and land use change (Fenner et al., 2009; Hope et al., 1997).

These observations have raised concerns over increasing water treatment costs (Ritson et al., 2014) as DOC is primarily removed to minimize the formation of disinfection by-products (DBPs) such as trihalomethanes (THMs) which are produced via the reactions between dissolved organic matter (DOM) and disinfectants such as chlorine (Richardson et al., 2007). DBPs are of a particular concern as they may have an impact on human health (Richardson et al., 2007). Current UK limits are that the total trihalomethane (THM) concentration should not exceed 100 µg/l and requires DBP formation to be minimised (DWI, 2017).

2.2. CDOM and the role of photodegradation in its transformations.

Depending on its catchment character photodegradation can be one of the largest pathways for removal and or transformation of DOM in aquatic systems (Mopper et al., 2015). For example, photodegradation can impact upon the breakdown of HMW compounds to LMW compounds that are more readily utilised by heterotrophs. Complete photodegradation of dissolved organic carbon (DOC) to inorganic forms (carbon dioxide (CO_2), and carbon monoxide (CO)) and photochemically-mediated alterations in DOM composition play a significant role in global carbon cycling (Helms et al., 2008; Mopper et al., 2015, 1991; Stubbins et al., 2011). For instance, exposure to sunlight, particularly ultra-violet (UV) radiation, can affect the chemical composition and biological availability of DOM by increasing or decreasing the rate of biodegradation of HMW compounds instream (Helms et al., 2014).

Photodegradation usually occurs mostly in the UV region, as it has a higher frequency than infrared and visible radiation which means more energy is transferred when a photon interacts with a molecule. However, the radiation received from the sun contains varying wavelengths of energy, but only a portion of this spectrum reaches the Earth's surface due to absorbance and reflectance by the Earth's atmosphere.

Structural changes in DOM caused by light exposure have several implications for processes in the water column, they can be caused by direct or indirect photodegradation. Direct photodegradation occurs when sunlight, especially UV radiation, interacts with molecules and causes bonds within the molecule to break, to form smaller molecules and/or produce radicals. For example, nitrate (NO_3^-) is a major precursor of the hydroxyl radical (OH*) which can react quickly with almost any organic compound (Haag and Hoigné, 1985). NO_3^- efficiently absorbs Ultraviolet B radiation (UVB: 280–315 nm) to produce free radicals such as an oxygen radical (O^*) (Equation 1), which is one of the most reactive species in natural waters.

$$NO_3^- + hv \rightarrow NO_2^- + O^*$$

Equation 1: Direct photodegradation of nitrate under UVB radiation

Indirect photodegradation is caused by sunlight that is absorbed by photoactive compounds called photosensitisers, such as nitrate (NO_3^-) nitrite (NO_2^-), hydrogen peroxide (H_2O_2), ferric iron (Fe^{3+}) (Equation 2) and CDOM. When photosensitisers interact with a photon they produce reactive species such as the hydroxyl radical (OH*), singlet oxygen (O_2^-), reactive oxygen species (ROS) and CDOM triplet states ($CDOM^3$) (see Figure 2) which can induce transformations in other molecules (Vione *et al.,* 2014).

$$FeOH^{2+} + h\nu \rightarrow Fe^{2+} + OH^*$$

Equation 2: Ferric Iron as a photosensitiser (Neyens and Baeyens, 2003).

Both Iron and H_2O_2 are common constituents of oxygenated natural waters (Voelker and Sulzberger, 1996). Fe(III), which exists in the form of complexes with DOM is photochemically reduced to Fe(II) under sunlight irradiation (Photo Fenton Equation 3) (Voelker et al., 1997).

$$Fe\ (III)\text{-}(DOM) + h\nu \rightarrow Fe\ (II)\text{-}DOM + DOM^*$$

Equation 3: Ferric Iron as a photosensitiser (Nakatani et al., 2007).

The reaction of Fe(II) with hydrogen peroxide (also called Fenton's reaction Equation 4) is therefore of interest in a variety of natural water systems as it also generates hydroxyl radicals that can break down DOM (Nakatani et al., 2007; Voelker and Sulzberger, 1996).

$$Fe\ (II) + H_2O_2 \rightarrow Fe\ (III) + OH^* + OH^-$$

Equation 4: Fenton reaction (Nakatani et al., 2007).

Hydrogen peroxide (H_2O_2) is a universal component of the hydrosphere. It can be found in most water bodies including rain and can be excreted via microbial processes and is generally produced in higher quantities from the breakdown of HMW DOM (Kim and Portis, 2004). In low concentrations, it can aid in disinfection and breaking down organic matter especially under UV radiation. H_2O_2 readily dissociates into hydroxyl radicals (see Equation 5) and is used by some water companies in the treatment of sewage (Ksibi, 2006). In high concentrations, it can be toxic to aquatic life and living cells.

$$H_2O_2 + \ hv\ (\leq 360\ nm) \rightarrow \ \ 2OH^*O$$

Equation 5: Hydrogen peroxide photodegradation

Surface concentrations of H_2O_2 typically vary in natural waters from 0.02 to 0.32 µM in rivers (Cooper and Zika, 1983). However, H_2O_2 concentrations in rain water have been reported up to approximately 200 µM, although concentrations are usually less than 50 µM (Willey et al., 1996). Rain contains higher levels of H_2O_2 due to the dissolution of gas phase H_2O_2 being produced in the upper atmosphere (Sakugawa *et al.,* 1990).

Concentrations of H_2O_2 in surface waters are usually higher in summer than in winter, due to more intense solar irradiation causing formation of H_2O_2 gas in the upper atmosphere, dissolving into water vapour and falling as rain before entering the aquatic environment via various flow pathways. In aquatic environments the increased product of reactions involving sunlight, DOM/CDOM with dissolved oxygen under natural sunlight (Equation 6) (Mostofa and Sakugawa, 2009; Peake and Mosley, 2004) also has an impact on the concentration of H_2O_2. $CDOM^3$ can be the main precursor of singlet molecular oxygen that is photo-produced in surface waters, followed closely by nitrate, but may also react directly with various substances present in natural waters (Wenk *et al.,* 2013).

$$CDOM + hv \rightarrow CDOM^*$$

$$CDOM^* \rightarrow CDOM^3$$

$$CDOM^* + O_2 \rightarrow CDOM^+ + O_2^-$$

$$2O_2^- + 2H^+ \rightarrow H_2O_2 + O_2$$

Equation 6: Hydrogen peroxide generation from CDOM (Peake and Mosley, 2004).

$CDOM^3$ has absorbed photons of light and excited its outer electrons from their ground state (S_0) to a highly reactive triplet state (S_3) (see Figure 1: CDOM Triplet states). Thus, once the triplet state has been reached, it has enough time (typically in the order of microseconds in solution) to undergo bimolecular reactions and cause the breakdown of surrounding molecules, when compared to singlet excited states that are active for only nanoseconds (Wenk *et al.,* 2013).

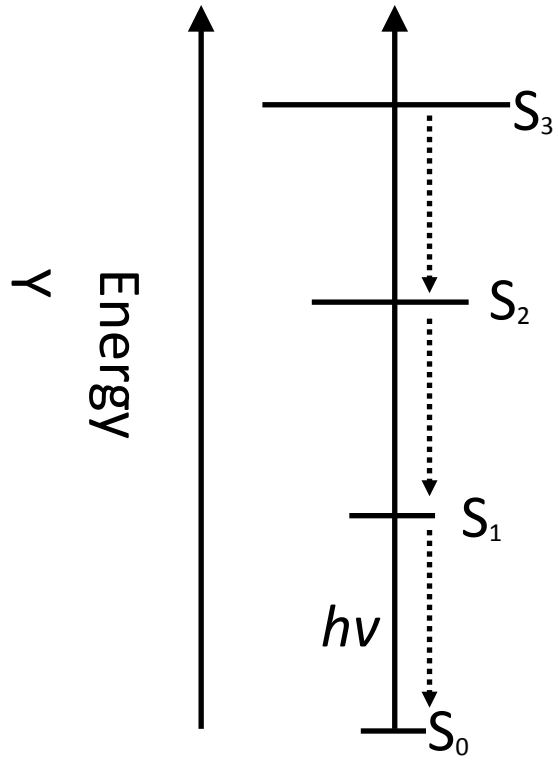

Figure 2: CDOM Triplet states

2.3. Fluorescent DOM (FDOM)

Fluorescence measurements can provide information on the likely composition of chromophoric (CDOM) and fluorescent DOM (FDOM) and can also be used as an indicator of the origin of the DOM as it will have a unique optical finger print. Fluorescence occurs when a molecule interacts with a wavelength of light, an electron is excited and promoted to an unoccupied orbital. The energy difference between the ground (S_0) and excited singlet states (S_1, S_2 or higher) determines the wavelengths at which light is absorbed when the electron then relaxes down to its original orbital and energy is released as light (fluorescence) (Matarazzo and Hudson, 2015).

DOM is difficult to analyse in high resolution, however in all natural waters, a fraction of the total dissolved organic matter pool that absorbs light (CDOM) also fluoresces in the UV and visible regions of the spectrum (Murphy et al., 2010). Fluorescence techniques have become increasingly popular due to their ability to attribute different peaks in the spectral response of DOM to types of compounds or sources of organic matter (Bridgeman et al., 2011) (see Table 1).

Table 1: Common labels for Identified regions of fluorescence peaks in an excitation emission spectrum of aquatic DOM (Oregon Water Science Centre, 2013).

Fluorescence Peak	Excitation/ Emission (nm)	Description	Reference
B	270/306	Tyrosine like-protein like, associated with autochthonous organic matter	(Coble, 2007, 1996)
T	270/340	Tryptophan-like, protein like, associated with phytoplankton productivity and has been associated with wastewater	(Coble, 2007; Goldman *et al.,* 2012; Stedmon *et al.,* 2003).
A	260/450	Humic-like	(Coble, 2007; Stedmon *et al.,* 2003).
M	300/390	Humic like, possibly marine, possible microbial reprocessing, more labile humic acids	(Coble, 2007; Stedmon *et al.,* 2003).
C	340/440	Humic-like, terrestrial, wide spread	(Coble, 2007; Stedmon *et al.,* 2003).
Fluorescence Index (FI)	370→470/ 520	Higher values indicate algal (microbial) vs. terrestrial derived DOC, values range from 1.3-1.9	(McKnight *et al.,* 2001).
FDOM	370/460	In-Situ fluorescence that is highly correlated to DOC (dissolved organic matter) concentrations	(Downing *et al.,* 2009; Spencer *et al.,* 2007).

Fluorescence can generally be divided into two groups, a protein-like and humic-like fluorescence. Within the protein-like group three fluorescent amino acids (tryptophan, tyrosine and phenylalanine) are indicative of proteins and peptides. The fluorescence of

these specific amino acids is due to the presence of an indole group (a fused ring heterocycle containing both a benzene ring and a heterocyclic aromatic ring in which a nitrogen atom occurs as part of a ring (Hudson et al., 2007).

Tyrosine (Peak B) is known to be responsible for the phenylalanine or tyrosine fluorescence intensity of proteins due to the fact that phenylalanine fluorescence is only observed only in the absence of tyrosine (Yamashita and Tanoue, 2003). The fluorophore associated with tyrosine is a simple phenol and tyrosine exhibits behaviour like that of phenols. However tyrosine fluorescence is almost completely quenched when it occurs within proteins, being only about 10-50% as intense in the protein form compared to free tyrosine (Wolfbeis, 1985).

Tryptophan-like fluorescence (Peak T) occurs in the low UV region and correlates strongly with an increasing bacterial population, but is dependent on microbial metabolic activity (Fox et al., 2017). As tryptophan is an essential amino acid, necessary for protein formation during growth and other metabolic pathways, it will be produced as a result of cell multiplication and metabolic processing (Coble et al., 2014). However, it should be noted that tryptophan is not unique in displaying these characteristics. Recent studies have demonstrated that other non-protein like compounds also fluoresce in the low-UV regions (Coble, 2007; Helms et al., 2014; Spencer et al., 2007), for example undegraded polyphenols are known to be present in vascular plant leachates that fluoresce in this region (Donham et al., 2014).

The occurrence of Peak M in its ‘‘pure’’ form correlates with other indicators of biological activity, such as chlorophyll concentration and high ammonium concentrations (Coble, 1996). It has been known that Peak M is originated from marine humic like substances but recently it has also been reported that Peak M is associated with microbe origin and the strong intensity of Peak M has been observed from sewage treatment water (Stedmon et al., 2007; Yamashita and Tanoue, 2003).

Although Peaks C and A are both commonly associated with humic-like material, they have been reported to vary independently, thus suggesting they originate from different pools of DOM (Kothawala et al., 2012). The humic like fluorescence is associated with Peaks A & C: The compounds associated with terrestrially derived FDOM are known to be stable higher

molecular weight aromatic compounds, generally considered non-labile (Cooper et al., 2016), with a shift to longer wavelengths of the humic-like peaks in freshwater samples, because terrestrial humic substances are more aromatic than marine humic substances (Benner, 2003). There is also recent evidence to suggest that Peak C is also produced *in situ* during the exponential stage of bacterial growth curves, likely to be produced via microbial metabolic pathways during microbial growth, or derived from metabolic by-products (Fox et al., 2017). This has also been supported by recent findings by (Kallenbach et al., 2016) showing the production of extracellular humic material by bacteria within soil organic matter.

The fluorescence index (FI) has been used in a wide range of studies to distinguish DOM derived from terrestrial sources (degraded plant and soil organic matter) that have lower values verses microbial sources (extracellular release and leachate from bacteria and algae) that have higher values (Hansen et al., 2016; Khamis et al., 2017). Samples from the Antarctic lakes had the high FI values (1.7–2.0), corresponding to DOM derived from a microbial source associated predominantly with phytoplankton productivity. In contrast, North American river samples had a lower FI (1.3–1.4), resulting from their origins in plant litter and soils. (Gabor et al., 2014) .

Peak ratios of C:T and A:T can be an indication of the amount of humic-like (recalcitrant) vs. freshly produced (labile) FDOM in a sample, with higher values indicating a higher proportion of degraded material. (Baker et al., 2008; Fox et al., 2017; Hansen et al., 2016). (Hansen et al., 2016) has suggested that suggest that if C:T is greater than approximately 5.0 and A:T is greater than 4.5 in natural waters, there is likely a greater relative contribution of soil-derived DOM than plant- or algae-derived DOM. (Hansen et al., 2016) has suggested that a C:A ratio below 0.6 can be associated with terrestrial soil-derived DOM.

The ratio of Peaks C to M was originally used to distinguish DOM derived from terrestrial vs. marine environments. Increased C:M ratio of all sources, resulting in overlapping values, suggesting that this fluorescence ratio is less promising at discriminating DOM origin in cases where both biological and photolytic processing is occurring (Hansen et al., 2016).

2.4. Dissolved Organic Nitrogen (DON)

Nitrogen is a naturally occurring element found in most natural systems. It is essential for the formation of amino acids and proteins and DNA in all biota. The natural source of nitrogen is the atmosphere, where N_2 gas comprises 70% of the system. However, this is biologically unavailable to all but N-fixing bacteria, including cyanobacteria and rhizobia in waters and soils. Following discovery of the Haber-Bosch process at the beginning of the C20th, fixing this nitrogen into a bioavailable form was possible on an industrial scale, allowing the expansion and intensification of farming in many catchments (Erisman et al., 2008).

No system is closed, so export of excess N applied that is greater than crop requirements to waters has become a major problem for water bodies in intensively farmed catchments. In excess, it can stimulate biological production in both terrestrial and aquatic ecosystems, leading to detrimental effects including eutrophication, and is a contributing factor in the acidification of upland and boreal soils and waters. Nitrogen can exist in a multitude of forms in the environment, for example, a large portion of nitrogen is bound to organic maternal in the form of DON and then nitrate (NO_3^-), nitrite (NO_2^-), ammonium (NH_4^+) and ammonia (NH_3) are the inorganic forms. When these are added to the dissolved organic nitrogen and particulate organic nitrogen compound classes commonly found in water bodies, these collectively comprise the total nitrogen load (TN) in the system (Durand *et al.,* 2011)

The bioavailability of bulk, uncharacterized DON entering aquatic systems has been shown to vary depending on its source (e.g., atmospheric, run-off from forested, agricultural, and urban/suburban lands) (Berman, 1999). DON transformation is an important process in the nitrogen cycle, as this controls the relative abundance of inorganic and organic nitrogenous compounds in water bodies, and thus their bioavailability to and impact on the instream biota.

It has also been implied that DON released from the soil is less bioavailable for microorganisms than DON originating from other sources, e.g. discharged from a treatment plant. This may be due to the fact that DON from agriculture and forest areas contains aromatic compounds, while municipal wastewater DON contains primarily aliphatic compounds (Czerwionka, 2015) which are easily hydrolysed by microorganisms. There is evidence from experimental and field monitoring studies that LMW DON (amino acids,

polyamines) is directly available for plant and algal uptake. Furthermore experimental data show that both PON and HMW DON are available for microbial assimilation in both terrestrial and aquatic systems (Durand et al., 2011). Non-photodegraded DON transformation in aquatic waters can include these steps:

1. Firstly, DON is metabolised or hydrolysed to ammonium through ammonification.
   1.1. $R–NH_2 + H_2O \rightarrow NH_3 + R\text{-}OH + Energy$
2. NH_4^+/NH_3 is transformed into nitrite, then into nitrate by nitrification.
   2.1. Nitrification is a two-step process involving two distinct microbial communities. Ammonia oxidizers (Nitrosomonas) transform ammonia to nitrite:
      2.1.1. $2NH_4^+ + 3O_2 \rightarrow 2NO_2^- + 2H_2O + 4H^+$
   2.2. Nitrite oxidizers (Nitrobacter species) use nitrite and generate nitrate (Raimonet et al., 2015).
      2.2.1. $2NO_2^- + O_2 \rightarrow 2NO_3^-$
3. Anaerobic ammonia oxidation (Anammox) uses ammonium and nitrite which act as electron donor and accepter, respectively, to yield nitrogen gas (Strous et al., 1997).
   3.1. $NH_4^+ + NO_2^- \rightarrow N_2 + 2H_2O$

Interactions of UV radiation and Dissolved Organic N (DON) provide a pathway for the conversion of HMW DON compounds to LMW DON compounds and inorganic N compounds that are more easily assimilated by aquatic microorganisms, including NH_4^+/NH_3, NO_2, urea (CH_4N_2O) and a range of LMW amino acids (Bronk et al., 2010; Zepp et al., 2003). This can impact upon the nitrogen cycle in aquatic ecosystems, increasing the rate of biotic uptake of N from the water column.

Photochemical reactions can also incorporate bioavailable N into biologically recalcitrant forms (Kieber et al., 1997; Reitner et al., 2002). The pathway of photochemical reactions (i.e., the production vs. the incorporation of bioavailable N) depends, in part, on the concentration of reactants. For example, photochemistry incorporates NH_4^+ into DON at high NH_4^+ concentrations) but produces NH_4^+ from DON at low NH_4^+ concentrations (Koopmans and Bronk, 2002; Tarr et al., 2001; Vähätalo et al., 2000).

2.5. Dissolved Organic Phosphorus (DOP)

Phosphorus is essential for aquatic life, as it is part of sugar-phosphate molecule that binds the DNA structure and cell membrane. It is derived from natural and anthropogenic sources. Natural sources include geological deposits, and, unlike nitrogen, it has no atmospheric phase, unless bound to dust particles eroded from agricultural land (George et al., 2018; Johnes and Hodgkinson, 1998). It has long been established that phosphorus, in excess, may significantly impair water quality by accelerating the growth of algae and aquatic plants. The specific bioavailability of DOP to aquatic organisms has also been reported for both marine (Björkman and Karl, 1994) and freshwater ecosystems (Bentzen et al., 1992; Berman, 1988).

Natural (or background) sources of P entering rivers are important where anthropogenic pressures are low/absent and can include the natural weathering and dissolution of geological parent materials, aeolian transport and deposition of dust from P rich soils (Holtan *et al.,* 1988), riparian vegetation (Meyer and Likens, 1979) and river bank erosion (Walling *et al.,* 2008). Anthropogenic phosphorus inputs are delivered to water bodies from point sources such as sewage treatment works (STWs) and septic tanks (Evans et al., 2004; Johnes and Hodgkinson, 1998) and diffuse sources such as agriculture (Heathwaite *et al.,* 1996). Septic tank inputs can either be a point source or discharge to the soil/unsaturated zone and are flushed to the streams during high rainfall events (May *et al.,* 2012).

Many authors have argued that in rural catchments point sources are not always the most significant contributors of phosphorus delivered to aquatic waters, as increasing phosphorus concentrations in many UK surface waters draining agricultural catchments, cannot be explained by export from point sources alone(Heathwaite et al., 1996; Johnes, 1996; Johnes and Hodgkinson, 1998; Muscutt and Withers, 1996).

Primary production in many natural water bodies is often limited by the availability of phosphorus (Edmondson and Vollenweider, 1970). Primary producers can easily utilize inorganic P forms such as orthophosphate (PO_4^{3-}), phosphorus pentoxide (P_2O_5) and a range of polyphosphate compounds. The research literature also indicates the importance of DOP as a nutrient source for microbiological and algal production, as a large fraction of DOP in

natural waters is amenable by hydrolysis by microbial populations, phytoplankton, and or zooplankton (Cotner and Wetzel, 1992). These organic forms are generally of biological origin and include but are not limited to nucleic acids, polyphosphates, phosphorus esters and phosphonates (Kolowith *et al.,* 2001).

In some cases, DOP can have similar and or greater concentrations than particulate and inorganic phosphorus, this is especially so in upland and semi-natural catchments where inorganic P sources are limited (Yates *et al.,* 2016) and highlights the importance of DOP as a bioavailable nutrient fraction in these waters. It has also been suggested that phosphate binds strongly to humic substances, particularly in the presence of high concentrations of ferric iron (Francko and Heath, 1979; Haan et al., 1990; JONES et al., 1988). In this way microbial access to phosphorus is restricted (Wetzel and Stewart, 1981).

As previously mentioned the majority of DOP is not readily available to microbes, as it cannot be directly accessed through the cell membrane; hence these compounds must be remineralized to bioavailable phosphate prior to uptake (Björkman and Karl, 2003; Cembella et al., 1982). The utilization of DOP is associated with a number of enzymes, among which phosphatases produced by algae in relatively large quantities correlated with their primary production (Babic et al., 2013). Phosphatases represent inducible catabolic ectoenzymes and their expression is generally regulated by the external concentration of inorganic phosphate (Hoppe, 2003). After the early phase of enzyme synthesis, phosphatases accumulate in the periplasmic space and at the later stage they are released outside the cell (Pandey, 2006).

Some DOP can absorb solar energy to produce labile LMW components (Lesueur et al., 2005) such as phosphonates that can be degraded indirectly by reactive oxygen species, such as hydroxyl radicals and superoxide oxygen radical (Liu et al., 2017). As mentioned previously phosphate binds readily to iron and the cleavage of the phosphate-iron-DOM complex is catalysed by solar radiation through the photochemical reduction of the iron to its ferrous form, releasing phosphate which then facilitates microbial utilization (Cotner and Heath, 1990; Francko and Heath, 1982).

2.6. Aims and objectives

Current expectations are that the UK climate will change in the future with higher temperatures, altered precipitation patterns and increased frequency and severity of extreme weather events (Jenkins et al., 2009). This will therefore impact upon the storage, processing and transport of DOM from terrestrial sources to the sea along aquatic pathways (Jones et al., 2016). Changes in climate and/or climate variability have already had significant effects on carbon dynamics in terrestrial ecosystems, in that greenness of vegetation, length of the growing season and biomass have increased in middle and northern latitudes of the Northern Hemisphere (Monteith et al., 2007; Myneni et al., 2001, 1997).

Any environmental change acting to destabilise the DOM pool has ensuing implications for in-stream quality and hence biological processes (Billett *et al.,* 2006). For example, increased levels of UV through ozone depletion (until ozone levels recover) will potentially mean greater bioavailability of DOC as it is the recalcitrant, aromatic compounds that are most prone to photo-oxidation (Zepp et al., 2007). However, increases in DOC concentrations especially from organic rich soils infer higher CDOM concentrations that can also inhibit photodegradation. UV exposure also enhances the decomposition of Particulate Organic C (POC) in freshwaters (Anesio et al., 1999), with implications for lowland catchments with generally higher concentrations of particulate matter exported to water bodies from their catchments.

The research of the last two decades has really highlighted the importance of DOM in biogeochemical cycles and how it plays a crucial part in nutrient transport and transformation in aquatic systems. There is a large body of research emerging on how photodegradation impacts DOM character in upland systems throughout the world. However, little has been done on how lowland catchments are impacted by photodegradation and even less so during the autumn and winter months. It is therefore essential to have a clear understanding of how photo degradation affects DOM relative to its catchment character to help understand how a changing climate might alter its composition and processing.

Therefore, this study focused on identifying sites with the greatest variation in hydrology and DOM composition in both upland and lowland catchments to assess the effects of photodegradation upon DOM. The samples collected were incubated for a week, whilst daily measurements were taken to look at the bulk transformation of DOM via photodegradation. Based on previous work it was hypothesised that:

a) DOM composition would alter between autumn and winter due to changes in hydrology throughout the year?
b) That photodegradation is still a critical pathway in the transformation of DOM in autumn and winter?
c) LMW compounds produced as a result of photodegradation would be utilised by biota present in the sample?

3. Site description

The resources available made selecting the Conwy Catchment in North Wales and the Hampshire Avon (HA) catchment in the South of England a good choice as an example of upland and lowland catchment in the UK (Figure 3). This is because high resolution nutrient sampling and analysis undertaken by the NERC DOMAINE programme (Characterising the Nature, Origins and Ecological Significance of Dissolved Organic Matter in Freshwater Ecosystems (NE/K010689/1) provided a data-rich platform for multiple sites in these catchments, within which context this study could be set. The samples collected, and experiments undertaken in this study were generated from October 2015 to February 2017.

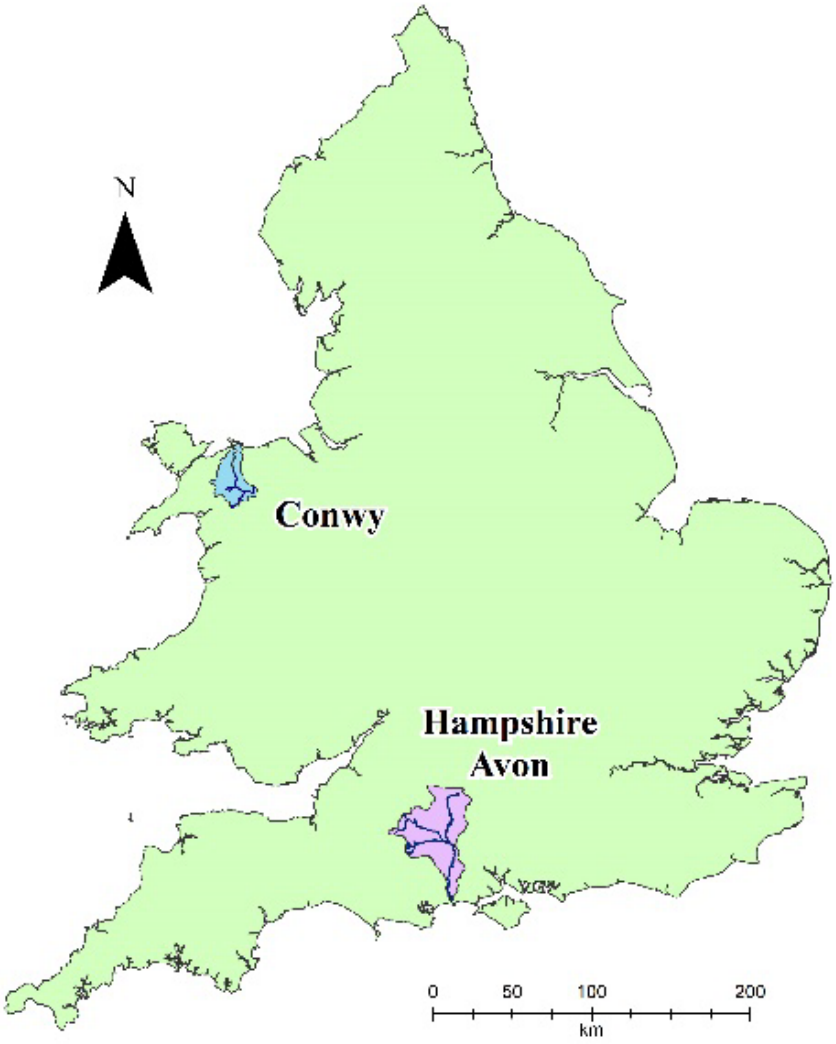

Figure 3: Map of the UK highlighting the Conwy & HA catchments (Yates, 2016)

The Conwy catchment is approximately 680 km^2 and is in North Wales (UK) with approximately half the catchment lying 300 m above sea level. The underlying geology is mainly comprised of sedimentary rocks, with high elevations comprising of igneous based rock types. Over a quarter of the Conwy catchment is covered by acid grassland, improved grassland dominates the eastern side of the catchment. This is then closely followed by bog dominating the south west of the catchment (Figure 3). Agricultural land use is largely low-density rough sheep grazing in the uplands, with more intensive sheep and cattle grazing on improved grassland in the lowlands of the catchment (Cooper et al., 2006; Yates et al., 2018). Due to the low population density any industrial activity is very minimal (Evans et al., 2006) and receives approximately 2042mm of rainfall annually.

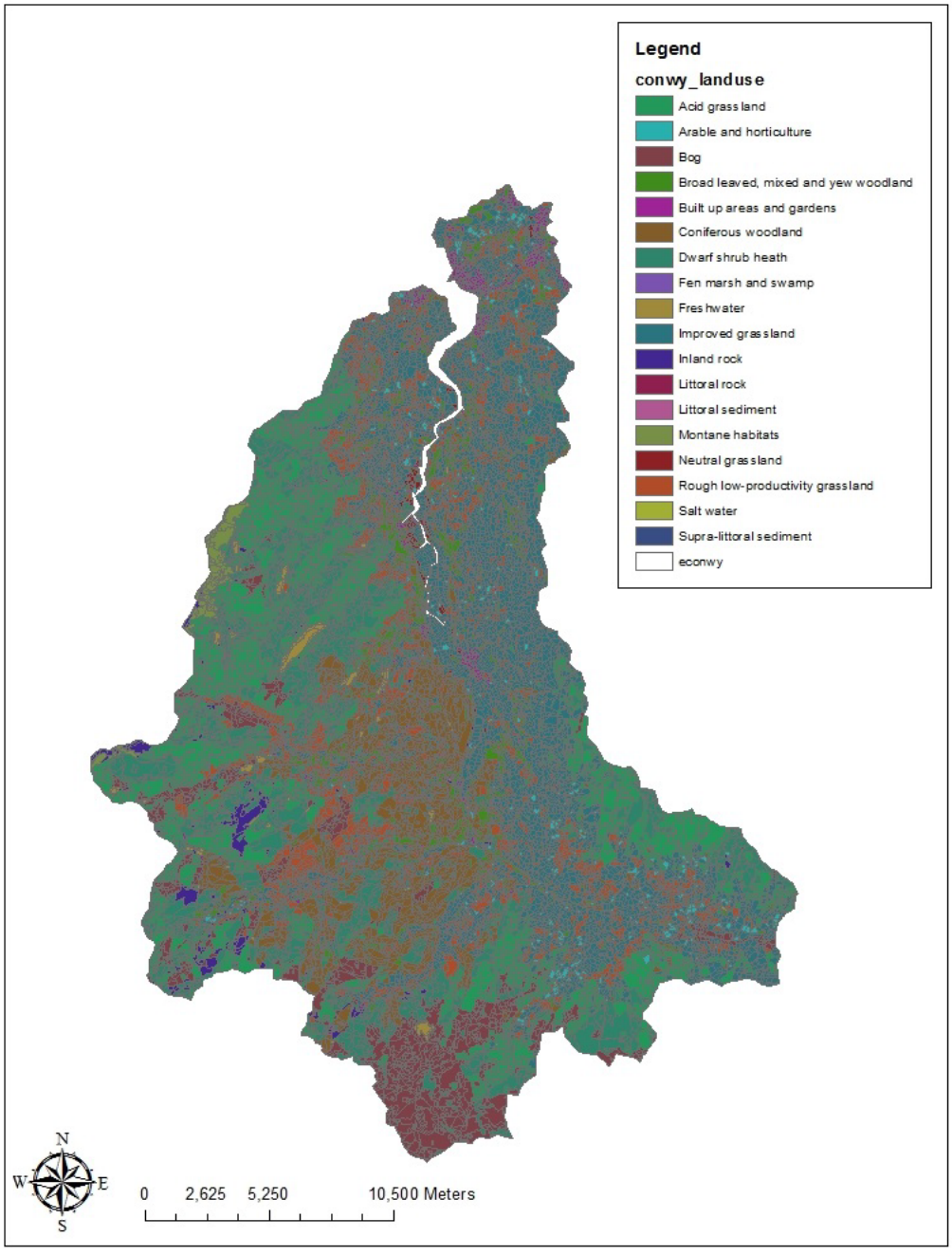

Figure 4: Land use summary of Conwy Catchment (Yates, 2016).

The Hampshire Avon is approximately 1700km^2 (Yates and Johnes, 2013) and although it is mostly underlain by chalk it encompasses geology ranging in age from the Late Jurassic Kimmeridge Clay Formation to the Palaeogene Barton 4 Group (Allen et al., 2014). Hence, streams draining the Chalk landscape are groundwater fed, which produces a slow response times to rainfall and or storm events (Berrie, 1992). The soils surrounding the Wylye

comprise of mostly calcareous brown earths, with a high infiltration capacity (base flow index 0.98) (Yates and Johnes, 2013) and receives approximately 832mm of rainfall annually.

The catchment is mainly rural with arable horticulture as the dominant land use type followed closely by calcareous grasslands (stemming from the rich chalk geology). These rivers tend to have distinctive aquatic plants (Bowes et al., 2005) dominated by *Ranunculus penicillatus* which is listed as a high ecological significance and is list as a priority habitat under the EC Habitats Directive (Council of European Communities, 1992). The Hampshire Avon contains several rivers and tributaries, but this study only focuses on the river Wylye and Sem.

A high proportion of the catchment has intensive farming as its major land use and so there are also concerns about nutrient leaching (particularly nitrate) to the aquifer (Limbrick, 2003) and diffuse inputs of nitrogen and phosphorus to the chalk streams generally (Bowes *et al.,* 2005; Prior and Johnes, 2002; Evans and Johnes, 2004) and specifically in the Hampshire Avon and its key tributary, the Wylye(Lloyd et al., 2019; Yates and Johnes, 2013). Septic tanks are in use throughout the catchment and the Wyle receives discharge from approximately 158 septic tanks under effluent discharge licences granted by the Environment Agency (Yates et al., 2016)

The Sem is a tributary of the Nadder and joins just West of Wardour. The catchment is mainly dominated by underlying impermeable Kimmeridge Clay, with surface runoff predominating (Allen et al., 2014). Lloyd et al. (2018) described the catchment as having a high proportion of rich intensive dairy farming and lowland grazing livestock production and suffering from the types of problems typically associated with manure production and management in these systems. Combined with the clay catchment hydrology which promotes a lower base flow index and a higher proportion of flow over the land surface, this leads to a high proportion of dissolved organic matter being delivered to the river through entrainment of manures via overland flow pathways as well as the delivery of inorganic nutrients and urea applied to the land as fertiliser via leaching along through flow pathways (Lloyd *et al.,* 2018).

The Conwy catchment had a total of 27 sites and the Hampshire Avon had 18 sites that could be used. Sites were selected based on their concentrations of DOC, N and P fractions and SUVA values. These parameters were picked as these play critical roles in the biological and photochemical transformations in aquatic systems. Some sites showed similar physiochemical parameters, so to obtain the greatest site variation possible, land use cover from LCM2007 was also used. This helped to remove sites of similar land use and physiochemical parameters to leave 3 sites in Conwy and 3 sites in the Hampshire Avon with different land use (Figure 5) and physiochemical parameters see (Figure 6 and Figure 7)

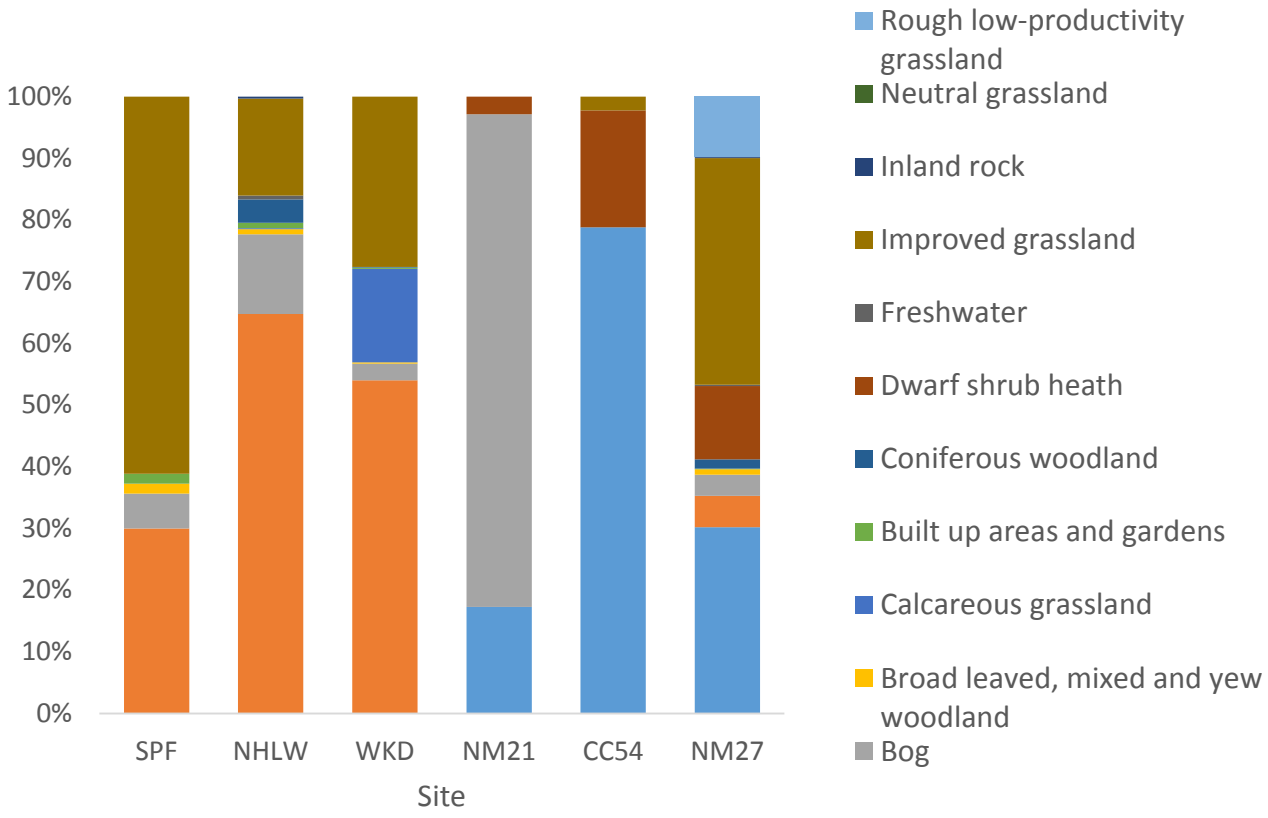

Figure 5: Percent land cover of selected field sites

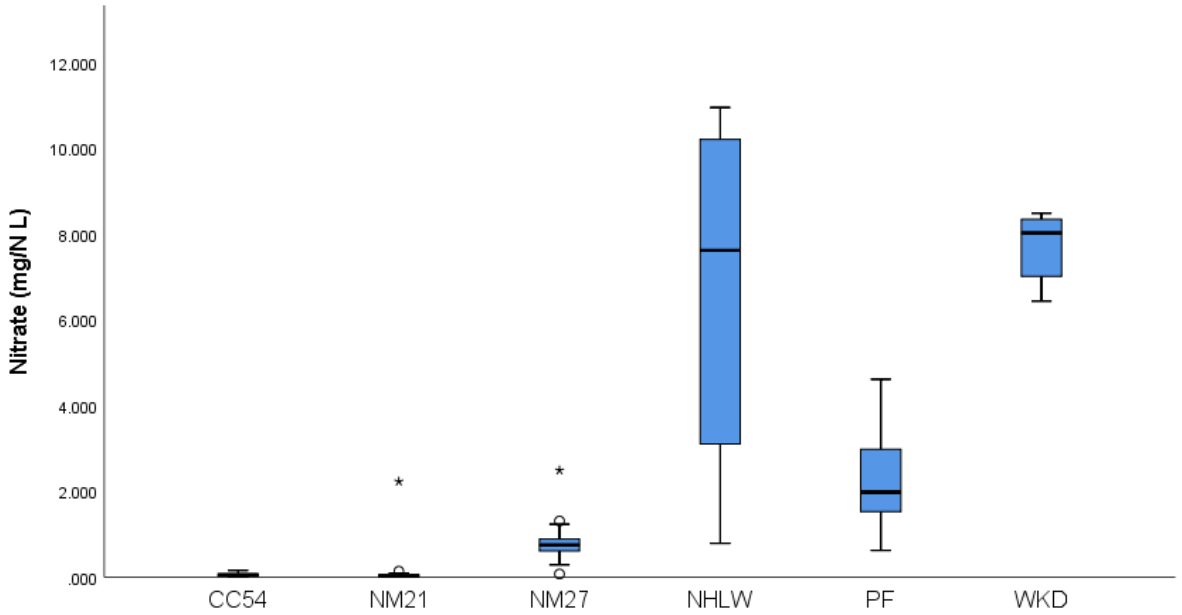

Figure 6: Average nitrate concentrations for the period 01/10/15 to 30/09/16

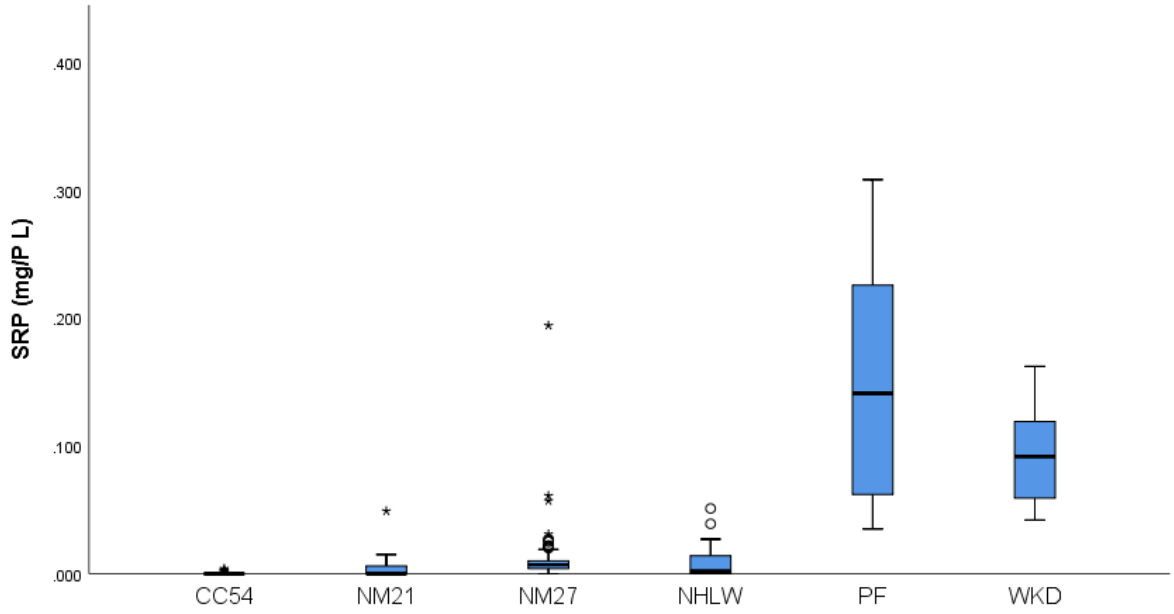

Figure 7: Average phosphate concentrations for the period 01/10/15 to 30/09/16

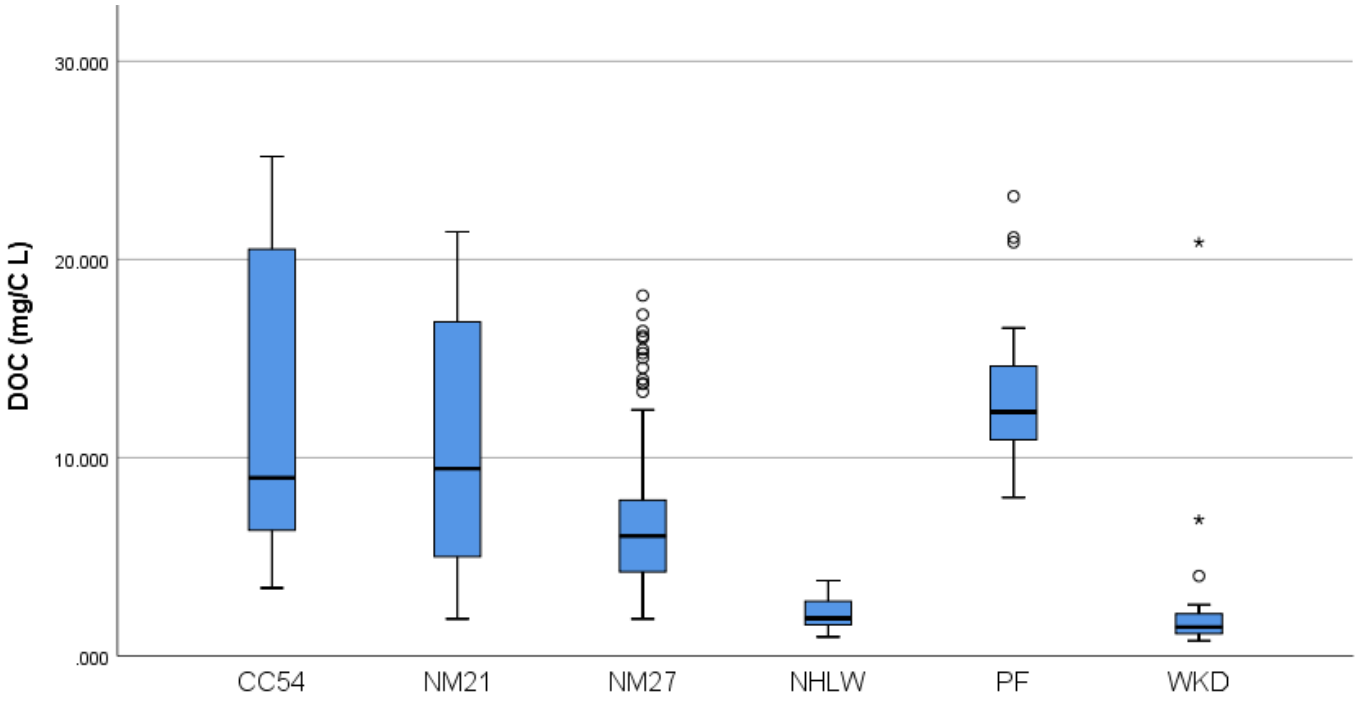

Figure 8: Average DOC concentrations for the period 01/10/15 to 30/09/16

3.1. Site description: Conwy sites

Three sites were selected from the Conwy catchment (Figure 9), comprising a peatland site (Nant y Brwyn) with heather moorland on blanket bog, an acid grassland site (Afon Cadnant) with low density sheep grazing, and a site combining acid and improved grassland which supported intensive sheep production on grass with some cattle production in its catchment (Pentrefoelas). Specific details of catchment character for each site are given below:

- Nant Y Brwyn Upper (NM21) is mainly covered by peatland. They are typically found in upland environments, where cooler temperatures and high levels of rainfall favour creating anaerobic environments that favour the formation of peat soils (Boothroyd *et al.,* 2015).
- Afon Cadnant (CC54) is mainly acid grassland. Upland acid grassland is characterised by vegetation dominated by grasses and herbs on a range of lime-deficient soils which have been derived from acid rocks such as sandstones, acid igneous rocks and on superficial deposits such as sands and gravels (JNCC, 2010a).
- Pentrefoelas (NM27) is comprised of mainly acid and improved grasslands and is a just downstream of Pentrefoelas. Improved grasslands are those meadows and pastures which have been so affected by heavy grazing, drainage, or the application

of herbicides, inorganic fertilisers, slurry or high doses or manure that they have lost many of the species which one could expect to find in unimproved grasslands (JNCC, 2010b).

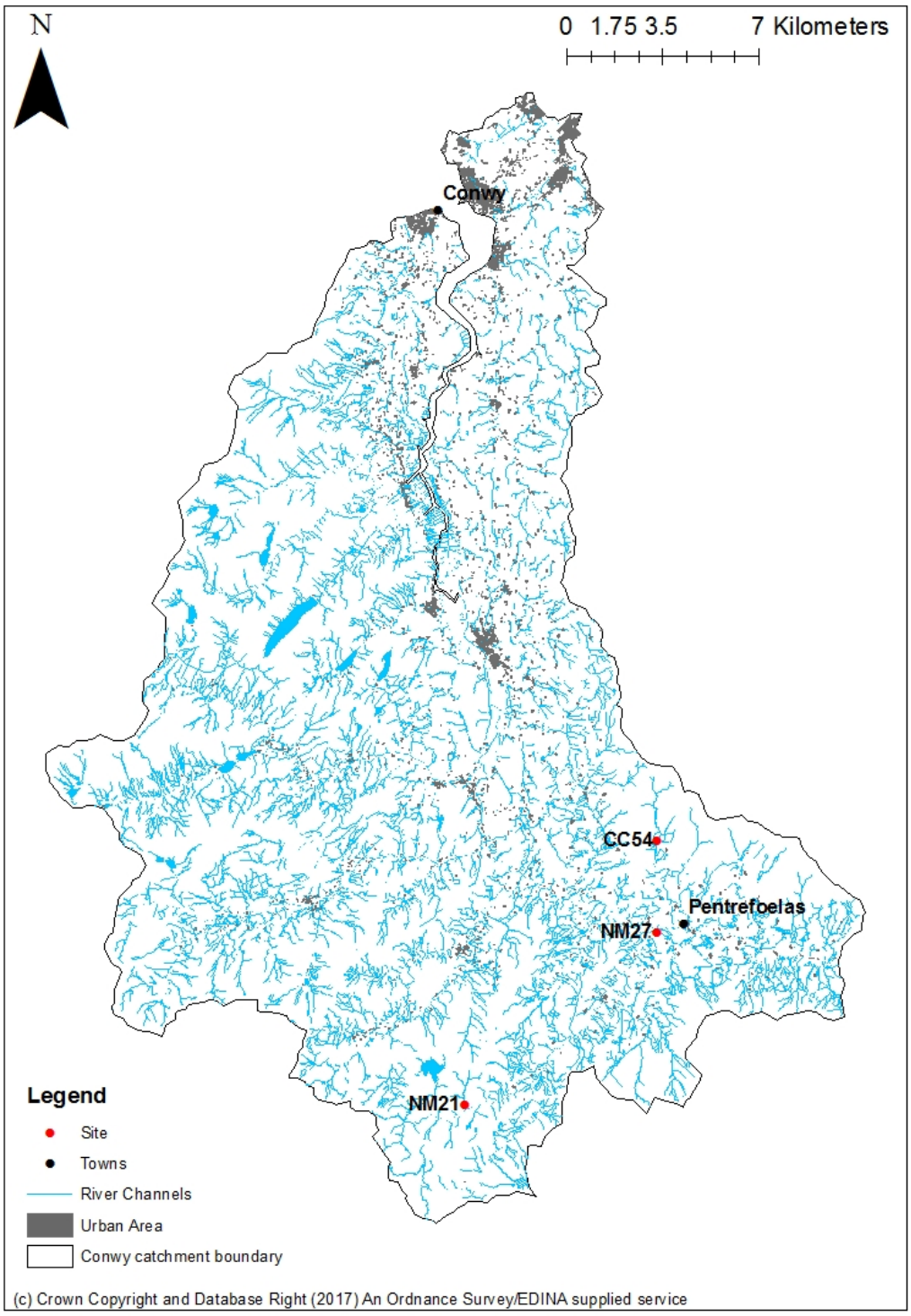

Figure 9: Sample sites in the Conwy Catchment.

3.2. Site description: Hampshire Avon sites

Three further sites with contrasting catchment character were selected in the Hampshire Avon catchment. These were the Wylye at Kingston Deverill, a chalk stream with a mixed arable catchment; the Sem at Priors Farm, a clay tributary of the Nadder catchment supporting intensive cattle production; and Hindon Lane Weir is a tributary in the Nadder, supporting mixed arable and intensive cattle production on chalk and clay. Specific details for each site are given below:

- Kingston Deverill is on the headwaters of the Wylye; the surrounding landscape is primarily arable and horticulture with extensive sheep grazing on hillslopes and some intensive cattle production in the valley bottom. The sampling site is downstream of an outflow pipe where Wessex Water optimise the flow conditions from the groundwater aquifer. Septic tanks in the upper reaches of the catchment are common in the villages and towns, contributing to both N and P enrichment of the Wylye (Lloyd et al., 2019).
- Priors Farm is on the headwaters of the Sem that flows into the Nadder, the Sem is a typical clay sub-catchment with large areas of intensive dairy and lowland grazing livestock production (Lloyd et al., 2019) with surface runoff predominating (Allen et al., 2014).
- Hindon Lane Weir is located below Fontill Lake and joins onto the Nadder by Tisbury. The catchment is mainly comprised to arable farmland and pasture with some broad-leafed woodland.

Table 2: Site co-ordinates for the Hampshire Avon & Conwy catchments

Site Name	Site Code	Latitude	Longitude
Kingston Deverill	WKD	51.133	-2.223
Priors Farm	PF	51.054	-2.156
Hindon Lane Weir	HLW	51.078	-2.090
Afon Cadnant	CC54	53.076	-3.700
Nant Y Brwyn	NM21	52.988	-3.801
Pentrefoelas	NM27	53.046	-3.699

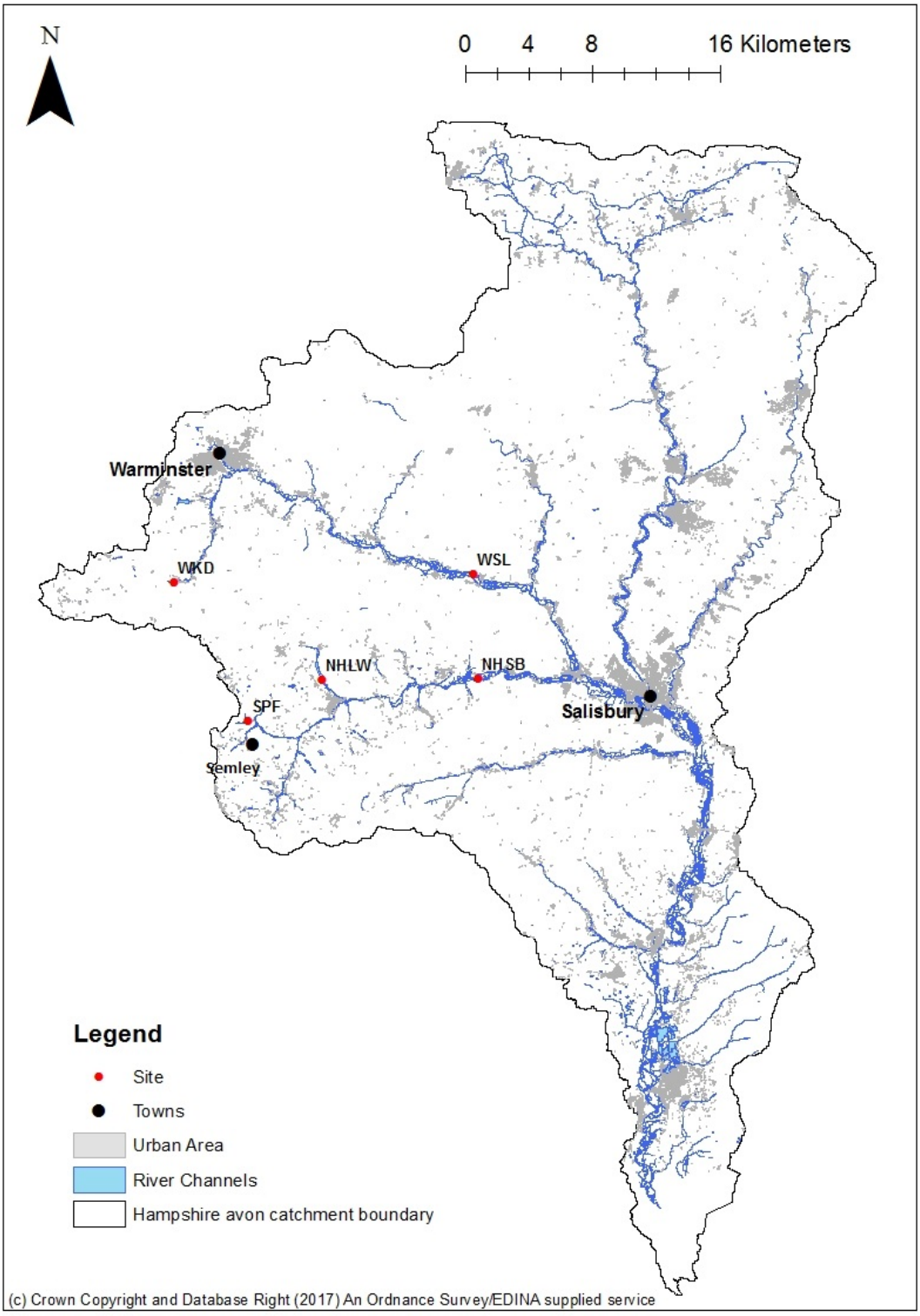

Figure 10: Sampling sites in the Hampshire Avon catchment

4. Methodology

River samples were collected in 1 litre, acid washed HDPE bottles and capped to eliminate any airspace in the sample bottle. Four 1 litre samples were collected from each site in amber glass bottles and placed inside a sealable cool box to limit any photo-oxidation during transit to the laboratory. Upon return to the laboratory the river samples were stored at <4ºC in the dark until filtering could commence (within 24h of sample collection), following the procedures outlined in Yates et al. (2016).

Prior to filtering, all the filtration equipment had been autoclaved at 105ºC for 1 hour to kill any bacteria present. The 4 separate 1 litre samples for each site were combined into 1 composite sample, with two litres of the new composite then filtered through a 0.45 µm cellulose nitrate filter that had been prewashed with 150ml of Milli Q water and dried. This new 0.45 µm filtrate was then filtered a second time through a 0.1 µm pre-washed cellulose nitrate filter to remove smaller microorganisms (Figure 11) from the sample.

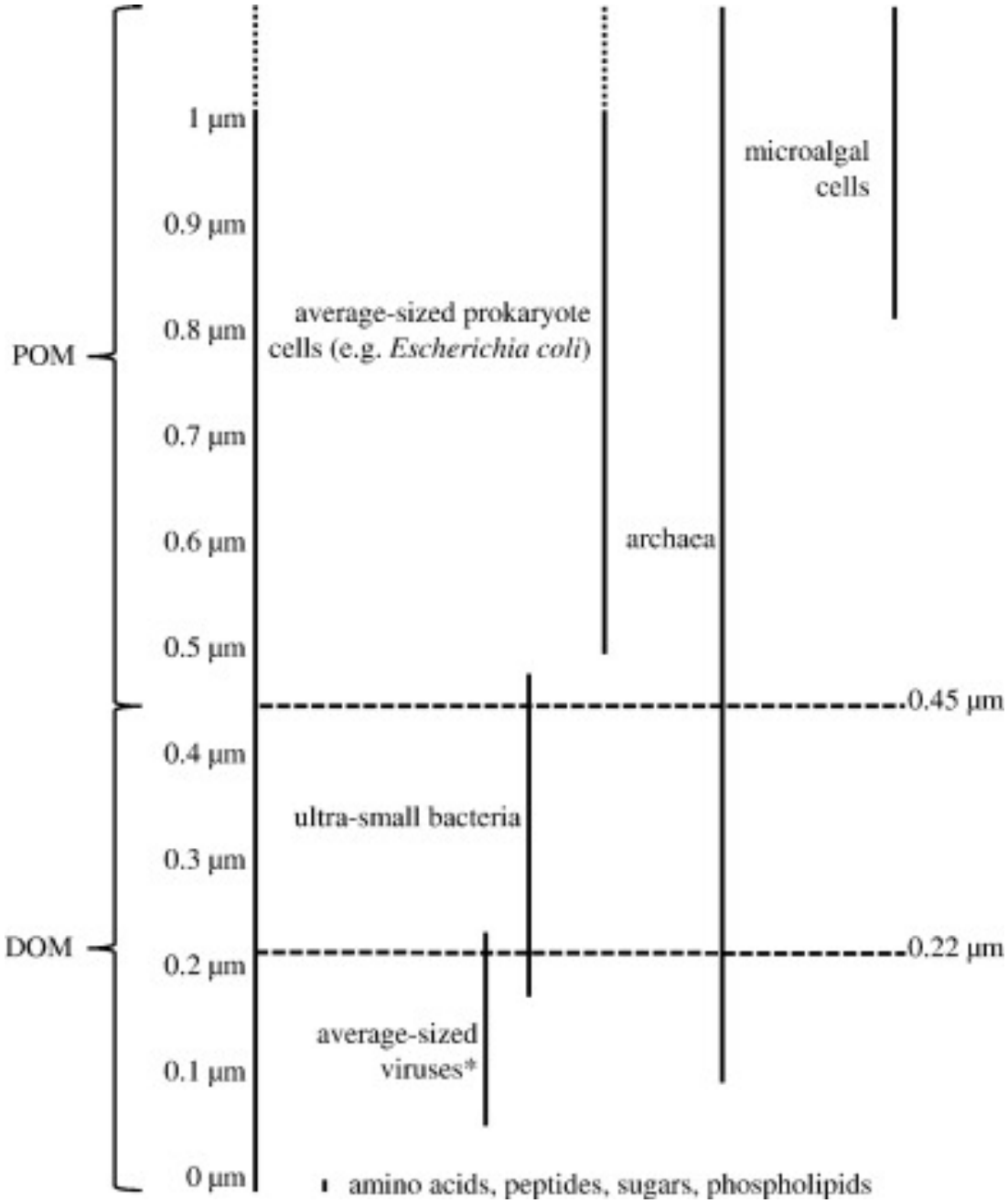

Figure 11: Relative size of dissolved organic matter (DOM) and particulate organic matter (POM) components in comparison to bacteria, archaea and viruses. POM N 0.45 µm N DOM. 0.45/0.22 µm filter cut-offs indicated by a dashed line (Brailsford et al., 2017).

The remaining two litres of unfiltered sample (UF) were then split between 3 quartz boiling flasks that had been acid washed in 10% hydrochloric acid (HCl) and then placed in a muffle furnace at 450ºC for 4 h and allowed to cool. The same procedure was also followed for the 0.1 µm filtrate fraction (F). A further UF and F sub-sample for each site was also placed into

an amber glass bottle as a dark control. In total, this generated 3 x UF, 3 x F and one UF dark control plus one F dark control for each site and sampling date.

A light box located in the School of Geographical Sciences LOWTEX Facility housed the samples for each site (see Figure 12). These were then subjected to the same daylight exposure (measured using a Jazz Spectrometer at 146 W/m^2 and temperature that would reflect the season in which samples were collected. This wattage reflects the expected energy seen in winter months but is lower than those expected in autumn (325 W/m^2) (Perry and Golding, 2011) The bulbs used were fluorescent 70W bulb emitting from 300nm-750nm (see Figure 13). Samples were subjected to a typical light/dark cycle for their respective season using a timer switch. Samples were placed into a shaker during incubation to mimic mixing in the river.

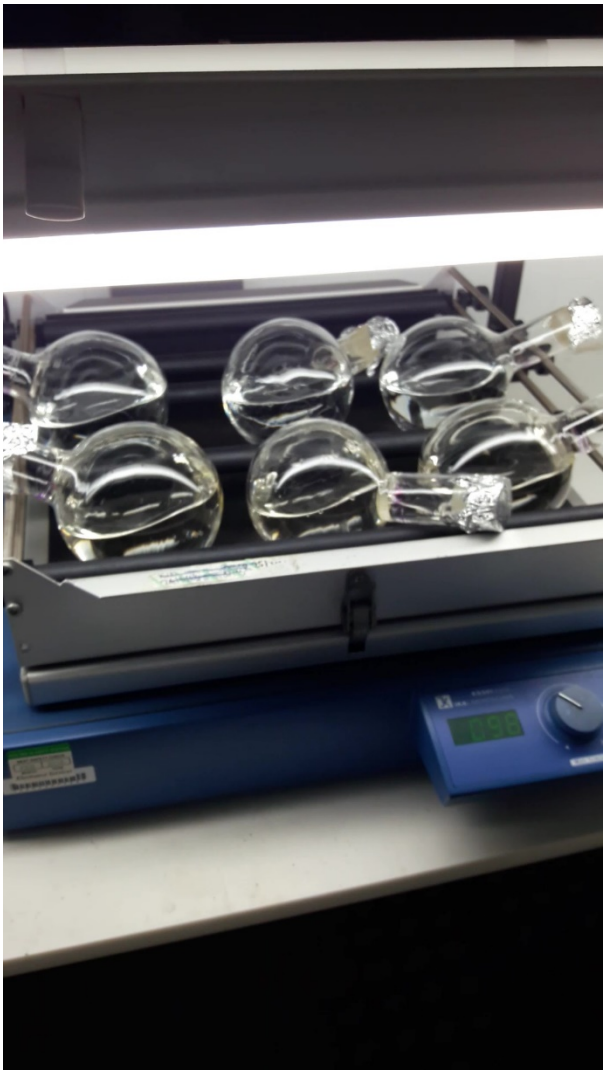

Figure 12: light box set up for incubations

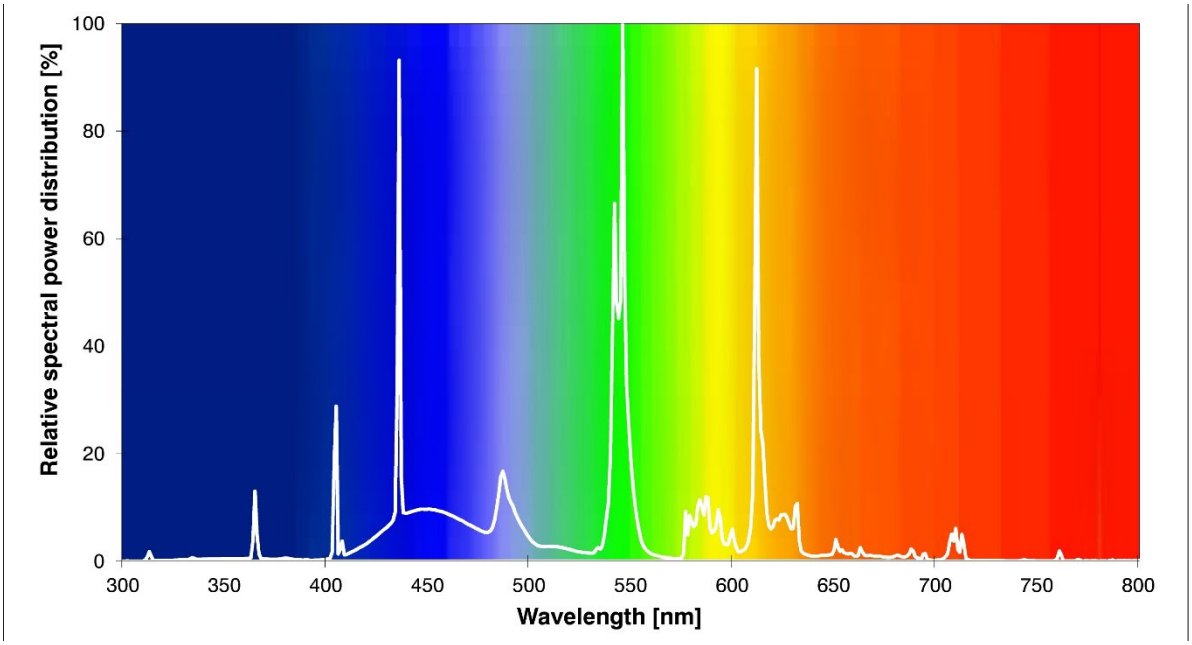

Figure 13: Spectral output from light source

Initial analysis commenced once the samples had been filtered and then analysed at time increments of 0, 24, 48, 72 and 168 h (7 days) from the start of the experiment. Samples were analysed to determine all N species (nitrate plus nitrite, measured as Total Oxidisable N (TON); ammonium plus unionised ammonia, measured as ammonium; Dissolved Organic N (DON); Particulate organic N (PON) and Total N (TN)). Phosphorus fractions (Soluble Reactive Phosphorus (SRP) measured as orthophosphate; Dissolved Organic P (DOP); Particulate P (PP) and Total P (TP)), and Dissolved Organic Carbon (DOC) using the approach outlined by (Yates et al., 2016; Yates and Johnes, 2013). Details for each analysis are given below in section 4.1, and a flow diagram summarising the sample analysis procedure is presented in Figure 12 (after Yates and Johnes, 2013). UV absorbance and fluorescence scans were also analysed.

4.1. Analytical Methods

4.1.1. DOC:

A Shimadzu TOC-L series analyser was used to automatically acidify samples to pH 2 to convert any inorganic carbon to carbon dioxide (CO_2) and then sparged with air to remove the produced CO_2. Samples were then passed through over a catalyst at 650ºC to convert any non-purgeable organic carbon (NPOC) to CO_2 that was analysed via infra-red.

4.1.2. Nutrient analysis

A Skalar San^{++} multi-channel continuous flow auto analyser was used to pump samples through the system with reagents added at various points through the process to produce a colour measured through a colorimeter at predetermined wavelengths:

4.1.3. Nitrate + Nitrite:

Samples were analysed using the hydrazine reduction method; nitrate was reduced to nitrite by hydrazinium sulphate and the nitrite (originally present plus reduced nitrate) is determined by diazotizing with sulphanilamide and coupling with N-(1-naphthyl) ethylenediamine dihydrochloride to form a highly coloured azo dye which was measured at 540 nm.

4.1.4. Nitrite:

Nitrite was determined by diazotizing with sulphanilamide and coupled with N-(1-naphthyl) ethylenediamine dihydrochloride to form a highly coloured azo dye which is measured at 540 nm.

4.1.5. Soluble Reactive Phosphate (SRP):

SRP was analysed by the addition of ammonium heptamolybdate and potassium antimony (III) oxide tartrate reacting in an acidic medium with phosphate to form an antimony-phospho-molybdate complex. This complex was reduced to an intensely blue-coloured complex by addition of ascorbic acid and is measured at 880 nm.

4.1.6. Ammonia (NH_3 + NH_4^+):

Using a modified Berthelot reaction, samples were buffered to an acidic pH and chlorinated (using sodium dichloroisocyanuric acid sodium salt) to monochloramine which reacts with salicylate to produce 5-aminosalicylate. This results in a green coloured complex that was measured at 660 nm.

4.1.7. Digestion Method

Total Dissolved Nitrogen (TDN) and Total Dissolved Phosphorus (TDP), were digested after filtration and Total Phosphorus (TP) and Total Nitrogen (TN) were digested without any filtration step, both using a persulphate oxidation method modified from (Johnes and Heathwaite, 1992).

The simultaneous digestion of all fractions of nitrogen and phosphate requires that there was a sufficiently alkaline and timed environment to transform all other forms of nitrogen to Nitrate. Whilst there being enough potassium sulphate after the alkaline phase to create an acidic enough environment to break down all fractions of phosphorus to SRP. These are then analysed on the Skalar using the Nitrate – Nitrite and SRP methods.

The fractions Dissolved Organic Nitrogen (DON), Particulate Organic Nitrogen (PON), Dissolved Organic Phosphorus (DOP) and Particulate Phosphorus (PP) were calculated by difference using the following chart:

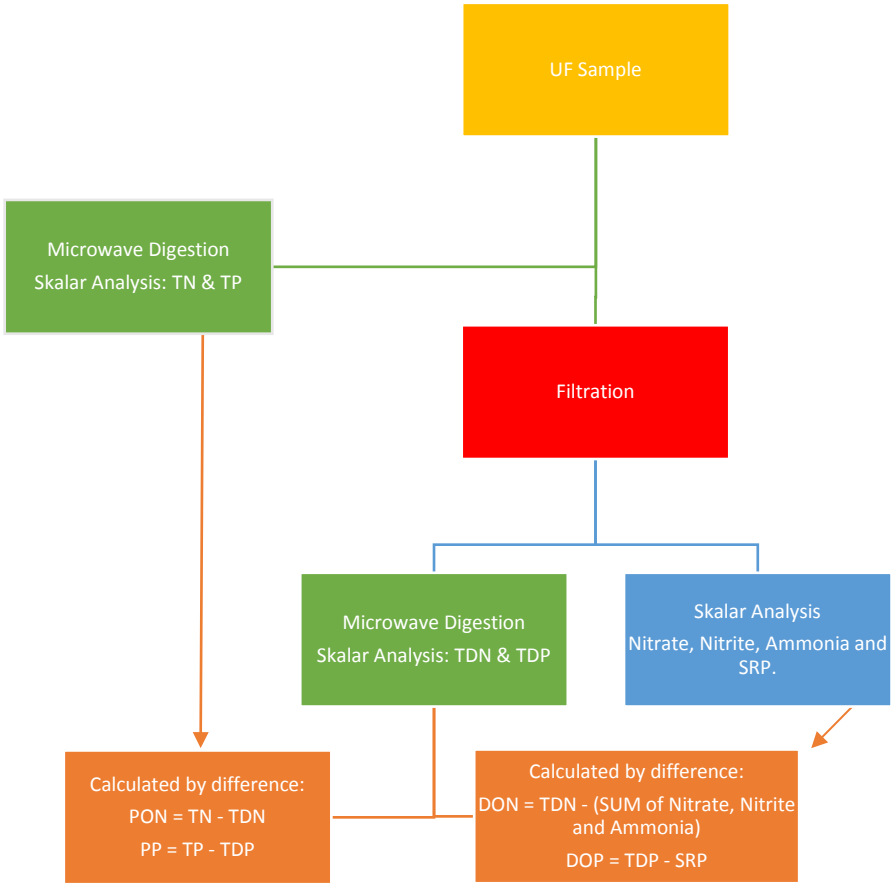

Figure 14: Sample analysis flow chart (Johnes and Heathwaite, 1992; Yates and Johnes, 2013))

4.1.8. UV Absorbance

Absorption for each individual wavelength was measured between a reference cell (I_0) and a sample (I). If the light intensity for the I was less than that of I_0 some light has been absorbed within the sample.

$$A = \mathrm{Log}_{10} \frac{I_0}{I}$$

Equation 7: Absorption of individual samples

Using A from the equation above, the molar absorbity was then calculated using Beer Lamberts law (Equation 8):

$$A = \epsilon l c$$

Equation 8: Beer Lamberts law

Where A is, the absorption calculated using ϵ is the molar absorptivity, l in the path length of the cuvette and c is the concentration of solution.

Samples were scanned using a Cary 60 UV Vis Spectrophotometer from 800nm to 200nm with an integration time of 0.1s using 10mm quartz cuvettes. To remove any interference from temperature samples were analysed once they had reached room temperature. To remove any instrumental bias an average of sample values between 750nm to 800nm was subtracted across all wavelengths. All UV results are reported as absorption coefficients unless otherwise specified. Absorption co-effects determine how far a wavelength of light can penetrate a substance before being absorbed. This was calculated using the equation below:

$$a(\lambda) = 2.303A(\lambda) / l$$

Equation 9: Absorption coefficient

Where a is the Napierian light absorption coefficient (m^{-1}) at λ (the wavelength in nm), A is the absorbance at λ wavelength, and l is the cell path length in meters (Green and Blough, 1994). The factor of 2.303 allows conversion of $\log_{10}$ to natural logarithm.

4.1.9. E ratios, Spectral Slopes, Slope ratio (S_r) and $SUVA_{254}$

UV-visible absorption spectra intensity for CDOM usually increases with lower wavelengths (Twardowski et al., 2004). This can be used to identify the variability in the DOM character (Blough and Green, 1995). For example, the slope can be used to identify transformations in the CDOM as a result of photodegradation (Twardowski and Donaghay, 2002; Vodacek et al., 1997).

Ratio of the absorption at 250nm to 365nm (also referred to as E2:E3 ratios) have been used to identify the alteration of HMW to LMW DOM (De Haan and De Boer, 1987; Peuravuori and Pihlaja, 1997). As molecular size increases the E2:E3 ratio decreases because of

stronger light absorption by high-molecular-weight (HMW) CDOM at longer wavelength (Helms et al., 2008).

Slope ratio (S_r) values were calculated using a non-linear fit of an exponential function to the absorption spectrum over the range 275-295nm and 350–400 nm (Helms et al., 2008).

$$a\lambda = a\lambda ref - S(\lambda - \lambda ref)$$

Equation 10: Slope ratio (Helms et al., 2008).

where a = Napierian absorption coefficient (m^{-1}), λ = wavelength (nm), λ_{ref} = reference wavelength (nm), and S = spectral slope (nm^{-1}) (Helms et al., 2008). The 275–295 nm slope and the 350–400 nm slope ranges were used as they have been demonstrated they contain the greatest variation in a wide range of samples, including DOM-rich terrestrial, estuarine, coastal, and highly photo bleached waters (Helms et al., 2008). All slopes have been reported as positive numbers so that the increase in steepness indicates a greater decrease in HMW.

Specific UV absorbance ($SUVA_{254}$) is defined as the UV absorbance of a water sample at a 254nm normalized for DOC concentration. SUVA has been widely used by researchers as it has been linked to the aromaticity of DOM (Weishaar et al., 2003).

4.1.10. Fluorescence

Fluorescence of DOM in aqueous samples can be determined by passing varying wavelengths of light (excitation) through the sample and monitoring the intensity of fluorescence (emission) at specified wavelengths to produce Excitation Emission Matrices (EEMS). In this study this was undertaken on each sample at each time point using a Cary Eclipse Fluorescence Spectrophotometer with an integration time of 0.1s. The samples were excited from 240nm to 450nm and the emission was scanned at 300-600nm using 10mm quartz cuvette. Without further processing the produced EEMS drown out smaller contributing fluorophores as well as containing interferences from the aqueous matrix. To remove these interferences the following steps were performed using the drEEM and FDOM toolbox created by (Murphy *et al.,* 2013):

a) To remove instrumental bias a correction factor from the manufacturer for the excitation and emission was applied to allow EEM comparison between scans run on different fluorimeters.

b) Each EEM was blank subtracted using DI water; this removes the noise from Rayleigh and Tyndall lines. Rayleigh scatter is the direct scattering of the incident light and there focuses at the same wavelength as the excitation (Lawaetz, 2016). The Raman peak is the result of non-elastic scatter i.e. a fraction of incident photons lose energy to vibration in water molecules and the photon is scattered at a higher wavelength than the incident light. (Lawaetz, 2016). The data are then normalised to the area under the Raman peak Ex 350 and Em at 390 to 398nm

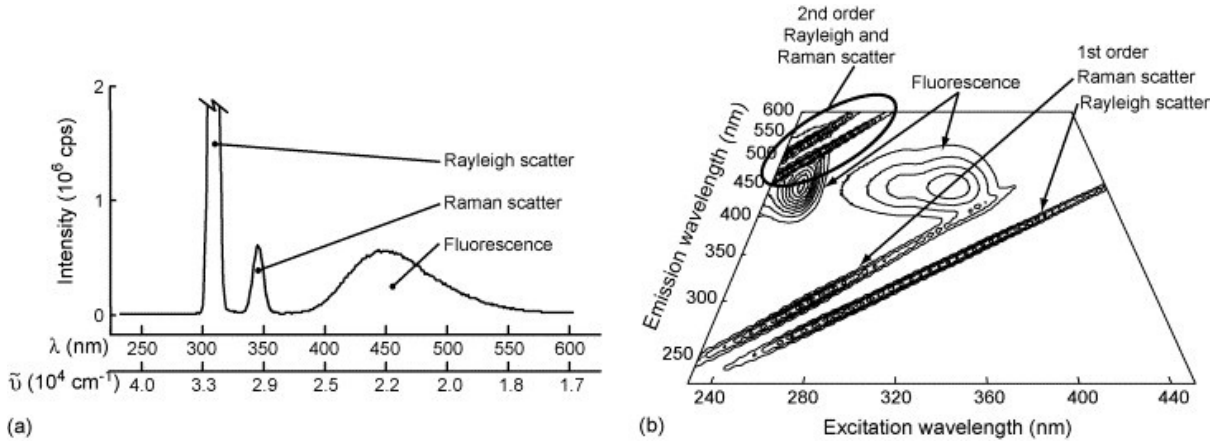

Figure 15: Raman and Rayleigh scatter in an EEM (Larsson et al., 2007).

c) Inner filter effects (IFE), can be caused by the absorption of the exciting as well as the fluorescent light (primary and secondary IFE, respectively) by the fluorophore itself, or by another component of the sample (Larsson et al., 2007), a correction factor was therefore needed to remove the IFE. Using equation 11 the UV scan of the same sample was applied to the fluorescence EEM to remove the IFE:

$$Fcor=Fobs\times10^{\,1(A_{Ex}+A_{Em})}$$

Equation 11: IFE correction value (Murphy et al., 2013)

Where F_{obs} and F_{cor} stand for the fluorescence intensity before and after calibration, respectively; and A_{Ex} and A_{Em} denote the absorbance at corresponding excitation and emission wavelengths, respectively. (Zhou et al., 2017).

d) Samples were then normalised to the area under the Raman peak (Ex 350 Em 380-426nm) to produce corrected fluorescence in Raman units (RU) see Equation 12. With Arp350 being the area underneath the Raman peak.

$$F^{cal}(RU) = \frac{1}{Arp350} F_{cor}$$

Equation 12: Raman normalisation (Murphy et al., 2013)

4.2. Quality assurance

For the DOC analyser and the Skalar each sample run was accompanied by an 8-point calibration with a correlation coefficient of ≥0.998. Every 20 samples were accompanied by a blank (≤LOD) and a high and low standard that to pass within ± 2 standard deviations of the validated mean.

Each batch of digested samples that was digested in the microwave was accompanied by a blank (≤LOD) and an organic N and P standard to check for total digestion of the organic fractions to nitrate and phosphate.

For the UV scans a holmium standard was scanned at the start and end of every day from 200nm to 800nm and every 50nm was used as a reference point that had limits of ±2 standard deviations of the validated mean applied.

4.3. Statistical Analysis

Using SPSS samples were analysed using a Shapiro-Wilk test that assessed whether the data are normally distributed, with 95% of the results falling within a normal distribution (Shapiro and Wilk, 1965). If data failed this test, they were transformed either by log, square root or reciprocal transformation. Data were also tested for assumed equal variance using Levene's test (Levene, 1960).

If the analysed data met the above criteria a one-way Anova test was used with a Tukey's Post Hoc to compare unfiltered and filtered samples and their dark counterparts at specified

time points. However, if data could not pass a Shapiro-WilK even after being transformed a Welch's test was performed with a Post Hoc Games-Howell test used instead of the Tukey test for data of unequal variance.

All results reported are means of the triplicate replicates of each day with error bars representing 1 standard deviation. The dark controls have not had any statistical analysis applied as there is only one value per day.

5. Results

5.1. Impacts of photodegradation processes on DOM character, as inferenced from fluorescence and UV-Visible spectrophotometry.

5.1.1. UV absorption at 254nm

Due to time constraints there are no autumn data for Nant Y Brwyn and no winter data for Pentrefoelas and Hindon Lane Weir. Afon Cadnant in autumn (see Figure 16) shows no change in the light and dark F fractions but a decrease in absorbance in both the light and dark UF fractions, with a reduction of 4.2%. During winter (see Figure 17) there is a similar decrease to autumn in the light and dark UF fractions, however there is a large increase (5.0%) in the light F fraction which is greater than the decrease in the UF fraction (4.4%).

Nant Y Brwyn shows a pattern like that of the autumn samples for Afon Cadnant with a decrease in the light and dark UF fractions (5.2%) with no change in the F fractions. Kingston Deverill in autumn showed no change in the dark UF and F light and dark and fractions but showed a substantial increase (17.7%) in the light UF fraction. The winter sample showed little or no variation.

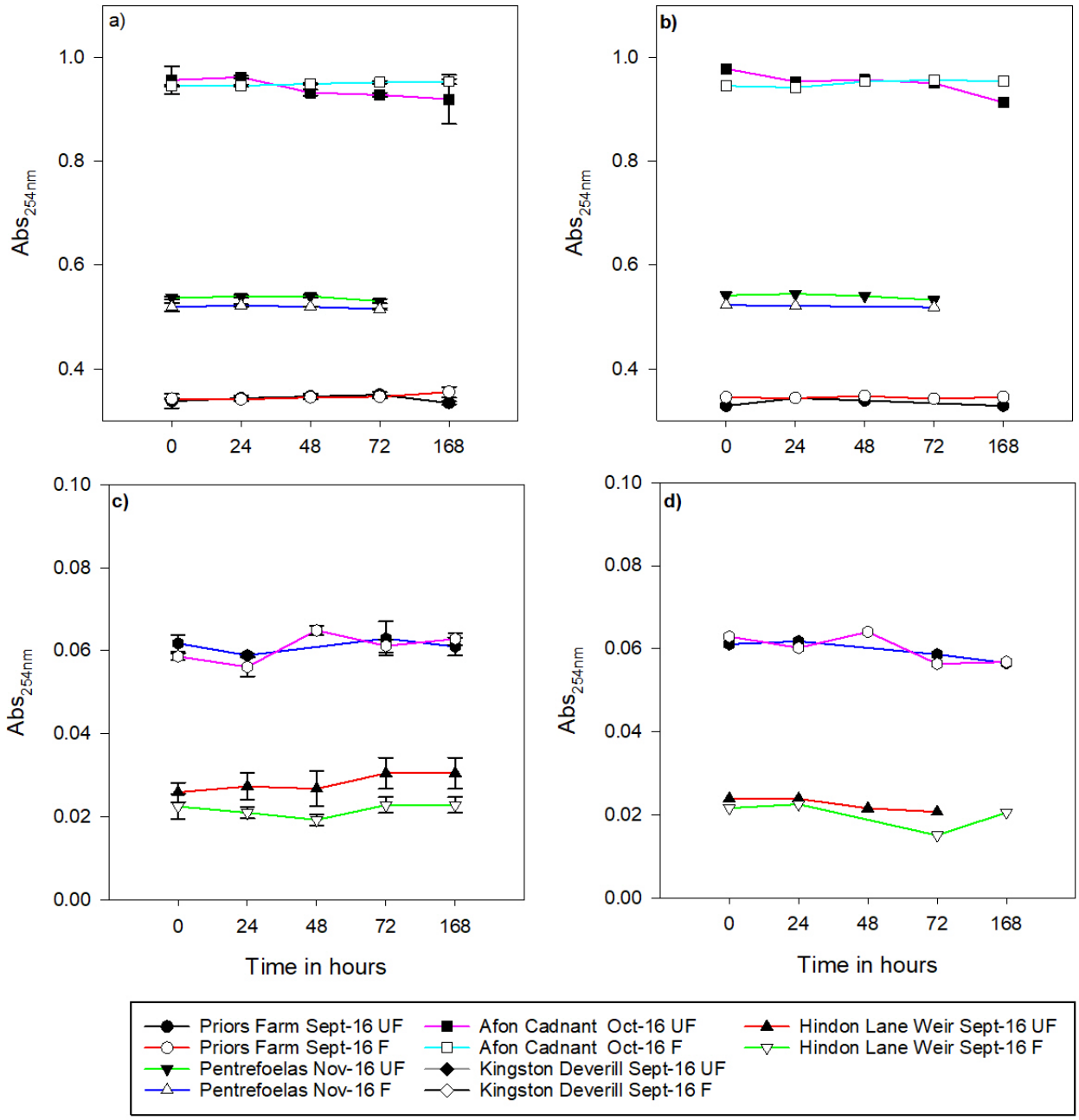

Figure 16: Absorption at 254nm change of UF and F (a & c) and UF and F dark (b & d) fractions in autumn.

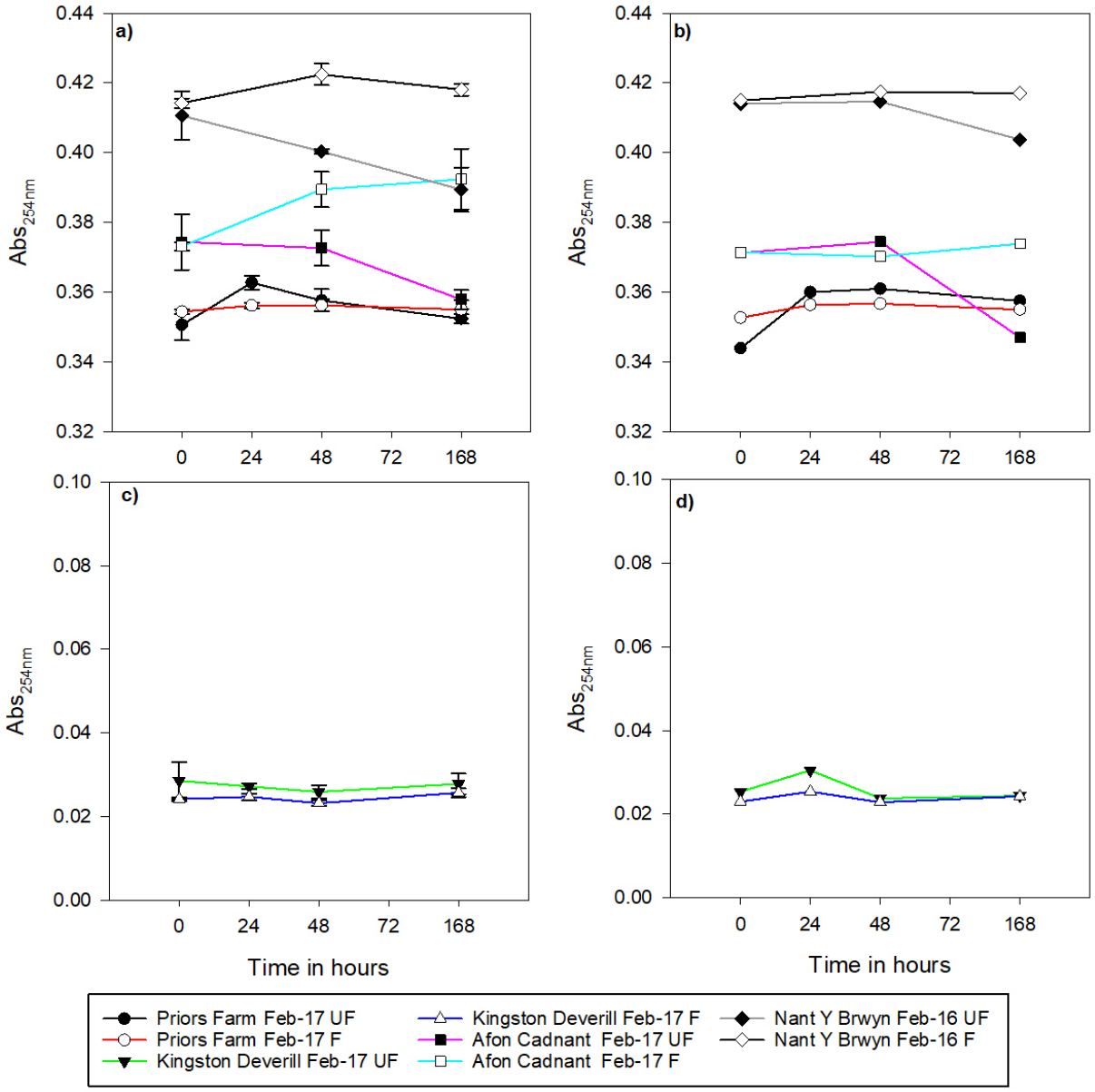

Figure 17: Transformation of absorption at 254nm of UF and F (a & c) and UF and F dark (b & d) fractions in winter.

5.1.2. Slope ratio (275-295 to 350-400nm)

S_r shows a large variation in the initial value between sites with Hindon Lane Weir having the highest value (1.2), followed by peatland sites at around 0.6 and Kingston Deverill had the lowest value at 0.25. Low S_r values are generally attributed to HMW DOM of terrestrial origin e.g. 0.7 terrestrial and 1.1 for estuarine and coastal samples, while increases in SR values over time can be photochemically induced, while decreases may be due to microbial processing (Helms et al., 2008). There is little variation overall in the initial S_r for the sites

between autumn (Figure 18) and winter (Figure 19). The data have been split into different scales of S_r values to aid the reader in viewing the trends and patterns.

Priors Farm shows little or no variation in either fraction for autumn. During winter there was no change in the dark samples, but both light fractions showed a statistically significant increase over 7 days (UF 4.3% & F 4.7%) but this increase did not occur initially and only occurred after 48 hours had passed.

Pentrefoelas showed no statistically significant change in autumn, which is evident in (Figure 18) as the F fraction remains unchanged, with a slight decrease after 48 hours in the UF fraction. In contrast there is a clear decline in S_r after 24 hours in both the UF and F dark fractions.

During autumn at Afon Cadnant in both the light and dark UF fractions shows an increase (4.7%) across 7 days, but the light and dark F fraction showed a slight decrease over 7 days in autumn. The dark fractions showed no change across 7 days. Winter had a similar significant increase in S_r in the F fraction (4.9%) which was statistically significant, with no change in the F dark fraction. The UF fraction showed a slight increase after 48 hours, but in the dark sample there is slow gradual decrease in S_r.

Nant Y Brwyn during winter shows trends like those shown in the Afon Cadnant samples, with a statistically significant increase in Sr (4.0%) in only the light filtered sample with no change in the F dark sample. But unlike Afon Cadnant, the light UF fraction slowly decreases and the UF dark samples increases after 7 days.

For both seasons Kingston Deverill had an initial difference between the UF and F fractions, but these were not statistically significant, nor were any of the changes in the autumn sample. The autumn light samples showed a gradual increase over 72 hours (12%) in the UF fraction. The F sample follows a U shape of decrease and increase over 72 hours. The dark fractions show an initial increase after 24 hours before gradually decreasing. In the light F sample, there is a gradual increase over 7 days but there were no statistically significant changes in the autumn sample.

In winter the light F sample had a statistically significant increase of 40% over 7 days which was the largest in increase across all sites over both seasons. The UF fraction shows a similar increase over 7 days but was not statistically significant. The dark samples behave similarly to that of the light samples suggesting that there may be biota present in the sample.

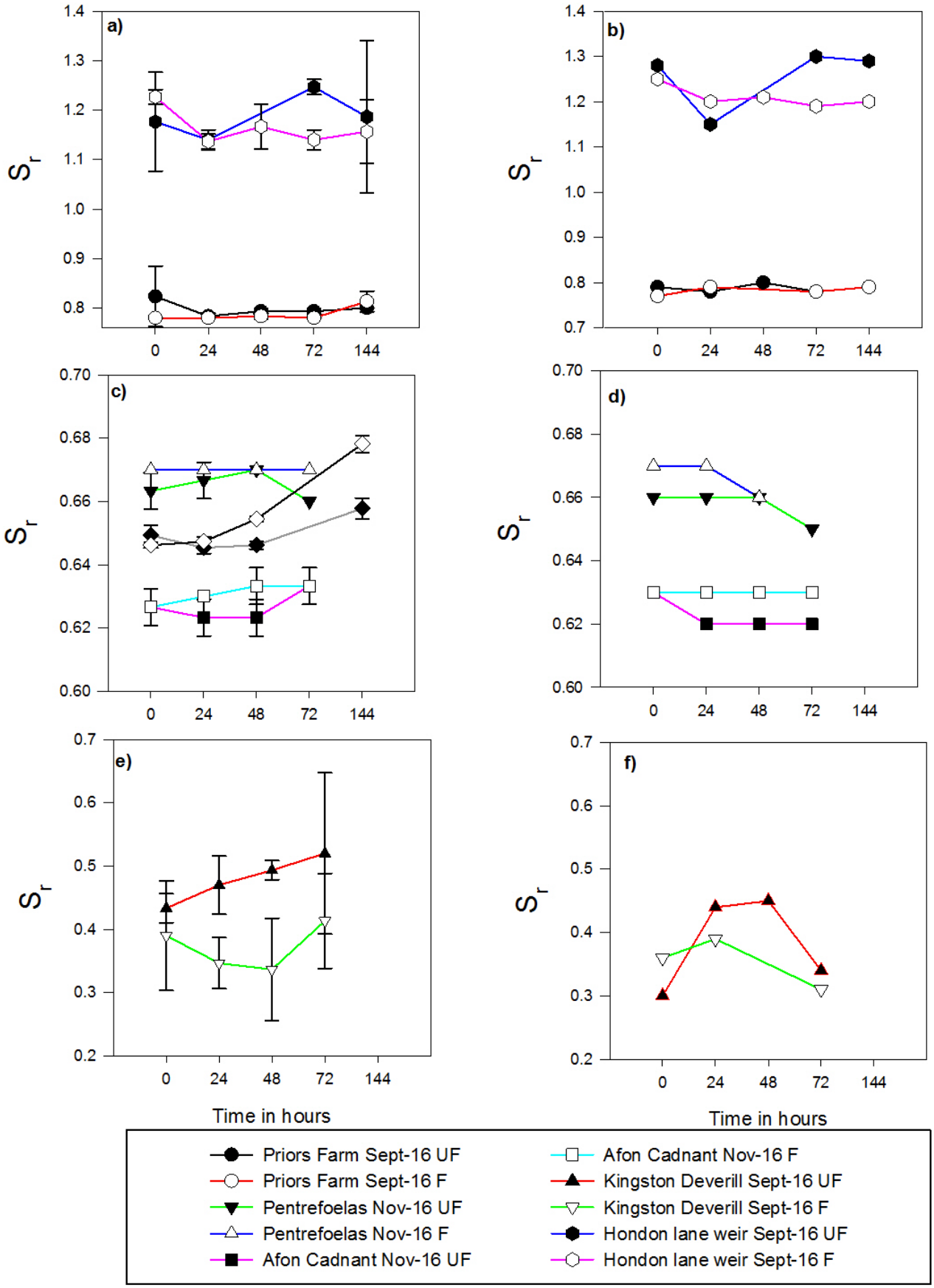

Figure 18: S_r change of UF and F (a, c & e) and UF and F dark (b, d & f) fractions in autumn.

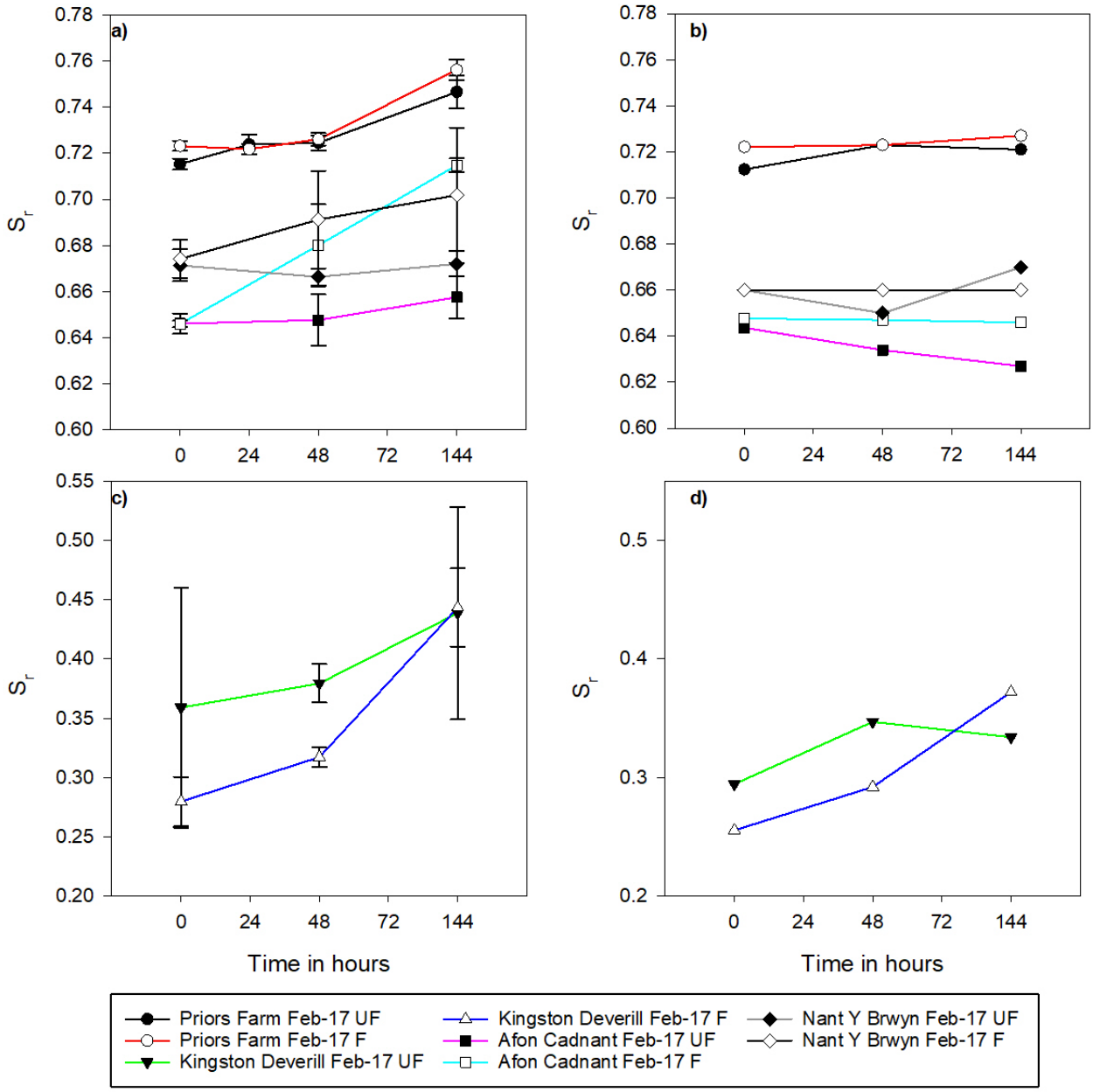

Figure 19: S_r change of UF and F (a & c) and UF and F dark (b & d) fractions in winter.

5.1.3. SUVA

There were no statistically significant changes in the SUVA values but examining Figure 20 & Figure 21 we can clearly see changes in some sites over 7 days. In autumn Pentrefoelas shows a U-shape gradual decrease with a maximum decrease at 24 hours before slowly increasing to approximately the original starting value. Afon Cadnant in autumn shows a slow increase for 48 hours in the light and dark UF fraction and remaining unchanged in the F light and dark fractions.

In winter in the light samples at Priors Farm, Afon Cadnant and Nant Y Brwyn show a very slight decrease in SUVA over 7 days. In the dark fractions there is little or no change in Priors Farm. Like the pattern observed in the S_r for Afon Cadnant and Nant Y Brwyn the SUVA value for Nant Y Brwyn increased and then decreased, with the opposite occurring in Afon Cadnant.

Kingston Deverill had the lowest initial SUVA value with concentrations similar to that of (Yates et al., 2016), yet there was a noticeable difference in SUVA values between autumn and winter. By winter SUVA had increased to 3.0mg/C L nm^{-1} double the value in autumn. Autumn showed no visible trends and or patterns. But In winter at Kingston Deverill there was a large decrease between 0 and 24 hours in both the light UF and F samples, before a slow gradual decrease between 24 and 168 hours (7 days). This is not mirrored in the dark fractions as there is a steep decrease over 7 days with a total reduction of 35% in SUVA concentration.

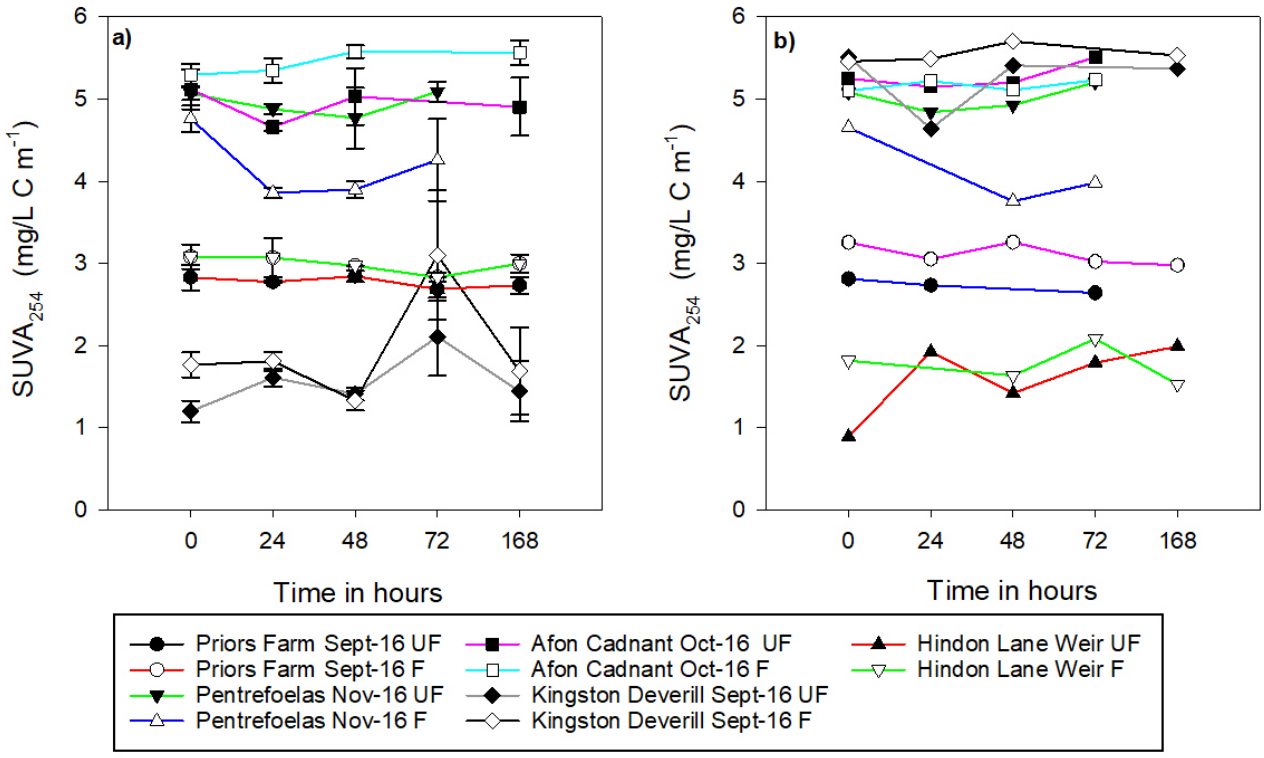

Figure 20: SUVA change of UF and F (a) and UF and F dark (b) fractions in autumn.

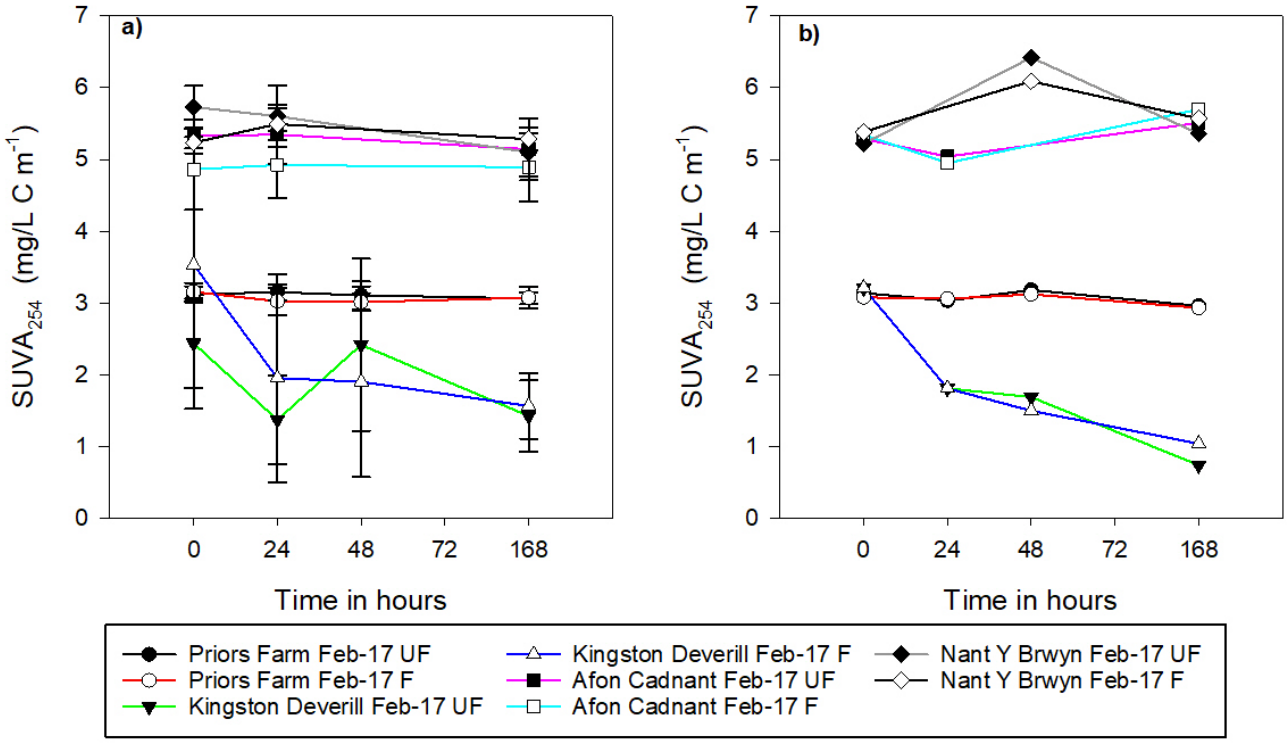

Figure 21: SUVA change of UF and F (a) and UF and F dark (b) fractions in winter.

5.1.4. Fluorescence

In autumn at Priors Farm there are only data for 0 and 72 hours and only in the UF fraction due to time constraints (see Table 3). All peaks decreased, with the biggest decrease in Peak A at 84%, although the FI did increase by 17%.

Table 3: Fluorescence (RU) change at Priors Farm in autumn

	0 hours	72 hours	% change
Peak B UF	1.58	0.87	-44.98
Peak T UF	7.23	1.75	-75.75
Peak A UF	49.58	7.87	-84.12
Peak C UF	29.88	4.96	-83.40
FI UF	1.44	1.69	17.50

Table 4: Peak ratio change (RU) at Priors Farm in autumn

	0 hours	72 hours	% change
Peak C:A UF	0.87	0.63	-27.21
Peak C:T UF	2.41	2.83	17.35
Peak A:T UF	3.79	4.49	18.42

In winter (see Table 5) in contrast to autumn all the light UF fractions increased in peak intensity and for all F fractions there was a decrease is peak intensity. The biggest increase in the UF fraction was in Peak C (69%) with and the biggest decrease was in Peak B (-60%). Data is only present for 0 and 168 hours and no UF & F dark fraction data are available.

Table 5: Fluorescence (RU) change at Priors Farm in winter

	0 hours	168 hours	% change
Peak B UF	3.39	4.44	30.99
Peak B F	4.27	1.69	-60.37
Peak T UF	4.79	7.36	53.71
Peak T F	6.48	3.50	-46.01
Peak A UF	30.75	52.48	70.66
Peak A F	38.20	22.83	-40.22
Peak C UF	19.49	33.02	69.39
Peak C F	23.40	13.66	-41.62
FI UF	1.65	1.66	1.11
FI F	1.61	1.70	6.01

Table 6: % change in the ratio of peaks (RU) at Priors Farm in winter:

	0 hours	168 hours	% change
Peak C:A UF	0.63	0.63	-0.74
Peak C:A F	0.62	0.62	-0.20
Peak C:T UF	4.09	4.50	9.90
Peak C:T F	3.64	3.36	-7.68
Peak A:T UF	6.45	7.15	10.74
Peak A:T F	5.89	5.50	-6.71

All the peaks decreased in intensity at Pentrefoelas with the biggest decrease in Peak B in the light UF and F fractions with -111% and -100% respectively. This was also the case for the dark UF and F fractions (see Table ***7***)

Table 7: Fluorescence (RU) change at Pentrefoelas in autumn

	0 hours	72 hours	% change
Peak B UF	5.95	-0.70	-111.70
Peak B F	6.25	-0.05	-100.83
Peak B Dark UF	8.67	1.59	-81.68
Peak B Dark F	9.25	1.00	-89.20
Peak T UF	7.85	0.71	-90.96
Peak T F	7.44	0.98	-86.86
Peak T Dark UF	8.97	1.62	-81.94
Peak T Dark F	10.32	1.46	-85.82
Peak A UF	66.54	21.95	-67.01
Peak A F	69.34	22.42	-67.67
Peak A Dark UF	65.63	24.85	-62.14
Peak A Dark F	71.39	19.03	-73.34
Peak C UF	35.41	11.63	-67.15
Peak C F	36.92	11.73	-68.22
Peak C Dark UF	33.65	13.00	-61.37
Peak C Dark F	35.00	10.45	-70.13
FI UF	1.43	1.34	-6.31
FI F	1.41	1.37	-3.15
FI Dark UF	1.40	1.43	2.50
FI Dark F	1.43	1.35	-5.52

Table 8: % change in the ratio of peaks (RU) at Pentrefoelas in autumn.

	0 hours	72 hours	% change
Peak C:A UF	0.53	0.53	-0.16
Peak C:A F	0.53	0.52	-1.62
Peak C:A UF dark	0.51	0.52	2.03
Peak C:A F dark	0.49	0.55	12.06
Peak C:T UF	4.60	19.60	325.97
Peak C:T F	5.08	13.05	156.85
Peak C:T UF dark	3.75	8.02	113.86
Peak C:T F dark	3.39	7.15	110.67
Peak A:T UF	8.65	36.65	323.80
Peak A:T F	9.57	24.81	159.35
Peak A:T UF dark	7.31	15.33	109.61
Peak A:T F dark	6.92	13.01	88.01

Afon Cadnant in autumn shows a stark contrast to that of Pentrefoelas in Autumn with the biggest decreases in Peak B in both the light and dark UF and F fractions (see Table 9), but all other peaks increase over 7 days.

Table 9: Fluorescence (RU) change at Afon Cadnant in autumn

	0 hours	168 hours	% change
Peak B UF	2.20	-18.15	-923.70
Peak B F	0.21	-16.19	-7771.25
Peak B Dark UF	1.79	-26.08	-1560.03
Peak T UF	2.99	-7.47	-349.59
Peak T F	1.73	-0.95	-154.87
Peak T Dark UF	2.93	-13.10	-546.76
Peak A UF	76.57	137.34	79.37
Peak A F	58.29	132.99	128.14
Peak A Dark UF	56.56	129.84	129.58
Peak C UF	41.66	83.72	100.96
Peak C F	34.68	76.28	119.95
Peak C Dark UF	35.08	77.44	120.76
FI UF	1.30	1.30	-0.18
FI F	1.31	1.35	3.28
FI Dark UF	1.30	1.27	-2.08

Table 10: % change in the ratio of peaks (RU) at Afon Cadnant in autumn

	0 hours	168 hours	% change
Peak C:A UF	0.54	0.61	12.08
Peak C:A F	0.60	0.57	-3.61
Peak C:A UF dark	0.62	0.60	-3.84
Peak C:T UF	24.28	-11.84	-148.76
Peak C:T F	-1.14	-11.68	-921.86
Peak C:T UF dark	11.96	-5.91	-149.41
Peak A:T UF	44.58	-19.54	-143.83
Peak A:T F	-1.83	-19.91	-989.38
Peak A:T UF dark	19.29	-9.91	-151.39

Kingston Deverill in winter showed a statistically significant increase in Peak A of 62% over 7 days in the light F fraction. We also see a 234% increase in Peak C in the UF fraction but then only a 58% increase in the F fraction. The ratio of Peak C:A tells us that there a clear increase in the UF fraction, but in the F fraction Peak A has increased more over 7 days than Peak C. No data are available in autumn due to time constraints.

Table 11: Fluorescence (RU) change at Kingston Deverill in winter

	0 hours	168 hours	% change
Peak B UF	1.62	3.51	117.12
Peak B F	0.80	1.63	102.93
Peak T UF	1.37	2.85	107.83
Peak T F	0.99	4.50	352.81
Peak A UF	3.80	6.33	66.70
Peak A F	3.46	5.64	62.81
Peak C UF	1.04	3.47	234.03
Peak C F	1.88	2.97	57.92
FI UF	1.40	1.80	28.55
FI F	2.25	1.67	-25.66
FDOM UF	1.00	2.18	118.16
FDOM UF	1.17	2.06	75.62

Table 12: Peak ratio (RU) % change at Kingston Deverill in winter

	0 hours	168 hours	% change
Peak C:A UF	0.28	0.56	98.23
Peak C:A F	0.55	0.53	-3.53
Peak C:T UF	0.93	1.23	31.26
Peak C:T F	2.14	0.88	-58.78
Peak A:T UF	2.88	2.25	-21.87
Peak A:T F	3.84	1.68	-56.21

Hindon Lane Weir showed a decrease in all Peaks, but the F fraction shows a larger decrease in all peaks (see Table 13). The biggest decrease was seen in Peak T light F

Table 13: Fluorescence (RU) change at Hindon Lane Weir in autumn

	0 hours	72 hours	% change
Peak B UF	8.65	1.05	-87.89
Peak B F	14.93	1.34	-91.01
Peak T UF	5.60	1.12	-79.95
Peak T F	13.67	1.13	-91.74
Peak A UF	3.47	0.58	-83.36
Peak A F	6.15	0.70	-88.69
Peak C UF	4.41	0.57	-87.16
Peak C F	6.30	0.56	-91.04
FI UF	1.24	1.51	21.95
FI F	1.69	1.76	4.05

Table 14: Peak ration (RU) % change at Hindon Lane Weir in autumn

	0 hours	72 hours	% change
Peak C:A UF	1.27	0.98	-22.75
Peak C:A F	1.01	0.82	-18.70
Peak C:T UF	0.80	0.51	-36.82
Peak C:T F	0.45	0.50	10.59
Peak A:T UF	0.63	0.51	-18.65
Peak A:T F	0.45	0.62	36.88

Nant Y Brwyn shows the biggest increase in Peak B, followed closely by Peak T. Peaks A and C show similar degradation over 168 hours (see Table 15)

Table 15: Fluorescence (RU) change at Nant Y Brwyn in winter

	0 hours	168 hours	% change
Peak B UF	0.47	2.88	510.71
Peak T UF	0.65	1.45	123.41
Peak A UF	42.42	28.77	-32.17
Peak C UF	23.79	12.59	-47.07
FI UF	1.31	1.39	5.45

Table 16: Peak ratio (RU) % change at Nant Y Brwyn in winter

	0 hours	168 hours	% change
Peak C:A UF	0.56	0.44	-22.29
Peak C:T UF	-13.30	8.92	167.06
Peak A:T UF	-22.51	20.37	190.51

5.2. Impacts of photodegradation processes on C, N and P concentrations in waters

5.2.1. DOC

Across 7 days in the upland sites (Afon Cadnant, Nant y Brwyn, Pentrefoelas), the light UF fractions showed a general decrease in DOC concentration whereas the lowland sites on both chalk (Kingston Deverill) and clay (Priors Farm and Hindon Lane Weir) showed an increase. Fovet et al (2016) showed a similar pattern with an increase in DOC in an incubation of water samples collected from agricultural sites catchments and a decrease in DOC concentrations during incubation of water samples collected from peatland catchments.

Priors Farm although not statistically significant in the autumn (see Figure 22) light samples both showed a general increase over 7 days, with a similar pattern mirrored in the dark

samples. In winter (see Figure 23) the light samples showed an increase of just 0.9% in DOC concentration the UF fraction, but an increase of 9.7% the F fraction. The dark samples showed a 10% increase in DOC concentration in the UF fraction and 5% in the F fraction.

Hindon Lane Weir October the light and dark fractions show similar trends of a maximum decrease between 0-24/48 hours after which there is a sharp increase in DOC concentration. In the light samples the UF fraction increased by 17.42% and the F fraction increased by 25.3%.

In autumn Afon Cadnant showed a slow decrease (7.7%) the light UF fraction and the F fraction showed an increase of 1.69% before decreasing after 3 days but with overlapping error bars to the UF fraction. There was no change in the F dark fraction but there was a 7.5% decrease in the UF dark fraction over 7 days. In winter the light F fraction shows a slow maximum increase up to 48 hours, then the DOC concentration begins to decrease, this trend is also present in the light UF fraction, but the increase isn't as substantial. The dark samples both show a similar pattern to that of the light samples but there is very little variation in the initial increase and then decrease.

At Pentrefoelas the F samples shows a distinct U-shaped curve of increase and decrease across 7 days that is not mirrored in the UF samples that remains stable.

The UF fraction for Nant Y Brwyn in both the light and dark samples shows a distinct decrease around 48 hours before increasing again after 7 days. This pattern is the same for the F dark sample, but the light F sample remains unchanged.

Neither season had any statistically significant results at Kingston Deverill as autumn showed very little variation between UF and F fractions which was not affected by light or dark incubations. However, winter shows a steady increase over 7 days to a total increase of 30% in DOC concentration by day 7 in both the light and dark fraction.

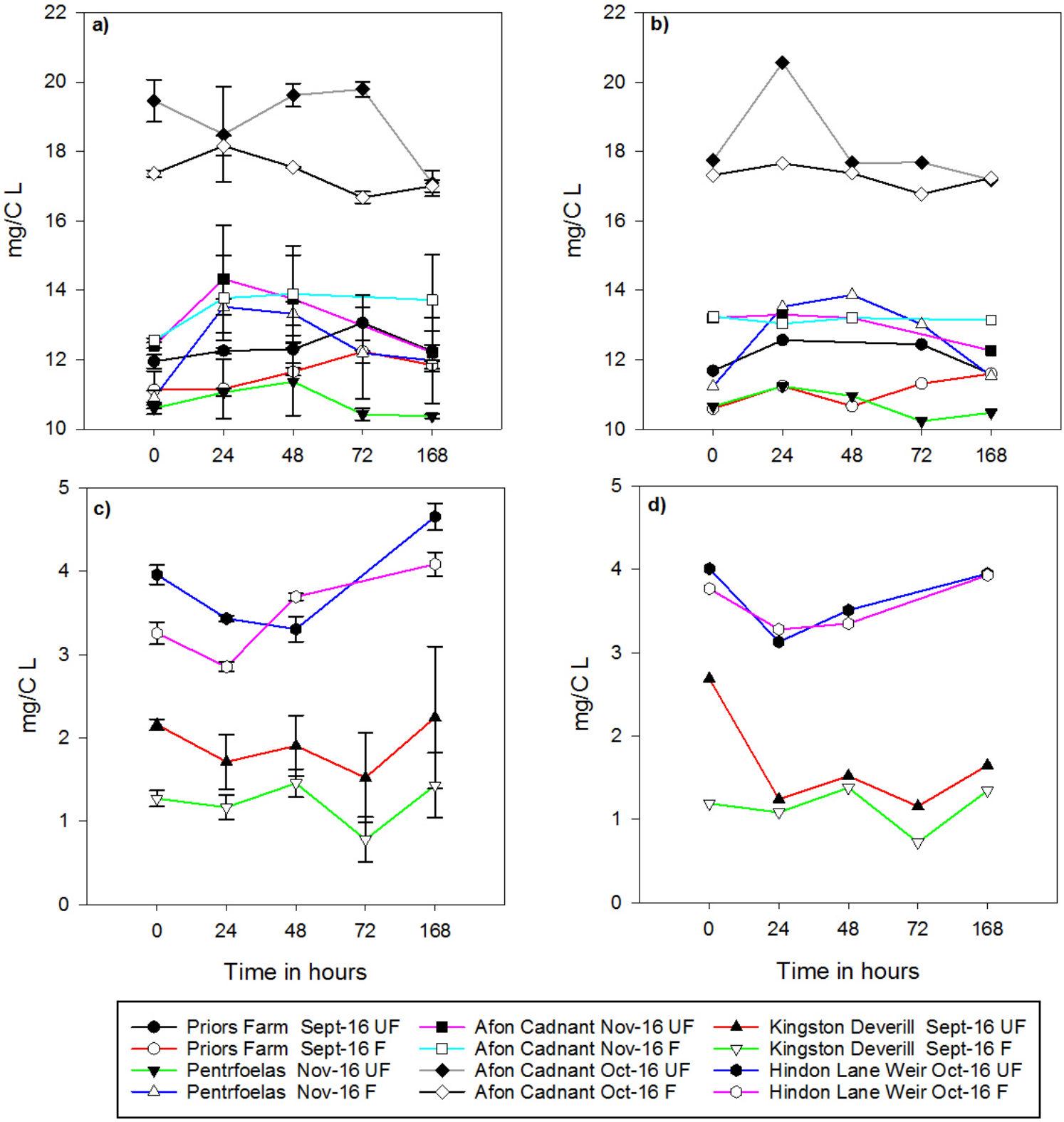

Figure 22: DOC change of light UF and F (a & c) and UF and F dark (b & d) fractions in autumn.

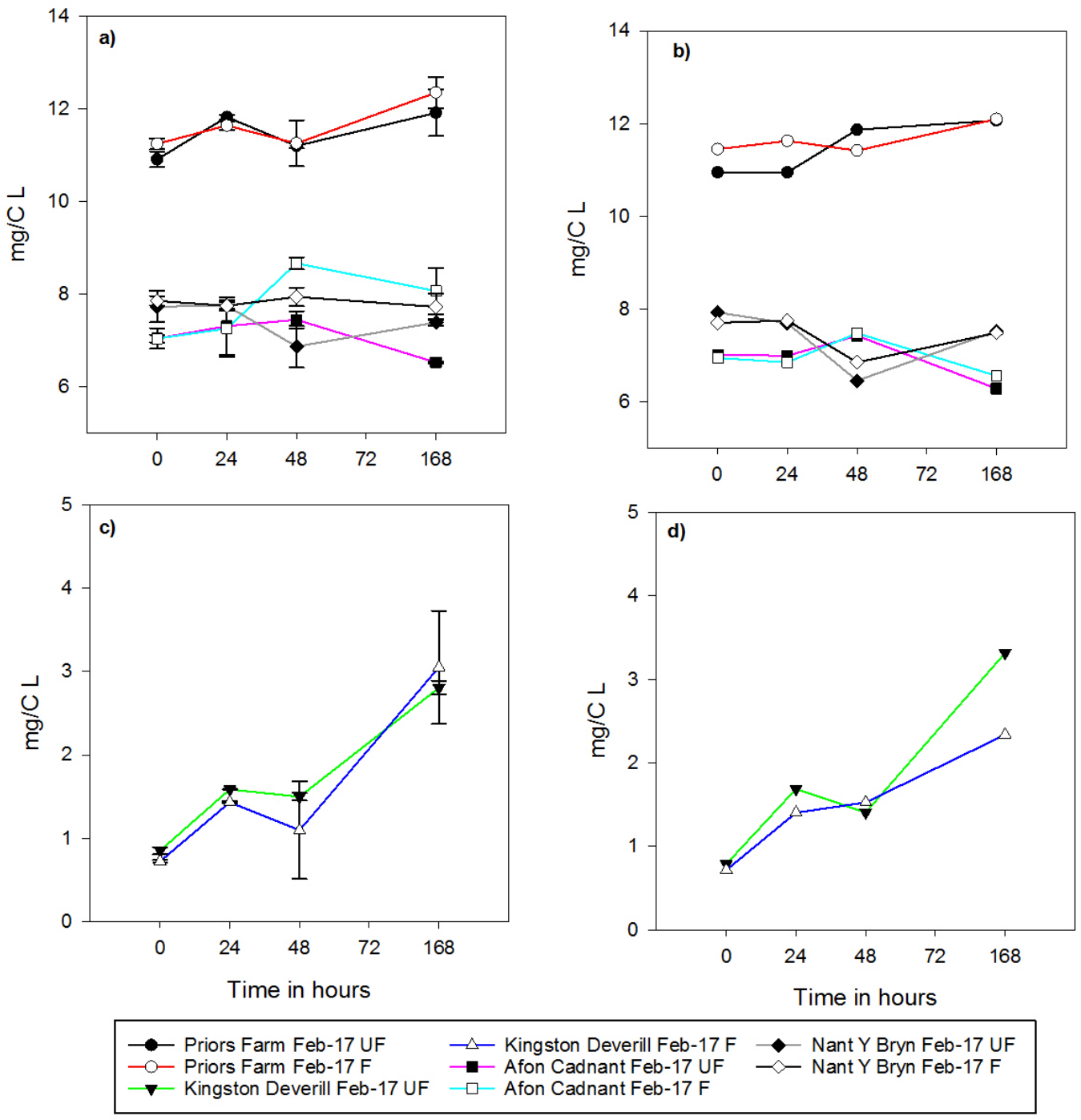

Figure 23: DOC change of UF and F (a & c) and UF and F dark (b & d) fractions in winter.

5.2.2. Nutrient speciation trends

The lowland sites had the highest concentrations of nitrate, ammonia and phosphate, with little or no inorganic nutrients in the upland sites. For all sites bar Priors Farm the nitrite concentration was below the LOD.

Hindon Lane Weir nitrate and ammonia (see Figure 24) showed no significant change in the filtered fraction, but there was a statistically significant reduction (60%) over 7 days in the nitrate light UF concentration and a 98% reduction in ammonia concentration after 48 hours at which point nitrate concentration takes a steep decline between 48 and 168 hours. But over 7 days there was a 50% increase in ammonia in the UF dark fraction, but no change in the F fraction. Phosphate remained below the LOD throughout the experiment.

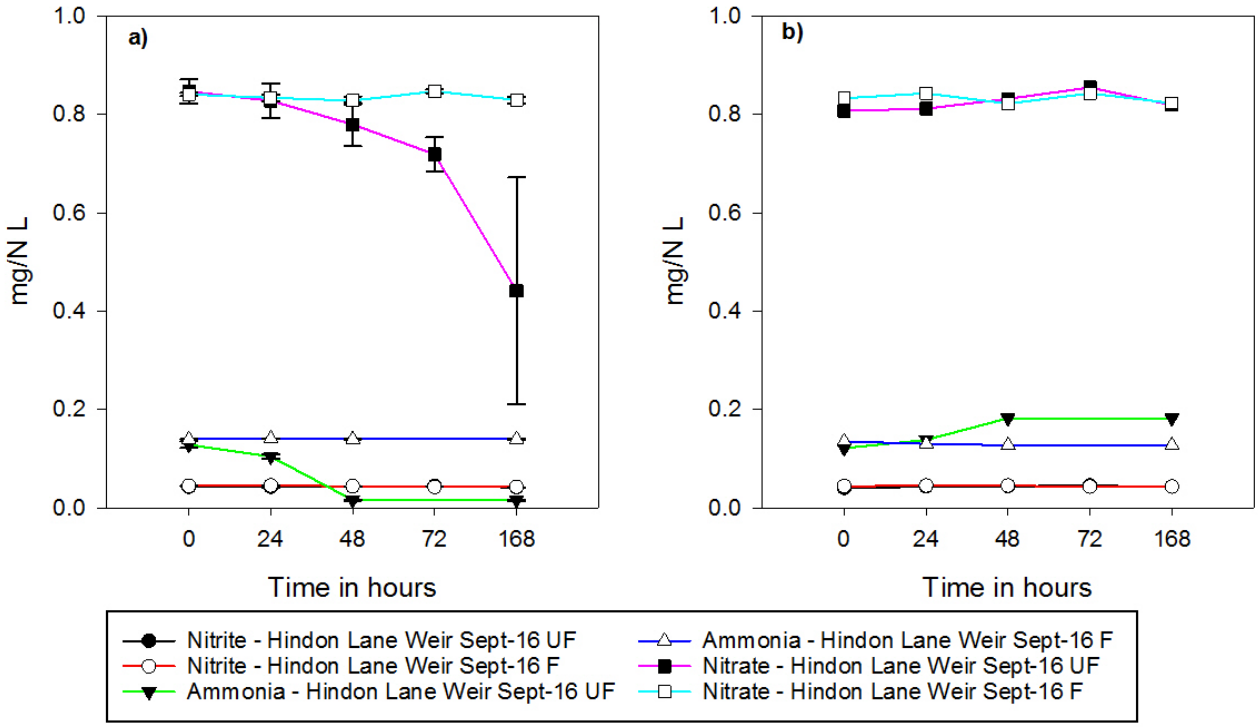

Figure 24: Hindon Lane Weir nitrate and ammonia change in light (a) and dark (b) in winter.

Priors Farm shows no changes in the inorganic fractions in autumn that were statistically significant (see Figure 25), although there is a clear decline in the nitrite concentration in all fractions over 7 days. There is also a slow decline in phosphate concentrations in the UF and F light samples,

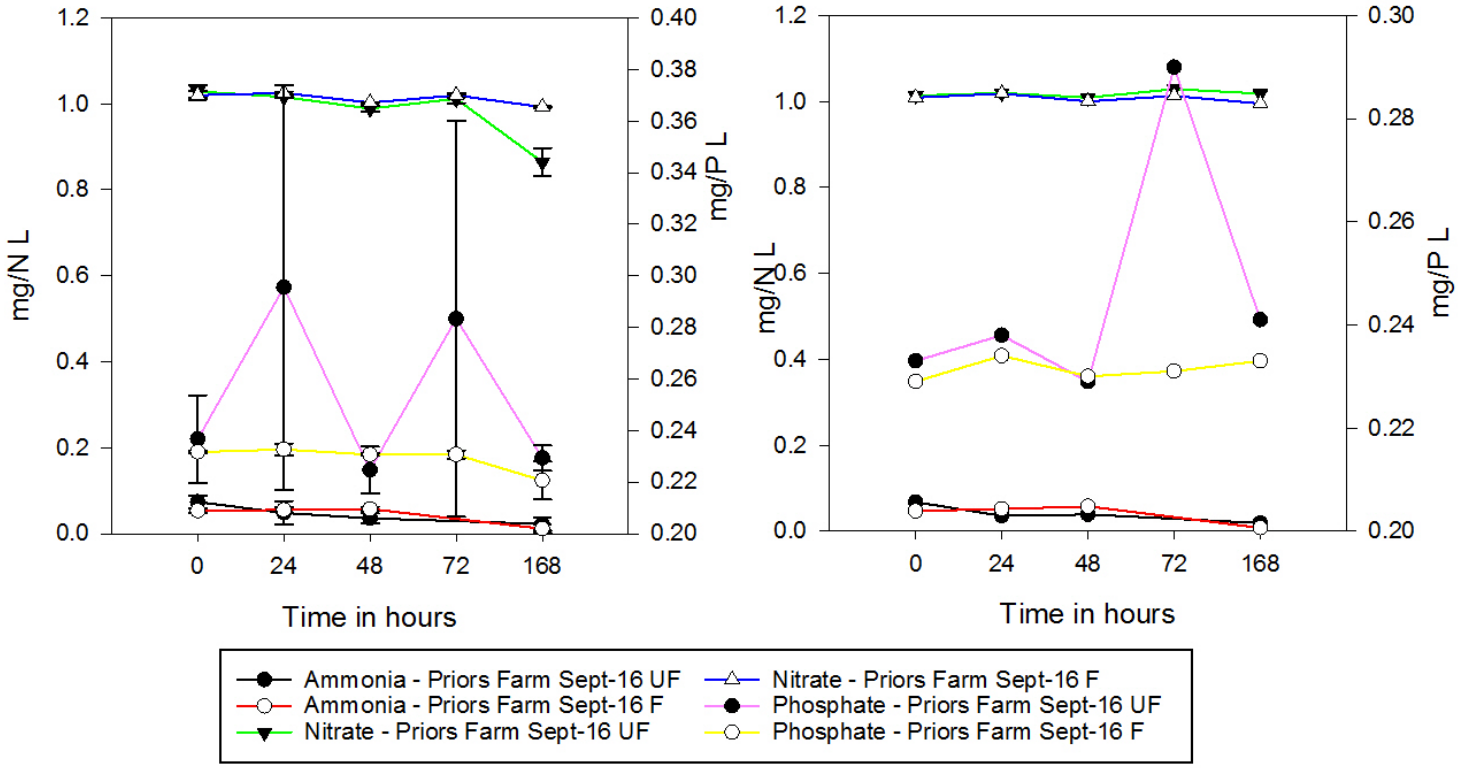

Figure 25: Priors Farm nutrient change in light (a) and dark (b) in autumn.

In contrast to autumn in winter there is a slow increase in nitrite concentration but only in the UF light and UF dark fractions (see Figure 26). The ammonia concentration in the F samples shows a similar increase after 3 days, this pattern is also present in the UF dark fraction, and however we see a decrease in the UF light sample that is reflected in the increase nitrite concentration. Phosphate concentrations display an inverse U-shape of increase and decrease in the light samples that is mirrored in the F dark sample but the UF dark samples shows a steady increase across 7 days.

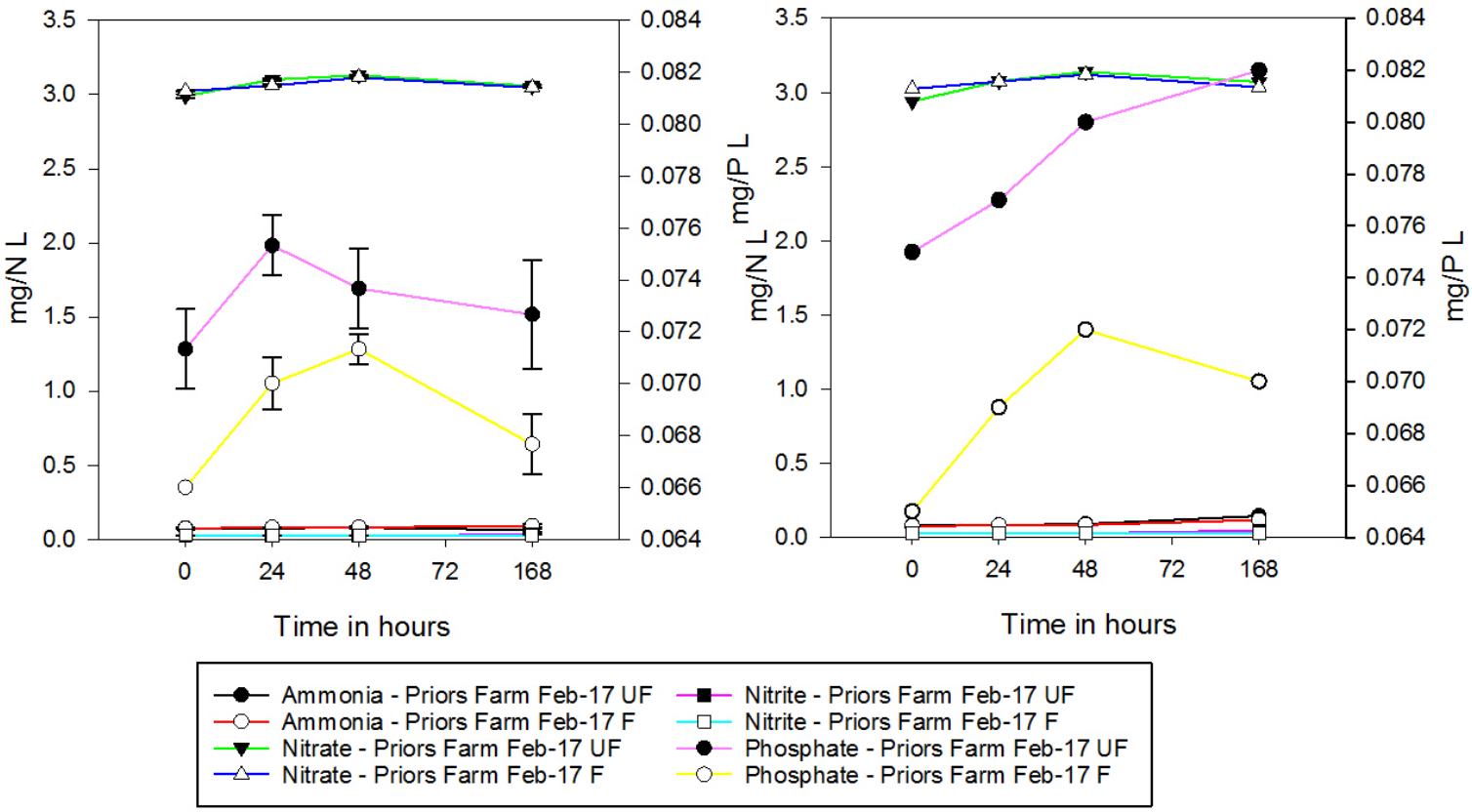

Figure 26: Priors Farm nutrient change in light (a) and dark (b) in winter.

A Statistically significant pattern is seen in both the light and dark fractions with a TDP decrease of 25% between day 1 & 3 days in UF fraction with a 2% decrease in the F fraction, with the DOP following a similar pattern in winter (see Figure 27). PP had the same trend but with an increase of 25% which matches the transformation of dissolved to particulate form. There are no data available for day 1 in the F and F dark fraction. Little or no change was observed in the nitrate values and at 0 hours PON and DON was less than the LOD in the light F fraction.

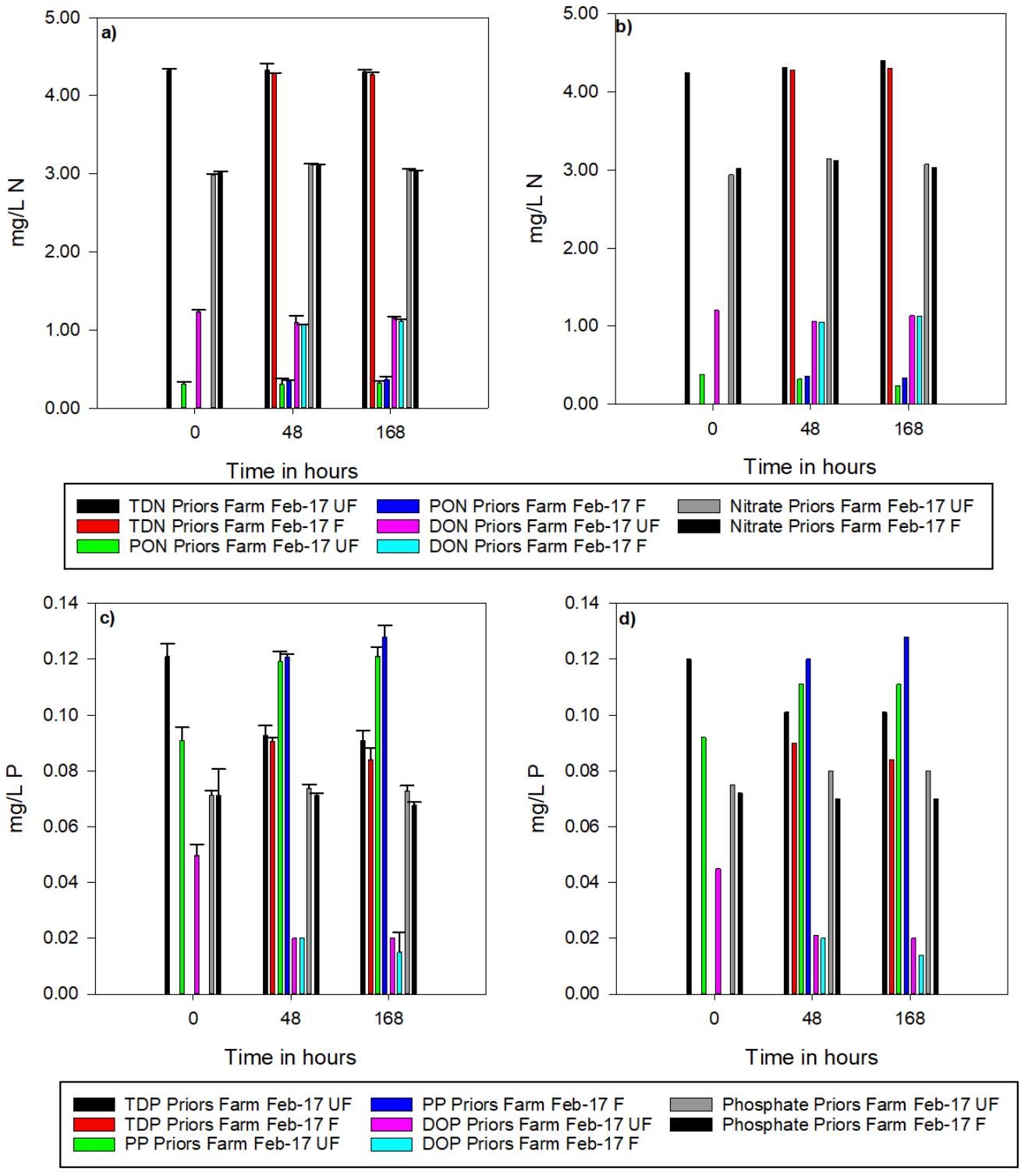

Figure 27: Priors Farm nitrate and phosphate transformation of light UF and F (a & c) and UF and F dark (b & d) fractions in winter.

Kingston Deverill showed no statistically significant changes in autumn, but there is a clear decrease in inorganic nutrients across 7 days (see Figure 28 and Figure 29)

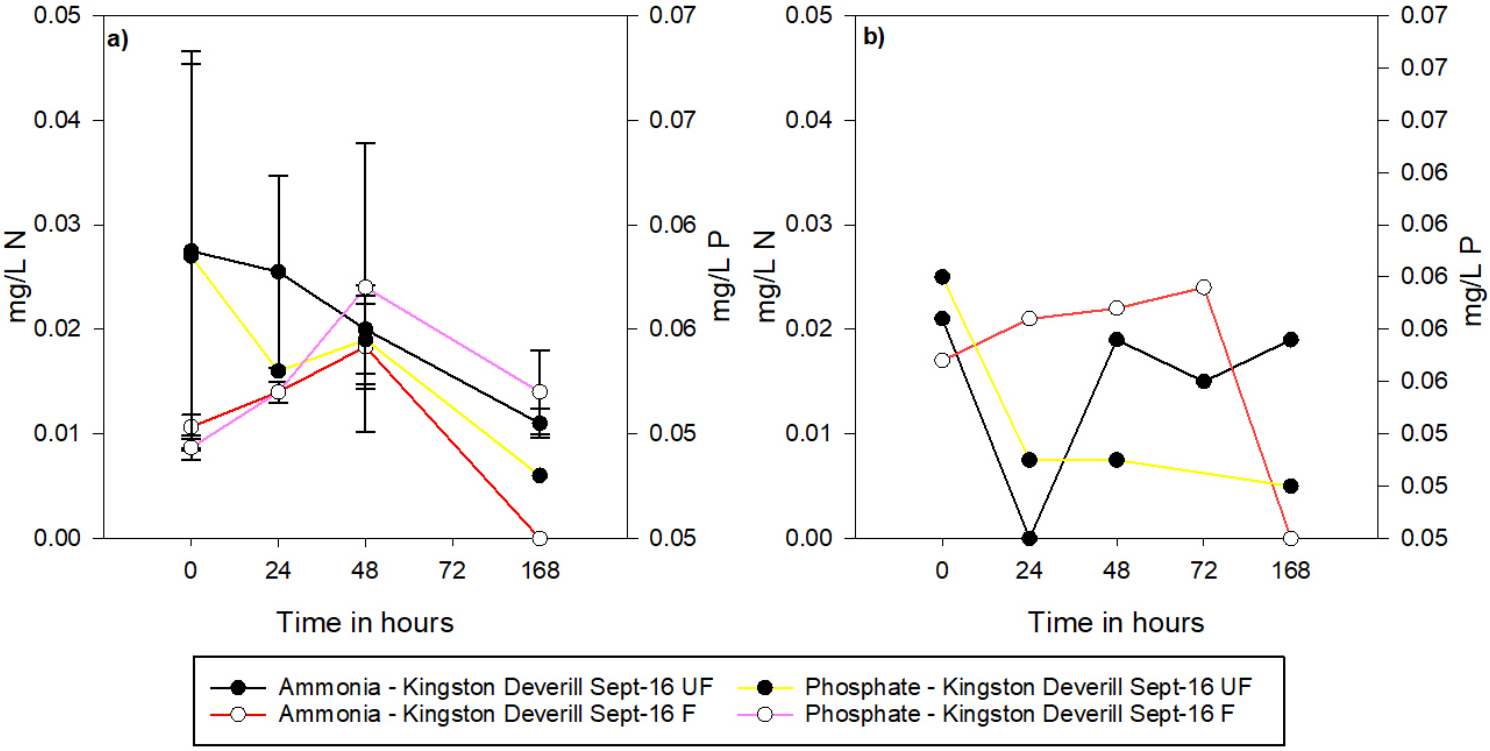

Figure 28: Kingston Deverill nutrient change in light (a) and dark (b) fractions in autumn

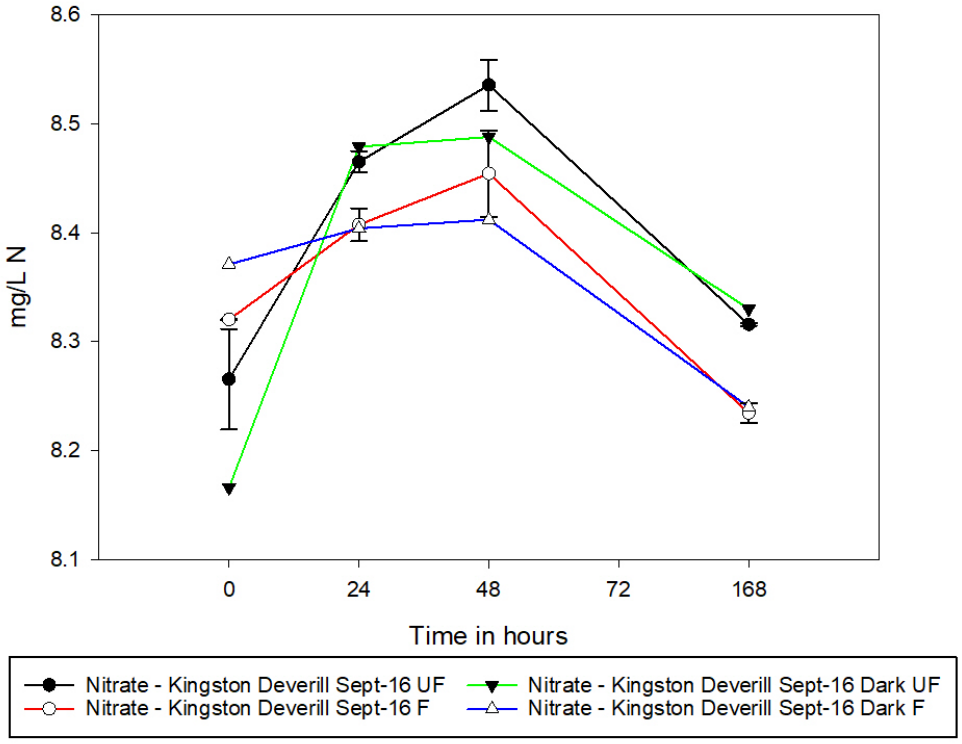

Figure 29: Kingston Deverill nitrate change over 7 days in autumn

The ammonia concentration remains relatively stable through the course of 7 days in the UF light and dark fractions but shows a decrease over 7 days in the F light and dark fractions in winter (see Figure 30).

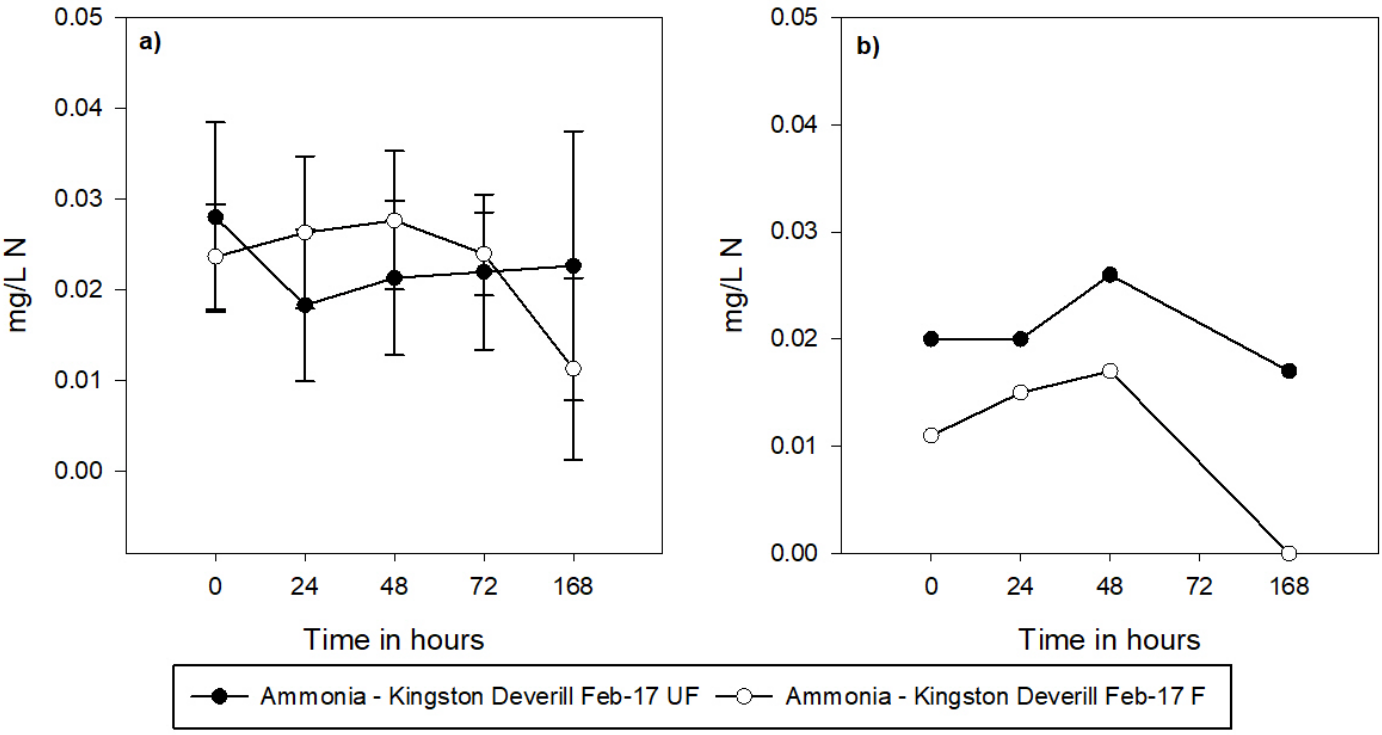

Figure 30: Kingston Deverill ammonia change in light (a) and dark (b) fractions in winter

In winter the following trends were statistically significant over 7 days (see Figure 31) the TDN changed in both fractions with a 2% increase in the UF fraction and a 3% decrease in the F fraction. This is mirrored with an increase in PON of 2%. No change in DON for both fractions, but in the UF fraction there was no change in nitrate, but F fraction decreased over 7 days. There are no data available for the dark fraction. There are no phosphate data due to erroneous results in the data.

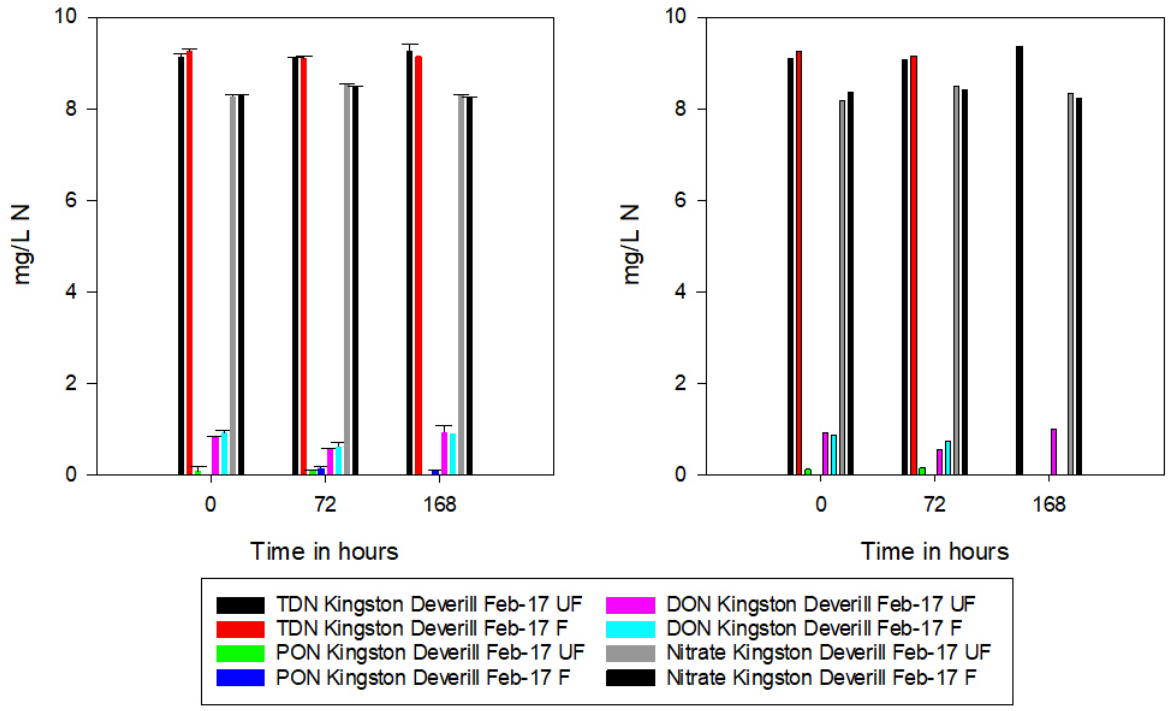

Figure 31: Kingston Deverill nitrogen transformation in light (a) and dark (b) in winter.

Autumn at Afon Cadnant showed a statistically significant gradual decrease for the nitrate concentration across 7 days with a total decrease of 56% in the light UF fraction and a 16% reduction in the light F fraction (see Figure 32), with a similar pattern seen in the dark controls but the decrease is not as great. This pattern is reversed in the ammonia concentrations with the biggest increase seen between 72 and 168 hours.

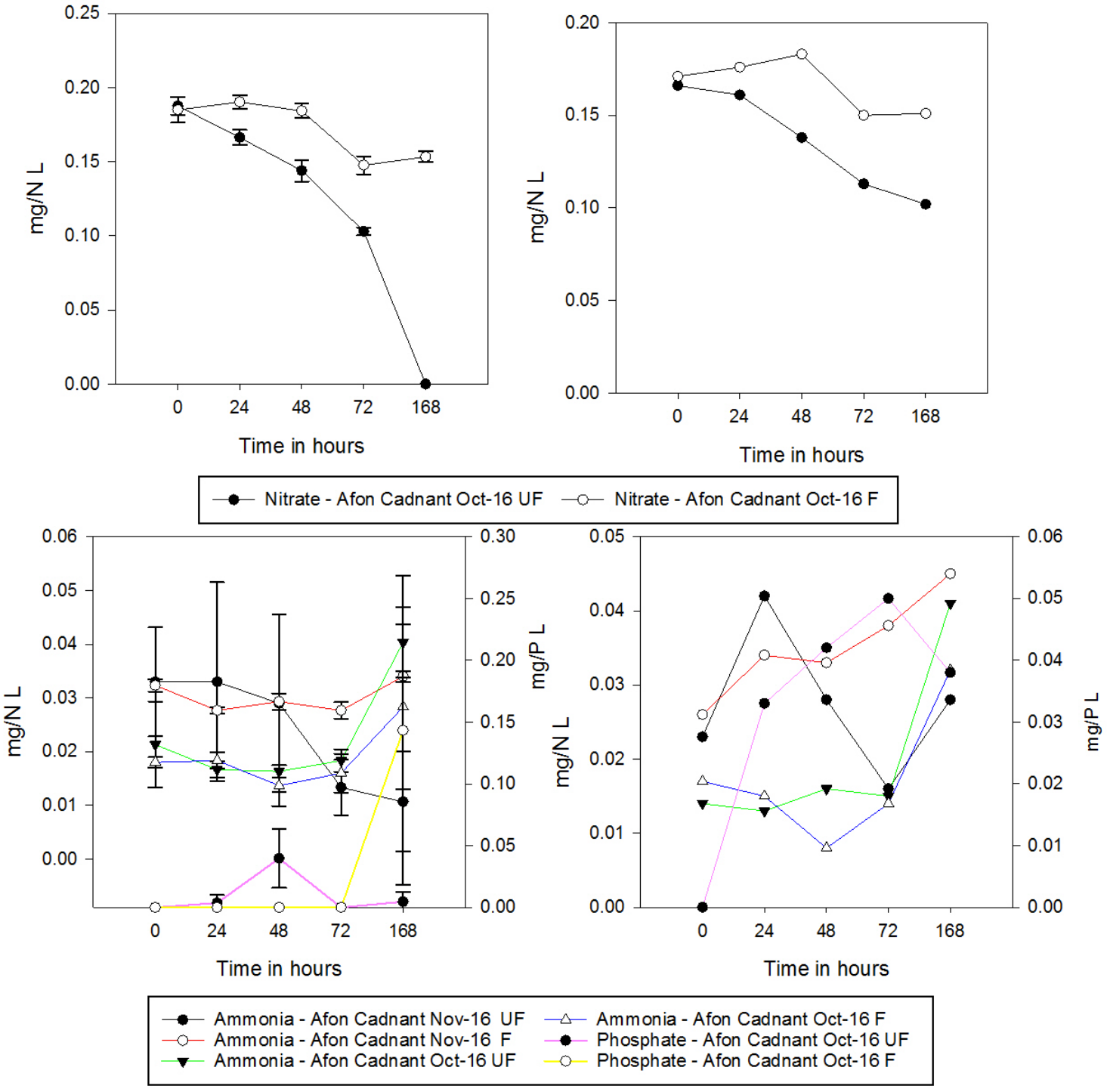

Figure 32: Afon Cadnant nutrient change in light (a & c) and dark (b & d) in autumn.

In contrast to autumn the ammonia concentration gradually decreases in the only the F fraction in both the light and dark samples, with little or no change in the UF samples (see Figure 33). There was a statistically significant decrease in TDN between days 1 and 3 in the

UF fraction that is mirrored in the UF DON (see Figure 34). Slight decrease in the F fraction for between day 1 and 3 but then remains stable in the TDN & DON. There are no dark data available and PON was below the LOD. Phosphate data have not been included due to erroneous results that displayed a DOP greater than TDP.

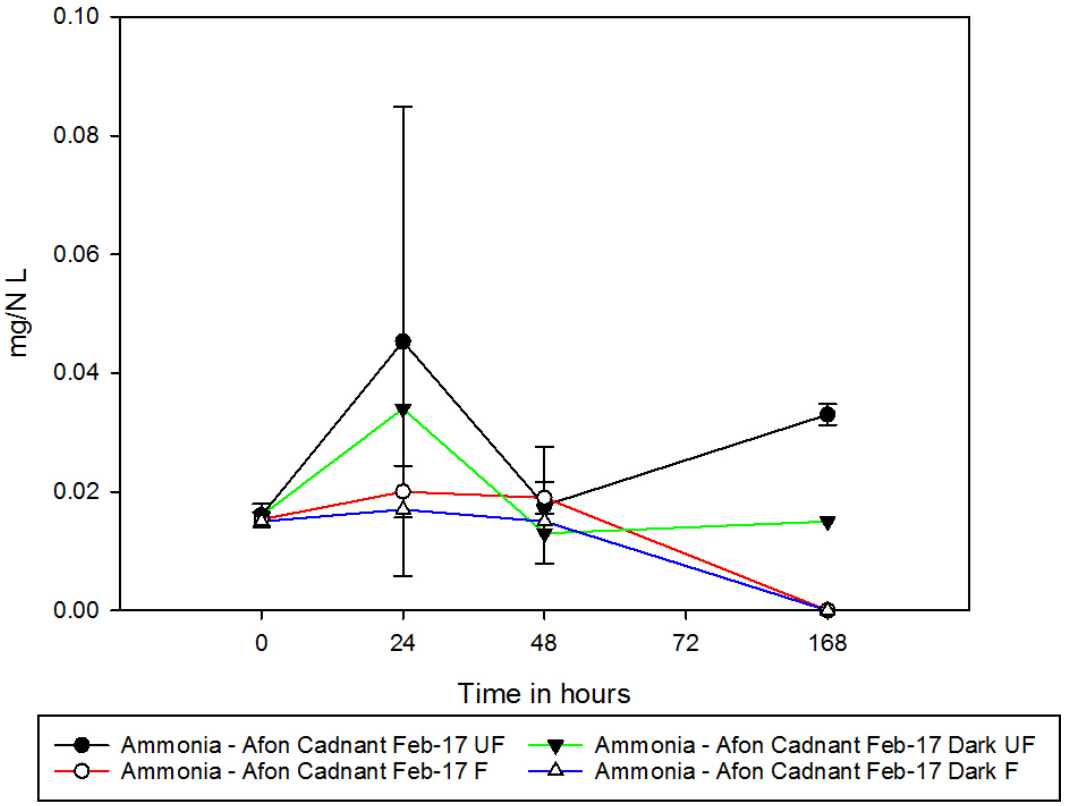

Figure 33: Afon Cadnant winter change in ammonia over in winter.

The initial decrease in TDN concentration between day 1 & 3 across all fractions, could be explained via a loss of nitrogen through denitrification, however this is unlikely as there are no statistically significant changes in ammonia nitrogen, nitrate and or Nitrite across 7 days. There is also no noticeable change in any other fractions between days 1 and 3, it more likely that this is an erroneous result.

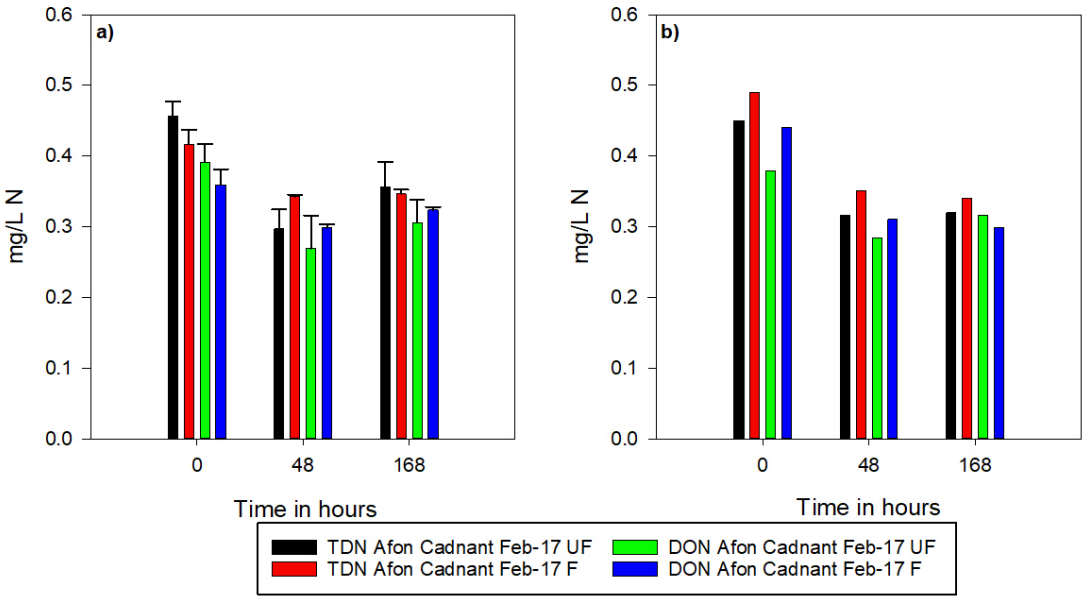

Figure 34: Afon Cadnant nitrate transformation in light (a) and dark (b) in winter.

Nant Y Brwyn follows the same pattern in ammonia transformation as the Afon Cadnant winter sample with a decrease in only the light and dark F sample (see Figure 35).

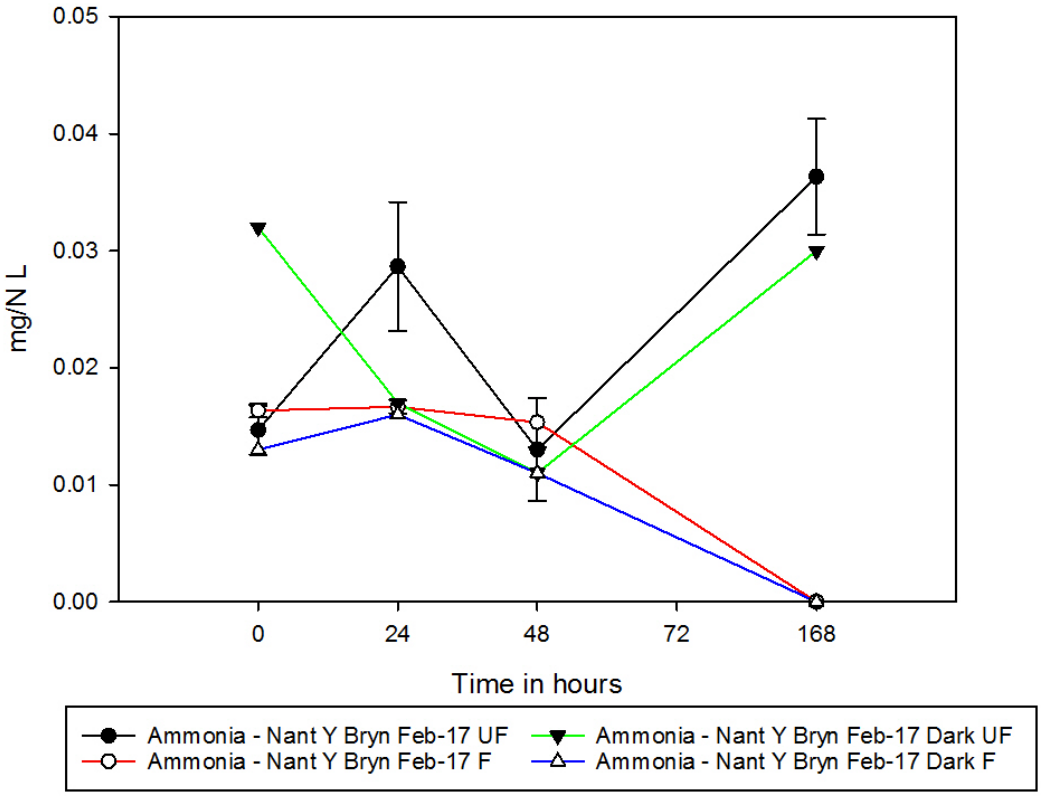

Figure 35: Nant Y Brwyn ammonia change in winter

The nitrate concentration at Pentrefoelas shows a slow decrease between 0 and 48 hours in both the UF and F light and dark samples before a slight increase and then decreasing again (see Figure 36). There is little or no change in the F ammonia in the light and dark samples, with a slow gradual decrease in the UF fractions. The UF and F fractions shows identical patterns in their light and dark counterparts; the UF samples remain stable for the first 72 hours then decrease to less than the LOD by 7 days. The Initial starting concentration for the F sample was below the LOD and did not increase until after 24 hours and shows an inverse U-shape before returning to less than the LOD by 7 days.

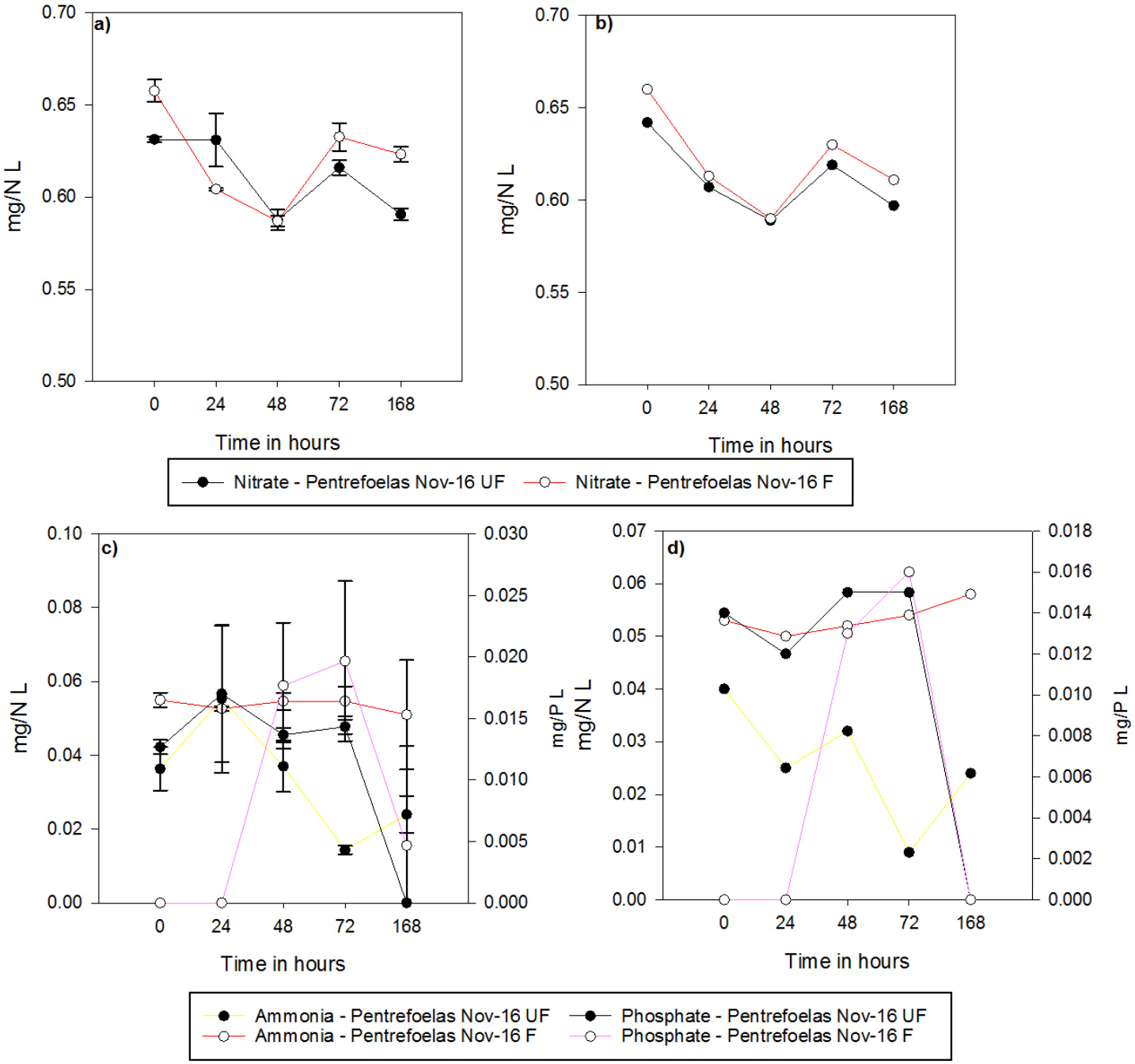

Figure 36: Nutrient change in light UF & F (a & c) and dark UF and F (b & d) at Pentrefoelas during autumn.

6. Discussion

6.1. Impacts of photodegradation processes on DOM character, as inferenced from UV-Visible spectrophotometry and fluorescence.

The DOM character At Afon Cadnant is dynamic and varies throughout the hydrological calendar. This variation affects the dominant pathway through which DOM is transformed: as the biota can metabolise DOM in autumn and winter but their substrate varies between these seasons, but photodegradation is only impacting upon the DOM present in winter.

Afon Cadnant had the highest SUVA values inferring a high content of aromaticity, With concentrations similar to those observed by (Fovet et al., 2016; Jones et al., 2016) with little variation between autumn and winter. In autumn the absorbance at 254nm highlights that the CDOM transformations are the result of microbial processing that is not light dependant as the decrease is mirrored in both the light and dark samples and not through the expected route of photodegradation. This decrease is reflected in an increase in the S_r as LMW DOM is being produced. This demonstrates that the biota present prefer to metabolise HWM DOM rather than use the easily available LMW DOM.

During winter both the absorbance at 254nm and the S_r are approximately half the original values when compared to autumn. Even though there is less chromophoric DOM present as inferred from the decrease in absorbance at 254nm, we now observe photodegradation of Particulate Organic Matter (POM), as the increase cannot be the result of microbial processing as we would see this process mirrored in the UF sample. What we see in the UF samples is a decrease in absorbance, demonstrating that in contrast to autumn the biota present are actively metabolising the freely available LMW DOM. Which is evidenced in the constant value in the S_r for the UF sample, but in the F sample we see an increase in the S_r from the freshly degraded POM.

During autumn Peaks B & T that are associated with algal and aromatic protein like fluorescence respectively both show a large decrease over 168 hours, this reduction insinuates the lack of microbial transformation in the samples occurring and as this degradation is also occurring in the dark samples, it must be the result of chemical degradation rather than that of photodegradation.

Peaks A & C increased between 0 hours and 168 hours in both the light and dark UF and Fractions. As highlighted earlier Peak C had the biggest increase in the UF fraction (100%) with only a 79% increase in Peak A again highlighting the difference in the DOM pools between these 2 peaks. However, looking at the peak ratios for each Peak There is a greater increase in the F fraction than the UF fraction and the UF dark fraction has a bigger increase in all peaks than the UF light fraction. This could indicate a large transformation of DOM by bacteria that are hindered through exposure to light as comparing the light UF and UF dark samples a similar pattern can be seen. However, exposing samples to a high dose of UV radiation may have increased microbial exudation of DOC (Jack et al., 2002) and therefore increasing all the fluorescent peaks.

Nant Y Brwyn showed a large decrease through photodegradation but also showed a highly active microbial community which was to be expected given the chromophoric nature of peatland DOM. Nant Y Brwyn displays a similar trend to that of the winter Afon Cadnant sample, in that the absorbance at 254nm decreases in both the UF light and dark sample that is the results of microbial processing, but there is little change in the S_r. The F fraction however, shows no change in absorbance at 254nm but shows a large increase in LMW DOM evidence by the increase in S_r proving that the LMW DOM produced does not absorb in the UV region a process also observed by (Xiaodong and Green, 2004) and that the lack of increase in the S_r in the UF fraction, tells us that the biota are metabolising the freshly produced LMW DOM.

The fluorescence peaks show a decrease in all but Peaks B & T that suggest there is a large bacterial and algal community metabolising in the UF sample. The decrease in all other peaks highlights the chromophoric nature of the DOM present in this peatland site due to the presence of high concentrations of HMW aliphatic and aromatic compounds derived from plant material that is not present at Afon Cadnant.

At Pentrefoelas the complete lack of change in S_r in the light F fraction highlights the lack of CDOM available for photodegradation and is a similar pattern to Priors Farm which is also mainly improved grasslands. The absorbance at 254nm SUVA remain unchanged in both the UF and F samples showing no biological and or photochemical transformation. However the

fluorescence peaks all degraded at the same rate as their light and dark, UF and F counterparts but as Peaks B & T are degrading it is assumed that there is no microbial transformation occurring and that the decreases observed are the result of photodegradation in the visible range and that there is some form of chemical degradation occurring in the dark samples.

Priors Farm showed little or no photodegradation which is a similar pattern to Pentrefoelas as the surrounding land use is mainly improved grasslands. Priors Farm was not very susceptible to photodegradation, but its microbial community showed a greater affinity for creating HWM DOM that was not chromophoric.

The difference in S_r at Priors Farm between autumn and winter is negligible and suggests that the catchment character has very little variation impacting upon the amount of LMW or HMW compounds present. The lack of change in autumn S_r suggests that there is little CDOM present and that the DOM is relatively recalcitrant to biota, this is further supported by the lack of change in absorbance at 254nm and SUVA. However, all the fluorescent peaks are decreasing which infers that there is CDOM present but is not absorbing in the UV spectrum and that is absorbing in the visible spectrum.

During winter a similar pattern is seen in the S_r between the UF and F fractions suggesting that the biota are not utilising the increased levels of LMW DOM and are inactive. This theory is supported by the fact that there is no decrease in the dark UF fraction i.e. there is no transformation of DOM occurring. As there is also no change in the absorbance at 254nm the increase in S_r in winter would be the result of the photodegradation of POM. As with autumn we can see a decrease in all F fraction fluorescence peaks that must be absorbing in the visible spectrum but in the UF fraction we can see an increase in both Peaks B & T that indicate microbial and algal processing and increase in Peaks A & C that highlights the biota are producing HMW humic like substances similar to the findings of (Fox et al., 2017) but the produced DOM does not absorb in the UV region. The biota is producing so much HMW DOM it negates any photodegradation occurring and is increasing the concentration of the DOM pool.

Kingston Deverill had the lowest initial S_r which is to be expected as this site is primarily groundwater fed and LMW compounds will have been metabolised first such as aliphatic

material, including proteins, carbohydrates, and organic acids (Coble et al., 2014; Hansen et al., 2016).

Kingston Deverill in autumn is demonstrating that photodegradation is not the sole cause of DOM transformation at this site as the UF fraction shows a greater increase in LMW DOM that must be the product of biological transformations occurring. Increasing concentrations of LMW DOM are also present in the UF winter sample and again there is no change in the absorption at 254nm. In parallel the SUVA values are decreasing highlighting that there is a biological transformation of HMW aromatic carbon possibly as the result of oligotrophs due to these changes being present in both the light and dark fractions. Due to similar trends seen in both the UF and F fractions in the light and dark samples, it is assumed that there is biota in the F sample, which is also evidenced by the increase in Peak T & B fluorescence.

Hindon Lane Weir in autumn had the highest initial S_r. Over 7 days the absorbance at 254nm increased in only the UF sample due to the biota producing chromophoric LMW DOM that is evidenced in the increase in S_r. The fact that the UF light and dark samples display a similar trend implies that non-photo dependant microbiological processes are occurring. Even though we do not see a change in the absorbance at 254nm in the F sample the decrease seen in fluorescence peaks at Hindon Lane Weir in both the light UF and F samples (which is greater in the F fraction) highlights a large portion of FDOM is susceptible to photodegradation but absorbs in the visible spectrum. A similar pattern was also seen by (Bertilsson and Tranvik, 2000) who stated that most lakes in the temperate climate region, are likely to be influenced by a solar driven photochemical production of DIC and carboxylic acids which would increase the levels of LMW DOM, but at this site the production of LMW DOM is the result of microbial processing.

6.2. Impacts of photodegradation and biodegradation on the processing on C, N and P concentrations in waters

Priors Farm in autumn thus shows an increase in DOC concentration in both unfiltered and filtered fractions and in both light and dark samples. This might indicate a breakdown of POC through photodegradation and or DOC production through photosynthesis which would be generally be of low molecular weight/size, highly labile and transparent (Brock and Clyne, 1984). If this was the case, we would expect to see an increase in the Sr for the UF fraction which we do not, but what we do see is a slow decrease in ammonia concentration but as there is no increase in nitrite and or nitrate, the ammonia must be undergoing conversion to nitrous oxide.

The DOC increase in winter in the UF dark fraction at Priors Farm is like that of the light control a process also observed by (Jones et al., 2016) and a few studies have considered the potential for chemolithoautotrophic bacteria in aquatic systems to utilise DIC to produce DOC. The most reported examples of dark carbon fixation are however associated with specific conditions that favour redox processes, such as very acidic rivers with high concentrations of heavy metals but the pH of this site was roughly 7.2 meaning that this might not apply at this site, given it is not acidic. The UF light and dark samples show clear ammonification through the decrease in DON, ammonia and then an increase in nitrite but no increase in nitrate results. This process is mirrored in the UF dark samples but there in a larger increase in nitrite and the ammonia concentration increased. The light F sample showed an increase in ammonia concentration through photodegradation as there is no reciprocal increase in nitrite concentration.

The photochemical release of ammonia from DOM likely occurs via more than one method as ammonia release is at least partially dependent upon hydroxyl radicals (Tarr et al., 2001; Wang et al., 2000). Filtering the samples likely removed smaller particulate phosphate that is incorporated into the dissolved phase and hence the difference in initial concentration between UF and F samples. A large fraction of phosphate is being converted to PP this is especially so in the light and dark F fraction.

Between autumn and winter at Afon Cadnant there is an 80% reduction in initial DOC concentration, a process also observed in the absorbance at 254nm and S_r highlighting the transformation and mobility of DOC concentrations in acid grassland systems through autumn and winter. Which is consistent with a flushing effect whereby DOM produced over the summer is transported and delivered to rivers by an increase in rainfall events (Eimers et al., 2008; Pickard et al., 1963) . At Afon Cadnant in autumn the initial increase in the F fraction and the then the lack of DOC decrease could indicate a lysing of the cells via filtration, but this is unlikely as it is not mirrored in the F dark fraction so could be an initial photodegradation of POC as it is mirrored in the UF fraction and that there is no initial increase in the UF dark fraction.

After 3 days the decrease in the UF and UF dark fraction DOC must be explained via microbial processing that is non-photosynthetic as biological activity in aquatic systems is usually considered to consume DOC (but not always) via respiration, and to contribute to the DOC pool only as dead cells, while production of DOC is attributed to either photosynthetic primary production or to the breakdown of POC (Dawson et al. 2001). Fovet et al (2016) had similar increases in DOC identifying the only potential carbon production sources as either POC, via desorption, photo-degradation or biodegradation, or DIC, via dark carbon fixation. The increase seen in only the light F fraction of Afon Cadnant in winter and Pentrefoelas in autumn could be through the degradation of POC that is being utilised by the biota in the UF sample.

The observed decrease and increase in nitrate and ammonia respectively could be an indication of fermentative dissimilatory nitrate reduction to ammonia (DNRA) as fermentative DNRA is thought to be favoured in nitrate-limited environments rich in labile carbon (Burgin and Hamilton, 2007). Nant Y Brwyn displays little or no variation in nutrient transformations in winter apart from a similar pattern to that of the winter Afon Cadnant site in that the decrease in ammonia concentration is only seen in the F samples.

During autumn at Hindon Lane Weir even though there was little or no change in the DOC pool, it was clear that during the first 3 days ammonia was being metabolised until this energy source was exhausted and at this point nitrate was then being metabolised. The dark controls show little or no variation in the nitrate concentration, and it is then assumed

that the biota present are photo reactive and due to the lack of light there is no energy available to metabolise the nitrate. But over 7 days there was a 50% increase in ammonia in the UF dark fraction, yet no change in the F fraction. The fact that we see a complete uptake of ammonia in the light samples highlights that the biota is unable to utilise the DON present and that there is little or no release of ammonia from the photodegradation of DON. The increase in ammonia concentration in the UF dark sample would suggest that there is a breakdown of DON in the dark.

In September at Kingston Deverill initial there is an initial dip then increase in both the light and dark fractions for DOC that is mirrored in the nitrogen transformations. The correlation between the decrease in ammonia and increase in nitrate concentration highlights ammonification occurring but after 48 hours the ammonia is exhausted and nitrate concentrations begin to decrease through denitrification. A similar decrease is observed in the F light winter sample but shows no increase in nitrate concentration. The slow decrease observed in the light UF ammonia and phosphate is the result of microbial degradation as an increase is observed in the light Fraction from the photodegradation of DON/PON and DOP/PP into ammonia and phosphate. This pattern of increasing ammonia concentration is also seen during the winter months but at a much smaller rate .

Pentrefoelas shows little or no metabolism of DOC in the light and dark UF fraction, but with large increases seen in the light F fraction that suggests that a large portion of POC is undergoing photodegradation, however this trend is mirrored in the dark F fraction. The slow decrease in ammonia over 7 days in both the UF light and dark fractions highlights that the transformation is not photo dependant (further supported via the lack of transformation in the F fractions). An expected increase in either DON and or nitrate concentration is also not observed and is decreasing over 7 days in both the UF light and dark samples, this would indicate that the metabolised ammonia is being converted into a gaseous form.

7. Conclusions

In the upland sites seasonality had a profound impact upon the DOM pool by altering the surrounding hydrology as evidenced by the fact that the peatland and acid grassland sites showed a vast difference in their DOM character. There were up to 80% reductions in the DOC concentrations between autumn and winter and large decreases in their absorbance at 254nm (which is highly susceptible to photodegradation) due to increasing rainfall events flushing out DOM. However, in contrast lowland areas showed little variation between autumn and winter highlighting a more stable hydrology which is to be expected as Kingston Deverill is supplied from aquifer source waters.

This thesis highlights that photodegradation is still a major pathway in the transformation of DOM during autumn and winter evidenced by the reduction in DOC and CDOM concentrations but that it is site and season specific. In terms of their spectroscopy upland sites had similar characteristics but behaved markedly different between autumn and winter, with photodegradation having the greatest impact during the winter months with large amounts of HMW DOM being converted to LMW DOM. In lowland sites photodegradation had little or no impact due to the low concentrations of CDOM and photoreactive compounds.

Even though LMW DOM is generally easier to metabolise for microorganism, the data has highlighted that the biota present does not always utilise this readily available food source. In the upland sites this is especially so during the autumn months, but during the winter the biota are actively metabolising LMW DOM produced from photodegradation. In the lowland sites there was a large variation in DOM transformation via biota that ranged from the production of HMW compounds to the transformation of HMW to LMW DOM with no evidences to suggest any metabolism of the newly produced LMW DOM.

Future work should focus on the qualitative analysis of the photodegradation products such as LMW DOM, as these can be metabolised by biota and how these photodegradation products vary seasonally. It is also crucial to investigate the LMW CDOM being produced as a bi product of metabolism and how the freshly produced CDOM is susceptible to photodegradation.

To conclude few studies have focused upon photodegradation during the autumn and winter months due to its perceived low impact upon DOM transformations. But this thesis has highlighted that even in the winter months photodegradation still plays a critical role and at some sites is the major pathway in the transformation of DOM.

8. Appendix

See attached CD for research data

9. Bibliography

Aitkenhead, J.A., McDowell, W.H., 2000. Soil C:N ratio as a predictor of annual riverine DOC flux at local and global scales. Global Biogeochem. Cycles 14, 127–138. doi:10.1029/1999GB900083

Allen, D.J., Darling, W.G., Davies, J., Newell, A.J., Gooddy, D.C., Collins, A.L., 2014. Groundwater conceptual models: implications for evaluating diffuse pollution mitigation measures. Q. J. Eng. Geol. Hydrogeol. 47, 65–80. doi:10.1144/qjegh2013-043

Anesio, A.M., Tranvik, L.J., Granéli, W., 1999. Production of inorganic carbon from aquatic macrophytes by solar radiation. Ecology 80, 1852–1859. doi:10.1890/0012-9658(1999)080[1852:POICFA]2.0.CO;2

Babic, O., Simeunovic, J., Skrbic, N., Kovac, D., Svircev, Z., 2013. Detection of phosphatase activity in aquatic and terrestrial cyanobacterial strains. Zb. Matice Srp. za Prir. Nauk. 31–42. doi:10.2298/ZMSPN1325031B

Baker, A., Tipping, E., Thacker, S.A., Gondar, D., 2008. Relating dissolved organic matter fluorescence and functional properties. Chemosphere 73, 1765–1772. doi:10.1016/j.chemosphere.2008.09.018

Benner, R., 2003. Molecular Indicators of the Bioavailability of Dissolved Organic Matter. Aquat. Ecosyst. 121–137. doi:10.1016/B978-012256371-3/50006-8

Benner, R., Kaiser, K., 2011. Biological and photochemical transformations of amino acids and lignin phenols in riverine dissolved organic matter. Biogeochemistry 102, 209–222. doi:10.1007/s10533-010-9435-4

Bentzen, E., Taylor, W.D., Millard, E.S., 1992. The importance of dissolved organic phosphorus to phosphorus uptake by limnetic plankton. Limnol. Oceanogr. 37, 217–231. doi:10.4319/lo.1992.37.2.0217

Berg, V.D., Leon, J., Shotbolt, L., Ashmore, M.R., 2012. Dissolved organic carbon (DOC) concentrations in UK soils and the influence of soil, vegetation type and seasonality. Sci. Total Environ. 427–428, 269–276. doi:10.1016/j.scitotenv.2012.03.069

Berman, T., 1999. Algal growth on organic compounds as nitrogen sources, Journal of Plankton Research. doi:10.1093/plankt/21.8.1423

Berman, T., 1988. Differential uptake of orthophosphate and organic phosphorus substrates by bacteria and algae in Lake Kinneret. J. Plankton Res. 10, 1239–1249. doi:10.1093/plankt/10.6.1239

Berrie, A.D., 1992. The chalk-stream environment. Hydrobiologia 248, 3–9. doi:10.1007/BF00008881

Bertilsson, S., Tranvik, L.J., 2000. Photochemical transformation of dissolved organic matter in lakes. Limnol. Oceanogr. 45, 753–762. doi:10.4319/lo.2000.45.4.0753

Billett, M.F., Deacon, C.M., Palmer, S.M., Dawson, J.J.C., Hope, D., 2006. Connecting organic carbon in stream water and soils in a peatland catchment. J. Geophys. Res. Biogeosciences 111, n/a-n/a. doi:10.1029/2005JG000065

Björkman, K.M., Karl, D.M., 2003. Bioavailability of dissolved organic phosphorus in the euphotic zone at Station ALOHA, North Pacific Subtropical Gyre. Limnol. Oceanogr. 48, 1049–1057. doi:10.4319/lo.2003.48.3.1049

Björkman, K.M., Karl, D.M., 1994. Bioavailability of inorganic and organic phosphorus compounds to natural assemblages of microorganisms in Hawaiian coastal waters. Mar. Ecol. Process Ser. 111, 265–273. doi:10.3354/meps111265

Bowes, M.J., Leach, D. V., House, W.A., 2005. Seasonal nutrient dynamics in a chalk stream: The River Frome, Dorset, UK. Sci. Total Environ. 336, 225–241. doi:10.1016/j.scitotenv.2004.05.026

Brailsford, F.L.L., Glanville, H.C.C., Marshall, M.R.R., Golyshin, P.N.N., Johnes, P.J.J., Yates, C.A.A., Owen, A.T.T., Jones, D.L.L., 2017. Microbial use of low molecular weight DOM in filtered and unfiltered freshwater: Role of ultra-small microorganisms and implications for water quality monitoring. Sci. Total Environ. 598, 377–384. doi:10.1016/j.scitotenv.2017.04.049

Bridgeman, J., Bieroza, M., Baker, A., 2011. The application of fluorescence spectroscopy to organic matter characterisation in drinking water treatment. Rev. Environ. Sci. Biotechnol. doi:10.1007/s11157-011-9243-x

Brock, T.D., Clyne, J., 1984. Significance of algal excretory products for growth of epilimnetic bacteria. Appl. Environ. Microbiol. 47, 731–4.

Bronk, D.A., Roberts, Q.N., Sanderson, M.P., Canuel, E.A., Hatcher, P.G., Mesfioui, R., Filippino, K.C., Mulholland, M.R., Love, N.G., 2010. Effluent organic nitrogen (EON): Bioavailability and photochemical and salinity-mediated release. Environ. Sci. Technol. 44, 5830–5835. doi:10.1021/es101115g

Burgin, A.J., Hamilton, S.K., 2007. Have we overemphasized the role of denitrification in aquatic ecosystems? A review of nitrate removal pathways. Front. Ecol. Environ. 5, 89–

96. doi:10.1890/1540-9295(2007)5[89:HWOTRO]2.0.CO;2

Cembella, A.D., Antia, N.J., Harrison, P.J., 1982. The utilization of inorganic and organic phosphorous compounds as nutrients by eukaryotic microalgae: A multidisciplinary perspective: Part i. Crit. Rev. Microbiol. 10, 317–391. doi:10.3109/10408418209113567

Chróst, R., Faust, M., 1983. Organic carbon release by phytoplankton: its composition and utilisation by bacterioplankton. J Plankt. Res 5, 477–493. doi:10.1093/plankt/5.4.477

Coble, P.G., 2007. Marine optical biogeochemistry: The chemistry of ocean color. Chem. Rev. 107, 402–418. doi:10.1021/cr050350+

Coble, P.G., 1996. Characterization of marine and terrestrial DOM in seawater using excitation-emission matrix spectroscopy. Mar. Chem. 51, 325–346. doi:10.1016/0304-4203(95)00062-3

Coble, P.G., Spencer, R.G.M., Baker, A., Reynolds, D.M., Gabor, R., Baker, A., Dianne, M., Millller, M., 2014. Aquatic Organic Matter Fluorescence, First. ed, Aquatic Organic Matter Fluorescence. Cambrige University Press, Cambridge. doi:10.1017/CBO9781139045452.006

Cole, J.J., Prairie, Y.T., Caraco, N.F., McDowell, W.H., Tranvik, L.J., Striegl, R.G., Duarte, C.M., Kortelainen, P., Downing, J.A., Middelburg, J.J., Melack, J., 2007. Plumbing the global carbon cycle: Integrating inland waters into the terrestrial carbon budget. Ecosystems 10, 171–184. doi:10.1007/s10021-006-9013-8

Cooper, D.M., Jenkins, A., Norris, D., Evans, C.D., Juggins, S., 2006. A linked spatial and temporal model of the chemical and biological status of a large, acid-sensitive river network. Sci. Total Environ. 365, 167–185. doi:10.1016/j.scitotenv.2006.02.037

Cooper, K.J., Whitaker, F.F., Anesio, A.M., Naish, M., Reynolds, D.M., Evans, E.L., 2016. Dissolved organic carbon transformations and microbial community response to variations in recharge waters in a shallow carbonate aquifer. Biogeochemistry 129, 215–234. doi:10.1007/s10533-016-0226-4

Cooper, W.J., Zika, R.G., 1983. Photochemical formation of hydrogen peroxide in surface and ground waters exposed to sunlight. Science 220, 711–712. doi:10.1126/science.220.4598.711

Cotner, J.B., Heath, R.T., 1990. Iron redox effects on photosensitive phosphorus release from dissolved humic materials. Limnol. Oceanogr. doi:10.4319/lo.1990.35.5.1175

Cotner, J.B., Wetzel, R.G., 1992. Uptake of dissolved inorganic and organic phosphorus

compounds by phytoplankton and bacterioplankton. Limonology Oceanogr. 37, 232–243.

Czerwionka, K., 2015. Influence of dissolved organic nitrogen on surface waters. Oceanologia 58, 39–45. doi:10.1016/j.oceano.2015.08.002

De Haan, H., De Boer, T., 1987. Applicability of light absorbance and fluorescence as measures of concentration and molecular size of dissolved organic carbon in humic Lake Tjeukemeer. Water Res. 21, 731–734. doi:10.1016/0043-1354(87)90086-8

Donham, J.E., Rosenfeldt, E.J., Wigginton, K.R., Qu, S., Kolodziej, E.P., Cwiertny, D.M., Zepp, R.G., Hoigne, J., Bader, H., Vaughan, P.P., Blough, N. V., Dong, M.M., Rosario-Ortiz, F.L., Zepp, R.G., Bruce, C.F., Hoigne, J., Page, S.E., Kling, G.W., Sander, M., Harrold, K.H., Logan, J.R., McNeill, K., Cory, R.M., Hoigné, J., Jasper, J.T., Sedlak, D.L., Haidar, M., Dirany, A., Sirés, I., Oturan, N., Oturan, M.A., Mitra, P., Banerjee, P., Chakrabartia, S., Bhattacharjee, S., Katsoyiannis, I.A., Canonica, S., Gunten, U. von, McKay, G., Kleinman, J.L., Johnston, K.M., Dong, M.M., Rosario-Ortiz, F.L., Mezyk, S.P., Rosenfeldt, E.J., Linden, K.G., Grebel, J.E., Pignatello, J.J., Mitch, W.A., Liao, C.-H., Kang, S.-F., Wu, F.-A., Buxton, G. V., Greenstock, C.L., Helman, W.P., Ross, A.B., Hagg, W.R., Yao, C.C., Chen, S., Hoffman, M.Z., Buxton, G. V., Elliot, A.J., Goldstone, J. V., Pullin, M.J., Bertilsson, S., Voelker, B.M., Brezonik, P.L., Fulkerson-Brekken, J., Westerhoff, P., Aiken, G., Amy, G., Debbroux, J., Westerhoff, P., Mezyk, S.P., Cooper, W.J., Minakata, D., McKay, G., Dong, M.M., Kleinman, J.L., Mezyk, S.P., Rosario-Ortiz, F.L., Rosario-Ortiz, F.L., Mezyk, S.P., Doud, D.F., Snyder, S.A., Keen, O.S., McKay, G., Mezyk, S.P., Linden, K.G., Rosario-Ortiz, F.L., Rahn, R.O., Ou, B., Hampsh-Woodill, M., Flanagan, J., Deemer, E.K., Prior, R.L., Huang, D., Satoh, A.Y., Trosko, J.E., Masten, S.J., Sjöback, R., Nygren, J., Kubista, M., Banat, F., Al-Asheh, S., Al-Rawashdeh, M., Nusair, M., Singhal, G.S., Rabinowitch, E., Cordier, P., Grossweiner, L.I., 2014. Photometric hydroxyl radical scavenging analysis of standard natural organic matter isolates. Environ. Sci. Process. Impacts 16, 764. doi:10.1039/c3em00663h

Durand, P., Breuer, L., Johnes, P.J., Billen, G., Butturini, A., Pinay, G., van Grinsven, H., Garnier, J., Rivett, M., Reay, D.S., Curtis, C., Siemens, J., Maberly, S., Kaste, O., Humborg, C., Loeb, R., de Klein, J., Hejzlar, J., Skoulikidis, N., Kortelainen, P., Lepisto, A., Wright, R., 2011. Nitrogen processes in aquatic ecosystems, The European Nitrogen Assessment. doi:10.1126/science.333.6046.1083

DWI, 2017. What are the drinking water standards? [WWW Document]. Defra. URL http://dwi.defra.gov.uk/consumers/advice-leaflets/standards.pdf (accessed 6.6.17).

Edmondson, W.T., Vollenweider, R.A., 1970. Scientific fundamentals of the eutrophication of lakes and flowing waters with particular reference to nitrogen and phosphorus as factors in eutrophication. Limnol. Oceanogr. 15, 169–170. doi:10.4319/lo.1970.15.1.0169

Eimers, M.C., Buttle, J., Watmough, S.A., 2008. Influence of seasonal changes in runoff and extreme events on dissolved organic carbon trends in wetland- and upland-draining streams. Can. J. Fish. Aquat. Sci. 65, 796–808. doi:10.1139/f07-194

Erisman, J.W., Sutton, M.A., Galloway, J., Klimont, Z., Winiwarter, W., 2008. How a century of ammonia synthesis changed the world. Nat. Geosci. 1, 636–639. doi:10.1038/ngeo325

Evans, C.D., Cooper, D.M., Juggins, S., Jenkins, A., Norris, D., 2006. A linked spatial and temporal model of the chemical and biological status of a large, acid-sensitive river network. Sci. Total Environ. 365, 167–185. doi:10.1016/j.scitotenv.2006.02.037

Evans, C.D., Monteith, D.T., Cooper, D.M., 2005. Long-term increases in surface water dissolved organic carbon: Observations, possible causes and environmental impacts. Environ. Pollut. doi:10.1016/j.envpol.2004.12.031

Evans, D.J., Johnes, P.J., Lawrence, D.S., 2004. Physico-chemical controls on phosphorus cycling in two lowland streams. Part 2-The sediment phase. Sci. Total Environ. 329, 165–182. doi:10.1016/j.scitotenv.2004.02.023

Fagerberg, T., Carlsson, P., Lundgren, M., 2009. A large molecular size fraction of riverine high molecular weight dissolved organic matter (HMW DOM) stimulates growth of the harmful dinoflagellate Alexandrium minutum. Harmful Algae 8, 823–831. doi:10.1016/j.hal.2009.02.002

Fenner, N., Freeman, C., Worrall, F., 2009. Hydrological Controls on Dissolved Organic Carbon Production and Release from UK Peatlands, in: Carbon Cycling in Northern Peatlands. pp. 237–249. doi:10.1029/2008GM000823

Findlay, R.L., Sinsabaugh, R.., 2003. Aquatic Ecosystems – Interactivity of Dissolved Organic Matter Academic Press (2003).

Fovet, O., Evans, C.D., Jones, D.L., Jones, T.G., Cooper, D.M., Bell, V., Davies, H., 2016. Reactivity of stream dissolved organic matter in headwater catchments: Photo-

degradation versus nutrient-limited production.

Fox, B.G., Thorn, R.M.S., Anesio, A.M., Reynolds, D.M., 2017. The in situ bacterial production of fluorescent organic matter; an investigation at a species level. Water Res. 125, 350–359. doi:10.1016/j.watres.2017.08.040

Francko, D.A., Heath, R.T., 1982. UV sensitive complex phosphorus: Association with dissolved humic material and iron in a bog lake. Limnol. Oceanogr. doi:10.4319/lo.1982.27.3.0564

Francko, D.A., Heath, R.T., 1979. Functionally distinct classes of complex phosphorus compounds in lake water. Limnol. Oceanogr. 24, 463–473. doi:10.4319/lo.1979.24.3.0463

Freeman, C., Evans, C.D., Monteith, D.T., Reynolds, B., Fenner, N., 2001. Export of organic carbon from peat soils. Nature 412, 785. doi:10.1038/35090628

Gabor, R.S., McKnight, D.M., Miller, M.P., 2014. Fluorescence Indices and Their Interpretation, in: Coble, P., Lead, J., Baker, A., Reynolds, D.M., Spencer, R.G.M. (Eds.), Aquatic Organic Matter Fluorescence. Cambridge University Press, Cambridge, pp. 303–338. doi:10.1017/CBO9781139045452.015

George, T.S., Giles, C.D., Menezes-Blackburn, D., Condron, L.M., Gama-Rodrigues, A.C., Jaisi, D., Lang, F., Neal, A.L., Stutter, M.I., Almeida, D.S., Bol, R., Cabugao, K.G., Celi, L., Cotner, J.B., Feng, G., Goll, D.S., Hallama, M., Krueger, J., Plassard, C., Rosling, A., Darch, T., Fraser, T., Giesler, R., Richardson, A.E., Tamburini, F., Shand, C.A., Lumsdon, D.G., Zhang, H., Blackwell, M.S.A., Wearing, C., Mezeli, M.M., Almås, R., Audette, Y., Bertrand, I., Beyhaut, E., Boitt, G., Bradshaw, N., Brearley, C.A., Bruulsema, T.W., Ciais, P., Cozzolino, V., Duran, P.C., Mora, M.L., de Menezes, A.B., Dodd, R.J., Dunfield, K., Engl, C., Frazão, J.J., Garland, G., González Jiménez, J.L., Graca, J., Granger, S.J., Harrison, A.F., Heuck, C., Hou, E.Q., Johnes, P.J., Kaiser, K., Kjær, H.A., Klumpp, E., Lamb, A.L., Macintosh, K.A., Mackay, E.B., McGrath, J., McIntyre, C., McLaren, T., Mészáros, E., Missong, A., Mooshammer, M., Negrón, C.P., Nelson, L.A., Pfahler, V., Poblete-Grant, P., Randall, M., Seguel, A., Seth, K., Smith, A.C., Smits, M.M., Sobarzo, J.A., Spohn, M., Tawaraya, K., Tibbett, M., Voroney, P., Wallander, H., Wang, L., Wasaki, J., Haygarth, P.M., 2018. Organic phosphorus in the terrestrial environment: a perspective on the state of the art and future priorities. Plant Soil 427, 191–208. doi:10.1007/s11104-017-3391-x

Green, S.A., Blough, N.V., 1994. Optical absorption and fluorescence properties of chromophoric dissolved organic matter in natural waters. Limnol. Ocean. 39, 1903–1916. doi:10.4319/lo.1994.39.8.1903

Grimm, N.B., Foster, D., Groffman, P., Grove, J.M., Hopkinson, C.S., Nadelhoffer, K.J., Pataki, D.E., Peters, D.P.C., 2008. The changing landscape: Ecosystem responses to urbanization and pollution across climatic and societal gradients. Front. Ecol. Environ. doi:10.1890/070147

Haag, W.R., Hoigné, J., 1985. Photo-sensitized oxidation in natural water via .OH radicals. Chemosphere 14, 1659–1671. doi:10.1016/0045-6535(85)90107-9

Haan, H., Jones, R.I., Salonen, K., 1990. Abiotic transformations of iron and phosphate in humic lake water revealed by double-isotope labeling and gel filtration. Limnol. Oceanogr. 35, 491–497. doi:10.4319/lo.1990.35.2.0491

Hansen, A.M., Kraus, T.E.C., Pellerin, B.A., Fleck, J.A., Downing, B.D., Bergamaschi, B.A., 2016. Optical properties of dissolved organic matter (DOM): Effects of biological and photolytic degradation. Limnol. Oceanogr. 61, 1015–1032. doi:10.1002/lno.10270

Harjung, A., Sabater, F., Butturini, A., 2016. Hydrological connectivity drives dissolved organic matter processing in an intermittent stream. Limnologica. doi:10.1016/j.limno.2017.02.007

Heathwaite, A.L., Johnes, P.J., Peters, N.E., 1996. Trends in nutrients. Hydrol. Process. 10, 263–293. doi:Doi 10.1002/(Sici)1099-1085(199602)10:2<263::Aid-Hyp441>3.0.Co;2-K

Hedges, J.I., 1992. Global biogeochemical cycles: progress and problems. Mar. Chem. 39, 67–93. doi:10.1016/0304-4203(92)90096-S

Helms, R., Mao, J., Stubbins, A., Schmidt-Rohr, K., Spencer, R.G.M., Hernes, P.J., Mopper, K., 2014. Loss of optical and molecular indicators of terrigenous dissolved organic matter during long-term photobleaching. Aquat. Sci. 76, 353–373. doi:10.1007/s00027-014-0340-0

Helms, Stubbins, A.A., Ritchie, J.D., Minor, E.C., David, J., Mopper, K., Helms, R., Stubbins, A.A., Kieber, D.J., Mopper, K., 2008. Absorption spectral slopes and slope ratios as indicators of molecular weight, source, and photobleaching of chromophoric dissolved organic matter. Limonology Oceanogr. 53, 955–969. doi:10.4319/lo.2008.53.3.0955

Hope, D., Billett, M.F., Cresser, M.S., 1997. Exports of organic carbon in two river systems in NE Scotland. J. Hydrol. 193, 61–82. doi:10.1016/S0022-1694(96)03150-2

Hoppe, H.G., 2003. Phosphatase activity in the sea. Hydrobiologia 493, 187–200. doi:10.1023/A:1025453918247

Hudson, N., Baker, A., Reynolds, D., 2007. Fluorescence analysis of dissolved organic matter in natural, waste and polluted waters - A review. River Res. Appl. 23, 631–649. doi:10.1002/rra

Jack, J., Sellers, T., Bukaveckas, P.A., 2002. Algal production and trihalomethane formation potential: an experimental assessment and inter-river comparison. Can. J. Fish. Aquat. Sci. 59, 1482–1491. doi:10.1139/f02-121

Jaffé, R., McKnight, D., Maie, N., Cory, R., McDowell, W.H., Campbell, J.L., 2008. Spatial and temporal variations in DOM composition in ecosystems: The importance of long-term monitoring of optical properties. J. Geophys. Res. Biogeosciences 113. doi:10.1029/2008JG000683

Jenkins, G., Murphy, J., Sexton, D., Lowe, J., Jones, P., Kilsby, P., 2009. UK Climate Projections: Briefing report. Exeter.

JNCC, 2010a. Acid grasslands - lowland.

JNCC, 2010b. Handbook for Phase 1 habitat survey - a technique for environmental audit. Jncc 40.

Johnes, P.J., 1996. Evaluation and management of the impact of land use change on the nitrogen and phosphorus load delivered to surface waters: The export coefficient modelling approach. J. Hydrol. 183, 323–349. doi:10.1016/0022-1694(95)02951-6

Johnes, P.J., Heathwaite, A.L., 1992. A procedure for the simultaneous determination of Total N and Total P in freshwater using persulphate microwave digestion. Water Res. 26, 1281–1287. doi:10.1016/0043-1354(92)90122-K

Johnes, P.J., Hodgkinson, R., 1998. Phosphorus loss from agricultural catchments: pathways and implications for management. Soil Use Manag. 14, 175–185. doi:10.1111/j.1475-2743.1998.tb00637.x

JONES, R.I., SALONEN, K., DE HAAN, H., 1988. Phosphorus transformations in the epilimnion of humic lakes: abiotic interactions between dissolved humic materials and phosphate. Freshw. Biol. 19, 357–369. doi:10.1111/j.1365-2427.1988.tb00357.x

Jones, T.G., Evans, C.D., Jones, D.L., Hill, P.W., Freeman, C., 2016. Transformations in DOC along a source to sea continuum; impacts of photo-degradation, biological processes and mixing. Aquat. Sci. 78, 433–446. doi:10.1007/s00027-015-0461-0

Kallenbach, C.M., Frey, S.D., Grandy, A.S., 2016. Direct evidence for microbial-derived soil organic matter formation and its ecophysiological controls. Nat. Commun. 7. doi:10.1038/ncomms13630

Khamis, K., Bradley, C., Hannah, D.M., 2017. Understanding dissolved organic matter dynamics in urban catchments: insights from in situ fluorescence sensor technology. Wiley Interdiscip. Rev. Water 5, e1259. doi:10.1002/wat2.1259

Kieber, R.J., Hydro, L.H., Seaton, P.J., 1997. Photooxidation of triglycerides and fatty acids in seawater: Implication toward the formation of marine humic substances. Limnol. Oceanogr. 42, 1454–1462. doi:10.4319/lo.1997.42.6.1454

Kim, K., Portis, A.R., 2004. Oxygen-dependent H2O2 production by Rubisco. FEBS Lett. 571, 124–128. doi:10.1016/j.febslet.2004.06.064

Koopmans, D.J., Bronk, D.A., 2002. Photochemical production of dissolved inorganic nitrogen and primary amines from dissolved organic nitrogen in waters of two estuaries and adjacent surficial groundwaters. Aquat. Microb. Ecol. 26, 295–304. doi:10.3354/ame026295

Kothawala, D.N., von Wachenfeldt, E., Koehler, B., Tranvik, L.J., 2012. Selective loss and preservation of lake water dissolved organic matter fluorescence during long-term dark incubations. Sci. Total Environ. 433, 238–246. doi:10.1016/j.scitotenv.2012.06.029

Ksibi, M., 2006. Chemical oxidation with hydrogen peroxide for domestic wastewater treatment. Chem. Eng. J. 119, 161–165. doi:10.1016/j.cej.2006.03.022

Larsson, T., Wedborg, M., Turner, D., 2007. Correction of inner-filter effect in fluorescence excitation-emission matrix spectrometry using Raman scatter. Anal. Chim. Acta 583, 357–363. doi:10.1016/J.ACA.2006.09.067

Lawaetz, A.J., 2016. Fluorescence Intensity Calibration Using the Raman Scatter Peak of Water Fluorescence Intensity Calibration Using the Raman Scatter Peak of Water. doi:10.1366/000370209788964548

Lesueur, C., Pfeffer, M., Fuerhacker, M., 2005. Photodegradation of phosphonates in water. Chemosphere 59, 685–691. doi:10.1016/j.chemosphere.2004.10.049

Levene, H., 1960. Robust Tests for Equality of Variances. Stanford University Press, Palo Alto.

Limbrick, K.J., 2003. Baseline nitrate concentration in groundwater of the Chalk in south Dorset, UK, in: Science of the Total Environment. pp. 89–98. doi:10.1016/S0048-9697(03)00098-6

Liu, G., Tang, Q., Zhou, Y., Cao, X., Zhao, J., Zhu, D., 2017. Photo-induced phosphate released from organic phosphorus degradation in deionized and natural water. Photochem. Photobiol. Sci. 16, 467–475. doi:10.1039/C6PP00313C

Lloyd, C.E.M., Johnes, P.J., Freer, J.E., Carswell, A.M., Jones, J.I., Stirling, M.W., Hodgkinson, R.A., Richmond, C., Collins, A.L., 2019. Determining the sources of nutrient flux to water in headwater catchments: Examining the speciation balance to inform the targeting of mitigation measures. Sci. Total Environ. 648, 1179–1200. doi:10.1016/J.SCITOTENV.2018.08.190

Marschner, B., Kalbitz, K., 2003. Controls of bioavailability and biodegradability of dissolved organic matter in soils, in: Geoderma. pp. 211–235. doi:10.1016/S0016-7061(02)00362-2

Matarazzo, A., Hudson, R.H.E., 2015. Fluorescent adenosine analogs: A comprehensive survey. Tetrahedron 71, 1627–1657. doi:10.1016/j.tet.2014.12.066

Mei, Z.P., Saucier, F.J., Le Fouest, V., Zakardjian, B., Sennville, S., Xie, H., Starr, M., 2010. Modeling the timing of spring phytoplankton bloom and biological production of the Gulf of St. Lawrence (Canada): Effects of colored dissolved organic matter and temperature. Cont. Shelf Res. 30, 2027–2042. doi:10.1016/j.csr.2010.10.003

Miller, W.L., Zepp, R.G., 1995. Photochemical production of dissolved inorganic carbon from terrestrial organic matter: Significance to the oceanic organic carbon cycle. Geophys. Res. Lett. 22, 417–420. doi:10.1029/94GL03344

Monteith, D.T., Stoddard, J.L., Evans, C.D., de Wit, H.A., Forsius, M., Høgåsen, T., Wilander, A., Skjelkvåle, B.L., Jeffries, D.S., Vuorenmaa, J., Keller, B., Kopácek, J., Vesely, J., 2007. Dissolved organic carbon trends resulting from changes in atmospheric deposition chemistry. Nature 450, 537–540. doi:10.1038/nature06316

Mopper, K., Bittar, T.B., Stubbins, A., Vieira, A.A.H., 2015. Characterization and photodegradation of dissolved organic matter (DOM) from a tropical lake and its dominant primary producer, the cyanobacteria Microcystis aeruginosa. Mar. Chem. 177, 205–217. doi:10.1016/j.marchem.2015.06.016

Mopper, K., Zhou, X., Kieber, R.J., Kieber, D.J., Sikorski, R.J., Jones, R.D., 1991. Photochemical degradation of dissolved organic carbon and its impact on the oceanic carbon cycle. Nature 353, 60–62. doi:10.1038/353060a0

Mosher, J.J., Kaplan, L.A., Podgorski, D.C., McKenna, A.M., Marshall, A.G., 2015. Longitudinal

shifts in dissolved organic matter chemogeography and chemodiversity within headwater streams: a river continuum reprise. Biogeochemistry 124, 371–385. doi:10.1007/s10533-015-0103-6

Mostofa, K.M.G., Sakugawa, H., 2009. Spatial and temporal variations and factors controlling the concentrations of hydrogen peroxide and organic peroxides in rivers. Environ. Chem. 6, 524–534. doi:10.1071/EN09070

Murphy, K.R., Butler, K.D., Spencer, R.G.M., Stedmon, C.A., Boehme, J.R., Aiken, G.R., 2010. Measurement of dissolved organic matter fluorescence in aquatic environments: An interlaboratory comparison. Environ. Sci. Technol. 44, 9405–9412. doi:10.1021/es102362t

Murphy, K.R., Stedmon, C.A., Graeber, D., Bro, R., Stedmon, C.A., Markager, S., Bro, R., Bro, R., Bro, R., Andersson, C.A., Kiers, H.A.L., Andersen, C.M., Bro, R., Murphy, K.R., Boehme, J.R., Noble, M., Brown, C., Smith, G., Sparks, D., Ruiz, G.M., Andersson, C.A., Bro, R., Stedmon, C.A., Bro, R., Murphy, K.R., Murphy, K.R., Butler, K.D., Spencer, R.G.M., Stedmon, C.A., Boehme, J.R., Aiken, G.R., Leibovici, D.G., Thomas, E. V., Bro, R., Smilde, A.K., DeRose, P.C., Early, E.A., Kramer, G.W., DeRose, P.C., Resch-Genger, U., Gilmore, A., Hurteaux, R., FitzGerald, S., Knowles, A., Gu, Q., Kenny, J.E., Holland, J.F., Teets, R.E., Kelly, P.M., Timnick, A., Christmann, D.R., Crouch, S.R., Holland, J.F., Timnick, A., Senesi, N., Coble, P.G., Green, S.A., Blough, N. V., Gagosian, R.B., Bahram, M., Bro, R., Stedmon, C.A., Afkhami, A., Zepp, R.G., Sheldon, W.M., Moran, M.A., Gurden, S.P., Westerhuis, J.A., Bro, R., Smilde, A.K., Riu, J., Bro, R., Bro, R., Kiers, H.A.L., Bosco, M. V., Garrido, M., Larrechi, M.S., Murphy, K.R., Hambly, A., Singh, S., Henderson, R.K., Baker, A., Stuetz, R., Khan, S.J., Murphy, K.R., Stedmon, C.A., Waite, T.D., Ruiz, G.M., Stedmon, C.A., Markager, S., Hurlbert, S.H., 2013. Fluorescence spectroscopy and multi-way techniques. PARAFAC. Anal. Methods 5, 6557. doi:10.1039/c3ay41160e

Muscutt, A.D., Withers, P.J.A., 1996. The phosphorus content of rivers in England and Wales. Water Res. 30, 1258–1268. doi:10.1016/0043-1354(95)00290-1

Myneni, R.B., Dong, J., Tucker, C.J., Kaufmann, R.K., Kauppi, P.E., Liski, J., Zhou, L., Alexeyev, V., Hughes, M.K., 2001. A large carbon sink in the woody biomass of Northern forests. Proc. Natl. Acad. Sci. U. S. A. 98, 14784–9. doi:10.1073/pnas.261555198

Myneni, R.B., Keeling, C.D., Tucker, C.J., Asrar, G., Nemani, R.R., 1997. Increased plant

growth in the northern high latitudes from 1981 to 1991. Nature. doi:10.1038/386698a0

Nakatani, N., Ueda, M., Shindo, H., Takeda, K., Sakugawa, H., 2007. Contribution of the photo-Fenton reaction to hydroxyl radical formation rates in river and rain water samples. Anal. Sci. 23, 1137–42. doi:10.2116/analsci.23.1137

Neyens, E., Baeyens, J., 2003. A review of classic Fenton's peroxidation as an advanced oxidation technique. J. Hazard. Mater. doi:10.1016/S0304-3894(02)00282-0

Pandey, M., 2006. Nutrient modulated alkaline phosphatase and associated processes in diazotrophic cyanobacteria. Polish J. Microbiol. 55, 53–62.

Peake, B.M., Mosley, L.M., 2004. Hydrogen peroxide concentrations in relation to optical properties in a fiord (Doubtful Sound, New Zealand). New Zeal. J. Mar. Freshw. Res. 38, 729–741. doi:10.1080/00288330.2004.9517272

Perry, A.M., Golding, N., 2011. Range of environmental temperature conditions in the United Kingdom.

Peuravuori, J., Pihlaja, K., 1997. Molecular size distribution and spectroscopic properties of aquatic humic substances. Anal. Chim. Acta 337, 133–149. doi:10.1016/S0003-2670(96)00412-6

Pickard, A.E., Heal, K. V, Mcleod, A.R., Dinsmore, K.J., 1963. Anterior Cervical Fusion. Solution of a Particular Problem. JAMA J. Am. Med. Assoc. 184, 165. doi:10.5194/bg-14-1793-2017

Prior, H., Johnes, P.J., 2002. Regulation of surface water quality in a Cretaceous Chalk catchment, UK: An assessment of the relative importance of instream and wetland processes. Sci. Total Environ. 282–283, 159–174. doi:10.1016/S0048-9697(01)00950-0

Raimonet, M., Vilmin, L., Flipo, N., Rocher, V., Laverman, A.M., 2015. Modelling the fate of nitrite in an urbanized river using experimentally obtained nitrifier growth parameters. Water Res. 73, 373–387. doi:10.1016/j.watres.2015.01.026

Reitner, B., Herzig, A., Herndl, G.J., 2002. Photoreactivity and bacterioplankton availability of aliphatic versus aromatic amino acids and a protein. Aquat. Microb. Ecol. 26, 305–311. doi:10.3354/ame0263055

Richardson, S.D., Plewa, M.J., Wagner, E.D., Schoeny, R., DeMarini, D.M., 2007. Occurrence, genotoxicity, and carcinogenicity of regulated and emerging disinfection by-products in drinking water: A review and roadmap for research. Mutat. Res. - Rev. Mutat. Res.

doi:10.1016/j.mrrev.2007.09.001

Ritson, J.P., Graham, N.J.D., Templeton, M.R., Clark, J.M., Gough, R., Freeman, C., 2014. The impact of climate change on the treatability of dissolved organic matter (DOM) in upland water supplies: A UK perspective. Sci. Total Environ. 473–474, 714–730. doi:10.1016/j.scitotenv.2013.12.095

Sawicka, K., Rowe, E.C., Evans, C.D., Monteith, D.T., E.I.Vanguelova, Wade, A.J., J.M.Clark, Vanguelova, E.I., Wade, A.J., Clark, J.M., 2017. Modelling impacts of atmospheric deposition and temperature on long-term DOC trends. Sci. Total Environ. 578, 323–336. doi:10.1016/j.scitotenv.2016.10.164

Seifert, A.-G., Roth, V.-N., Dittmar, T., Gleixner, G., Breuer, L., Houska, T., Marxsen, J., 2016. Comparing molecular composition of dissolved organic matter in soil and stream water: Influence of land use and chemical characteristics. Sci. Total Environ. 571, 142–152. doi:10.1016/j.scitotenv.2016.07.033

Seitzinger, S.P., Sanders, R.W., 1997. Contribution of dissolved organic nitrogen from rivers to estuarine eutrophication. Mar. Ecol. Prog. Ser. 159, 1–12. doi:10.3354/meps159001

Shapiro, S.S., Wilk, M.B., 1965. Biometrika Trust An Analysis of Variance Test for Normality (Complete Samples). Source Biometrika Biometrika Trust 52, 591–611. doi:10.1093/biomet/52.3-4.591

Simjouw, J.P., Minor, E.C., Mopper, K., 2005. Isolation and characterization of estuarine dissolved organic matter: Comparison of ultrafiltration and C18 solid-phase extraction techniques. Mar. Chem. 96, 219–235. doi:10.1016/j.marchem.2005.01.003

Spencer, R.G.M., Pellerin, B.A., Bergamaschi, B.A., Downing, B.D., Kraus, T.E.C., Smart, D.R., Dahlgren, R.A., Hernes, P.J., 2007. Diurnal variability in riverine dissolved organic matter composition determined by in situ optical measurement in the San Joaquin River (California, USA). Hydrol. Process. 21, 3181–3189. doi:10.1002/hyp.6887

Stedmon, C.A., Markager, S., Tranvik, L., Kronberg, L., Slätis, T., Martinsen, W., 2007. Photochemical production of ammonium and transformation of dissolved organic matter in the Baltic Sea. Mar. Chem. 104, 227–240. doi:10.1016/j.marchem.2006.11.005

Strous, M., Van Gerven, E., Kuenen, J.G., Jetten, M., 1997. Effects of aerobic and microaerobic conditions on anaerobic ammonium- oxidizing (anammox) sludge. Appl. Environ. Microbiol. 63, 2446–2448.

Stubbins, A., Law, C.S., Uher, G., Upstill-Goddard, R.C., 2011. Carbon monoxide apparent quantum yields and photoproduction in the Tyne estuary. Biogeosciences 8, 703–713. doi:10.5194/bg-8-703-2011

Su, R., Bai, Y., Zhang, C., Shi, X., 2015. The assessment of the spatial and seasonal variability of chromophoric dissolved organic matter in the Southern Yellow Sea and the East China Sea. Mar. Pollut. Bull. 100, 523–533. doi:10.1016/j.marpolbul.2015.09.002

Tarr, M.A., Wang, W., Bianchi, T.S., Engelhaupt, E., 2001. Mechanisms of ammonia and amino acid photoproduction from aquatic humic and colloidal matter. Water Res. 35, 3688–3696. doi:10.1016/S0043-1354(01)00101-4

Twardowski, M.S., Boss, E., Sullivan, J.M., Donaghay, P.L., 2004. Modeling the spectral shape of absorption by chromophoric dissolved organic matter. Mar. Chem. 89, 69–88. doi:10.1016/j.marchem.2004.02.008

Twardowski, M.S., Donaghay, P.L., 2002. Photobleaching of aquatic dissolved materials: Absorption removal, spectral alteration, and their interrelationship. J. Geophys. Res. 107, 3091. doi:10.1029/1999JC000281

U.S. Geological Survey, 2016. Organic Matter Research Lab - Optical Properties [WWW Document]. URL https://ca.water.usgs.gov/OMRL/OpticalProperties.html (accessed 2.5.19).

Vähätalo, A. V., Vähätalo, A. V., Salkinoja-salonen, M., Taalas, P., Salonen, K., Vähätalo, A. V., Salkinoja-salonen, M., Taalas, P., Salonen, K., Vähätalo, A. V., Vähätalo, A. V., Salkinoja-salonen, M., Taalas, P., Salonen, K., 2000. Spectrum of the quantum yield for photochemical mineralization of dissolved organic carbon in a humic lake. Limnol. Oceanogr. 45, 664–676. doi:10.4319/lo.2000.45.3.0664

Vodacek, A., Blough, N. V., Degrandpre, M.D., Peltzer, E.T., Nelson, R.K., 1997. Seasonal variation of CDOM and DOC in the Middle Atlantic Bight: Terrestrial inputs and photooxidation. Limnol. Oceanogr. 42, 674–686. doi:10.4319/lo.1997.42.4.0674

Voelker, B., Morel, F., Sulzberger, B., 1997. No Title. Environ. Sci. Technol 31.

Voelker, B.M., Sulzberger, B., 1996. Effects of fulvic acid on Fe(II) oxidation by hydrogen peroxide. Environ. Sci. Technol. 30, 1106–1114. doi:10.1021/es9502132

Walsh, J.J., Weisberg, R.H., Dieterle, D.A., He, R., Darrow, B.P., Jolliff, J.K., Lester, K.M., Vargo, G.A., Kirkpatrick, G., Fanning, K.A., Sutton, T.T., Jochens, A.E., Biggs, D.C., Nababan, B., Hu, C., Muller-Karger, F.E., 2003. Phytoplankton response to intrusions of

slope water on the West Florida Shelf: Models and observations. J. Geophys. Res. 108, 3190. doi:10.1029/2002JC001406

Wang, W., Tarr, M.A., Bianchi, T.S., Engelhaupt, E., 2000. Ammonium photoproduction from aquatic humic and colloidal matter. Aquat. Geochemistry 6, 275–292. doi:10.1023/A:1009679730079

Watts, C.D., Naden, P.S., Machell, J., Banks, J., 2001. Long term variation in water colour from Yorkshire catchments. Sci. Total Environ. 278, 57–72. doi:10.1016/S0048-9697(00)00888-3

Weishaar, J.L., Aiken, G.R., Bergamaschi, B.A., Fram, M.S., Fujii, R., Mopper, K., 2003. Evaluation of specific ultraviolet absorbance as an indicator of the chemical composition and reactivity of dissolved organic carbon. Environ. Sci. Technol. 37, 4702–4708. doi:10.1021/es030360x

Wetzel, R.G., Stewart, A.J., 1981. Dissovle humic materials: Photodegradation, sediment effects and reactivity with phosphate and calcium carbonate precipitation. Hydrobiologia 92, 265–286.

Willey, J.D., Kieber, R.J., Lancaster, R.D., 1996. Coastal rainwater hydrogen peroxide: Concentration and deposition. J. Atmos. Chem. 25, 149–165. doi:10.1007/BF00053789

Wolfbeis, O.S., 1985. The fluorescence of organic natural products, in: Molecular Luminescense Spectrospcopy. pp. 167–327.

Woods, G.C., Simpson, M.J., Kelleher, B.P., McCaul, M., Kingery, W.L., Simpson, A.J., 2010. Online High-Performance Size Exclusion Chromatography−Nuclear Magnetic Resonance for the Characterization of Dissolved Organic Matter. Environ. Sci. Technol. 44, 624–630. doi:10.1021/es903042s

Worrall, F., Harriman, R., Evans, C.D., Watts, C.D., Adamson, J., Neal, C., Tipping, E., Burt, T., Grieve, I., Monteith, D., Naden, P.S., Nisbet, T., Reynolds, B., Stevens, P., 2004. Trends in dissolved organic carbon in UK rivers and lakes. Biogeochemistry 70, 369–402. doi:10.1007/s10533-004-8131-7

Xiaodong, M., Green, S., 2004. Photochemical Transformation of Dissolved Organic Carbon in Lake Superior—An In-situ Experiment. Gt. Lakes 30, 97–112.

Yamashita, Y., Tanoue, E., 2008. Production of bio-refractory fluorescent dissolved organic matter in the ocean interior. Nat. Geosci. 1, 579–582. doi:10.1038/ngeo279

Yamashita, Y., Tanoue, E., 2003. Chemical characterization of protein-like fluorophores in

DOM in relation to aromatic amino acids. Mar. Chem. doi:10.1016/S0304-4203(03)00073-2

Yang, C., Liu, Y., Zhu, Y., Zhang, Y., 2016. Insights into the binding interactions of autochthonous dissolved organic matter released from Microcystis aeruginosa with pyrene using spectroscopy. Mar. Pollut. Bull. 104, 113–120. doi:10.1016/j.marpolbul.2016.01.053

Yates, C., 2016. Maps - DOMAINE [WWW Document]. URL http://www.nerc-domaine.uk/maps/ (accessed 4.28.17).

Yates, C.A., Johnes, P.J., 2013. Nitrogen speciation and phosphorus fractionation dynamics in a lowland Chalk catchment. Sci. Total Environ. 444, 466–479. doi:10.1016/j.scitotenv.2012.12.002

Yates, C.A., Johnes, P.J., Owen, A.T., Brailsford, F.L., Glanville, H.C., Evershed, R.., Jones, D.., Lloyd, C.E.M., Mayberly, S., Mackay, E.B., Jickells, T., 2018. Landscape scale variations in organic matter stoichiometry: assessing the role of land classification and soil C:N ratios. Biogeochem. (in Rev.

Yates, C.A., Johnes, P.J., Spencer, R.G.M., 2016. Assessing the drivers of dissolved organic matter export from two contrasting lowland catchments, U.K. Sci. Total Environ. 569–570, 1330–1340. doi:10.1016/j.scitotenv.2016.06.211

Zepp, R.G., Callaghan, T. V, Erickson III, D.J., 2003. Interactive effects of ozone depletion and climate change on biogeochemical cycles. Photochem. Photobiol. Sci. 2, 51. doi:10.1039/b211154n

Zepp, R.G., Erickson, D.J., Paul, N.D., Sulzberger, B., 2007. Interactive effects of solar UV radiation and climate change on biogeochemical cycling. Photochem. Photobiol. Sci. 6, 286–300. doi:10.1039/b700021a

Zhou, Y., Shi, K., Zhang, Y., Jeppesen, E., Liu, X., Zhou, Q., Wu, H., Tang, X., Zhu, G., 2017. Fluorescence peak integration ratio IC:ITas a new potential indicator tracing the compositional changes in chromophoric dissolved organic matter. Sci. Total Environ. 574, 1588–1598. doi:10.1016/j.scitotenv.2016.08.196

Zou, L., Wang, X.-C., Callahan, J., Culp, R.A., Chen, R.F., Altabet, M.A., Sun, M.-Y., 2004. Bacterial roles in the formation of high-molecular-weight dissolved organic matter in estuarine and coastal waters: Evidence from lipids and the compound-specific isotopic ratios. Limnol. Oceanogr. 49, 297–302. doi:10.4319/lo.2004.49.1.0297